Supporting information

Multivalent dextran hybrids for efficient cytosolic delivery of biomolecular cargoes

Table S1: Number, name and reference to synthesis/analysis of compounds used.

Number	Name	Reference to Synthesis/Analysis
1	L17E-Pra	2.4
2	dextran-*N*-Boc-Cad	2.7.2
3	CE(4.8)-dextran-*N*-Boc-Cad	2.7.2
4	Azide Linker	2.7.1
5	N_3(4.8)-dextran-*N*-Boc-Cad	2.7.2
6	N_3(4.8)-dextran-Cad	2.7.2
7	L17E(4.8)-dextran-Cad	2.7.3
8	L17E	2.1
9	CE(6.5)-dextran-*N*-Boc-Cad	2.8.3
10	*N*-Boc-ethylendiamine	2.8.1
11	1-((*N*-Boc)-2-aminoethyl)maleimide	2.8.1
12	*N*-(2-aminoethyl)maleimide	2.8.1
13	Maleimide-(6.5)-dextran-*N*-Boc-Cad	2.8.3
14	L17E-Cys	2.3
15	TAMRA-Thiol	2.8.2
16	TAMRA(1)-L17E(3.8)-dextran-*N*-Boc-Cad	2.8.4
17	CE(5.4)-dextran-*N*-Boc-Cad	2.9.1
18	N_3(5.4)-dextran-*N*-Boc-Cad	2.9.1
19	N_3(5.4)-dextran-Cad	2.9.1
20	N_3(5.4)-dextran-TAMRA	2.9.2
21	Alkyne-GFP11	2.5
22	L17E(2.7)-GFP11(2.7)-dextran-TAMRA	2.9.3
23	GFP11-dextran-TAMRA	2.9.4
24	GFP11	2.2
25	*S*-Trityl-3-mercaptopropionic acid	2.6.1
26	CE(10.5)-dextran-*N*-Boc-Cad	2.10.1
27	Maleimide-(10.5)-dextran-*N*-Boc-Cad	2.10.1

28	Thiol-PNA	2.6.2
29	L17E(5.3)-PNA(5.3)-dextran-*N*-Boc-Cad	2.10.2
30	DEACM	2.11.1
31	DEACM-OH	2.11.1
32	DEACM-*p*NP	2.11.2
33	Fmoc-L-Lys(DEACM)-OH	2.11.3
34	L17E-3PG	2.12
35	L17E-5PG	2.13

1 Results

1.1 TAMRA-L17E(3.8)-dextran **10** uptake in HeLa cells

1.1.1 Confocal Laser Scanning Microscopy

Uptake 25 µM TAMRA-dextran:

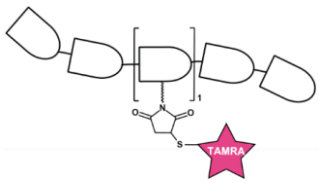

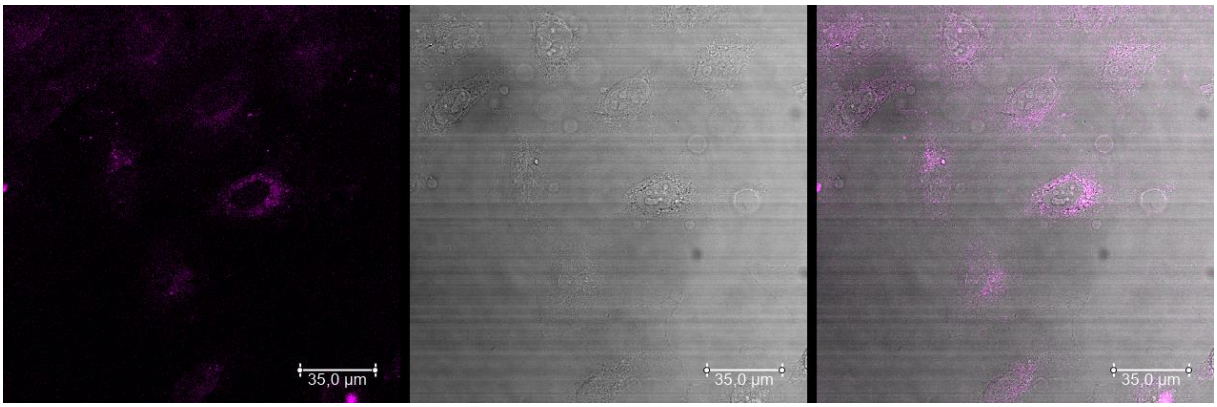

Figure S1: Fluorescence microscopy images (20x) of HeLa cells treated with 25 µM TAMRA-labelled dextran (10 kDa). TAMRA-fluorescence channel (left), brightfield (middle) and merge (right).

Uptake 25 µM TAMRA-dextran with 40 µM L17E coincubation:

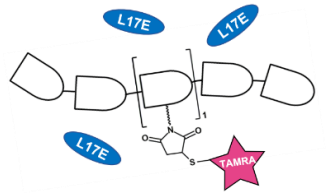

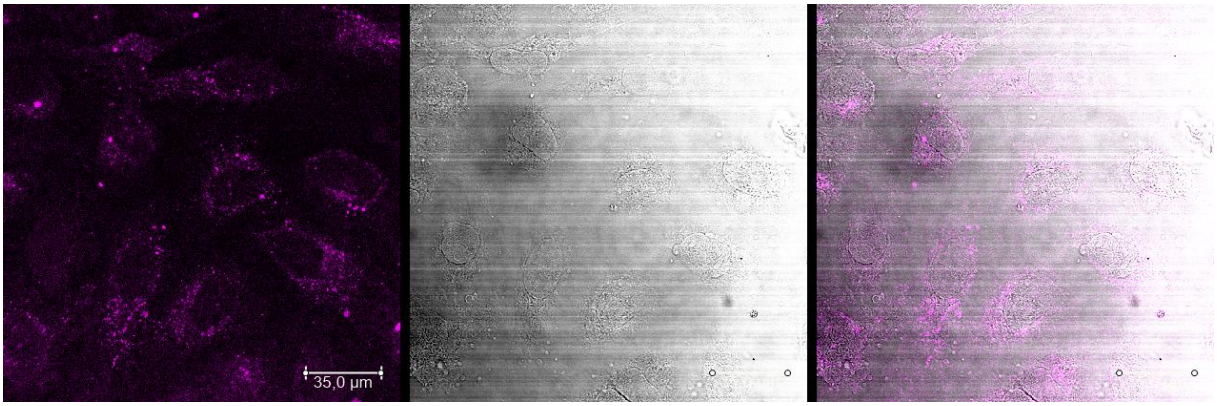

Figure S2: Fluorescence microscopy images (20x) of HeLa cells treated with 25 µM TAMRA-labelled dextran (10 kDa) with additional coincubation 40 µM solitary L17E. TAMRA-fluorescence channel (left), brightfield (middle) and merge (right).

Uptake 3.13 µM TAMRA-L17E(3.8)-dextran **10**:

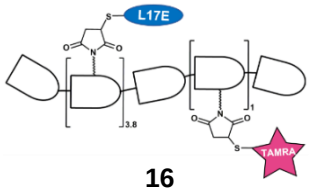

16

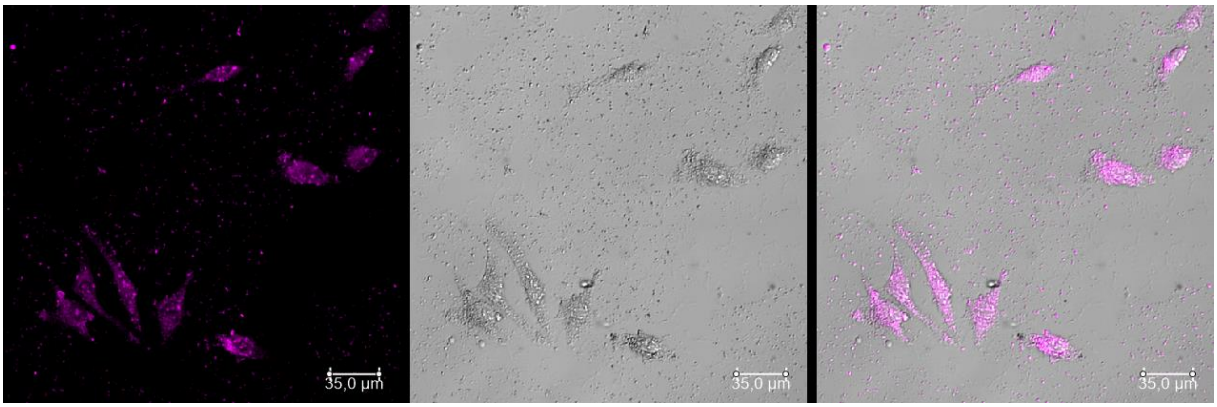

Figure S3: Fluorescence microscopy images (20x) of HeLa cells treated with 3.13 µM construct **16**, TAMRA-labelled dextran (10k Da) bearing 3.8 covalently conjugated L17E per dextran on average. TAMRA-fluorescence channel (left), brightfield (middle) and merge (right).

1.1.2 Cytotoxicity Assay of L17E(6)-dextran-TAMRA

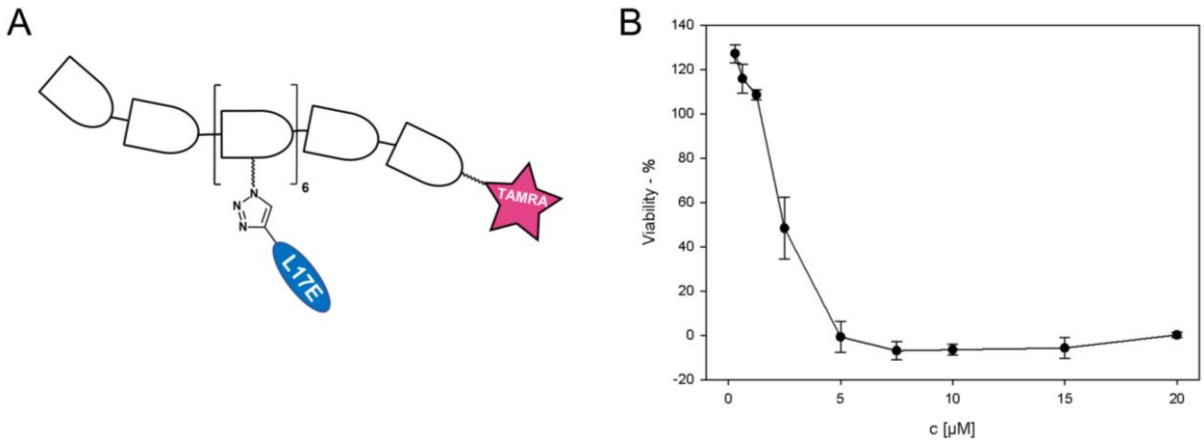

Figure S4: A: Schematic depiction of L17E(6)-dextran-TAMRA. This compound was synthesized and purified using the same procedure as described for TAMRA-labeled compound **22**. **B**: Cytotoxicity assay of L17E(6)-dextran-TAMRA, HeLa cells were incubated for 1 h with the compound (10 x concentrated in PBS) in serum-free DMEM, followed by incubation for 24 h in DMEM + 10 % FBS.

1.2 L17E-GFP11(5.4)-dextran-TAMRA **22** uptake in HeLa-GFP1-10 cells

1.2.1 Confocal Laser Scanning Microscopy

L17E-GFP11(5.4)-dextran-TAMRA **22,** 15 µM

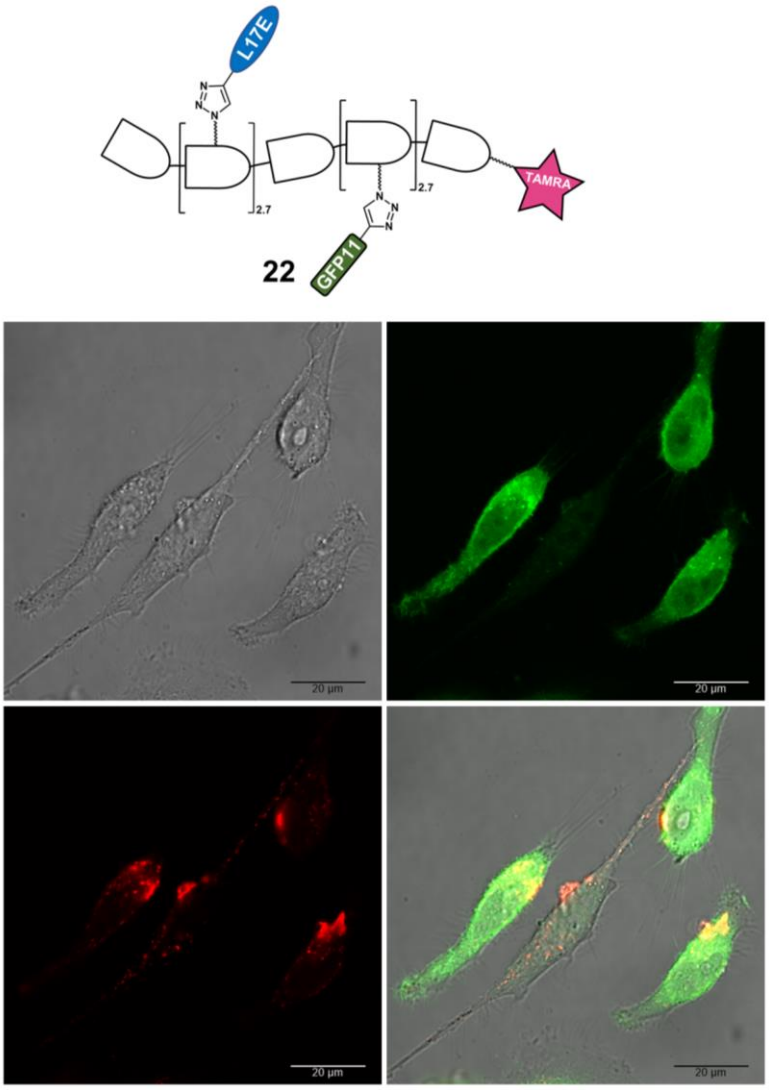

Figure S5: Live-cell CLSM images (63x) of HeLa cells treated with 15 µM construct **22**. Brightfield (top left), GFP-channel (top right), TAMRA-channel (bottom left), overlay (bottom right).

L17E-GFP11(5.4)-dextran-TAMRA **22,** 10 µM

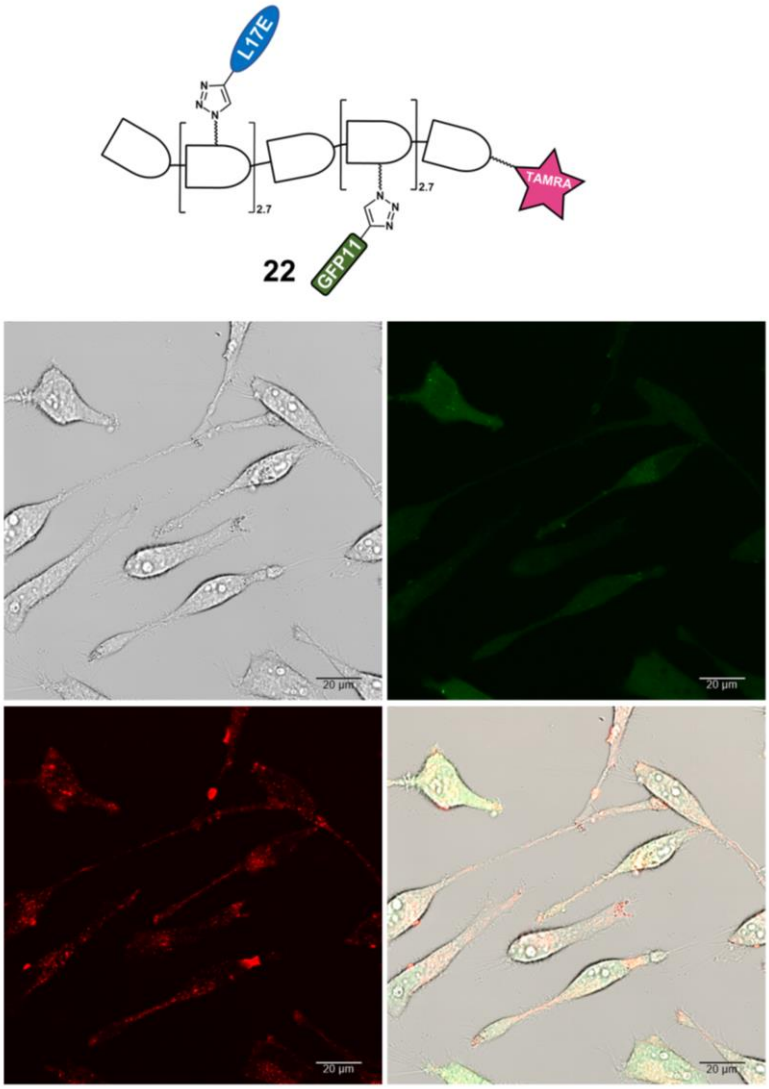

Figure S6: Live-cell CLSM images (20x) of HeLa cells treated with 10 µM construct **22**. Brightfield (top left), GFP-channel (top right), TAMRA-channel (bottom left), overlay (bottom right).

L17E-GFP11(5.4)-dextran-TAMRA **22,** 15 and 10 µM

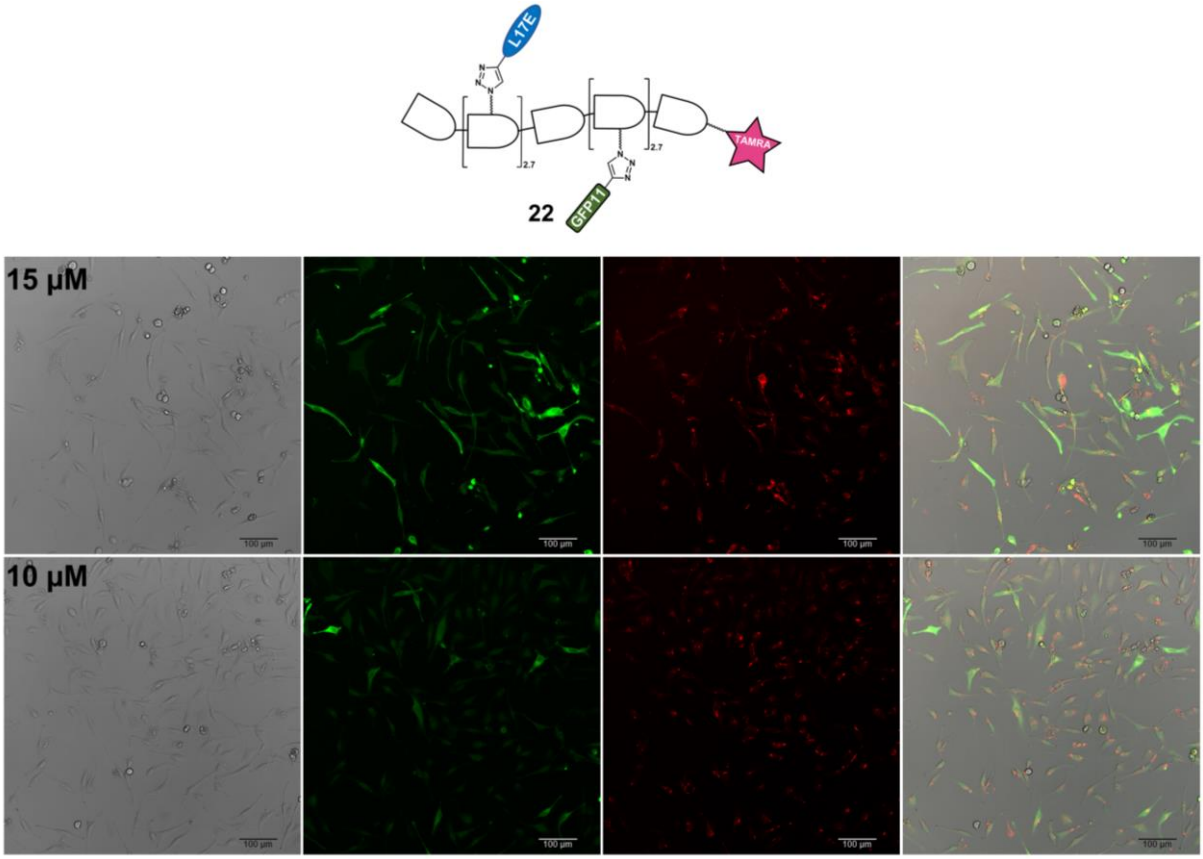

Figure S7: Live-cell CLSM images (20x) of HeLa cells treated with 15 µM construct **22** (top) and 10 µM construct **22** (bottom).

GFP11-dextran-TAMRA **23,** 10 µM

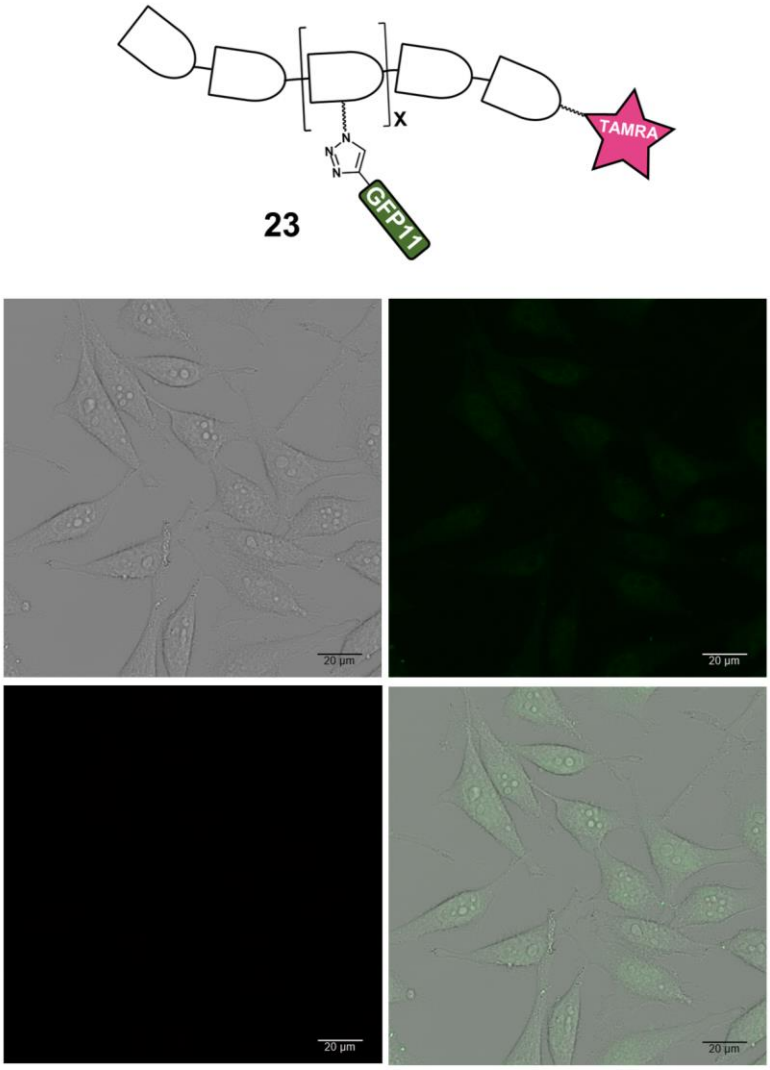

Figure S8: Live-cell CLSM images (20x) of HeLa cells treated with 10 µM construct **23**. Brightfield (top left), GFP-channel (top right), TAMRA-channel (bottom left), overlay (bottom right).

40.5 µM GFP11 **24,** 40.5 µM L17E **8:**

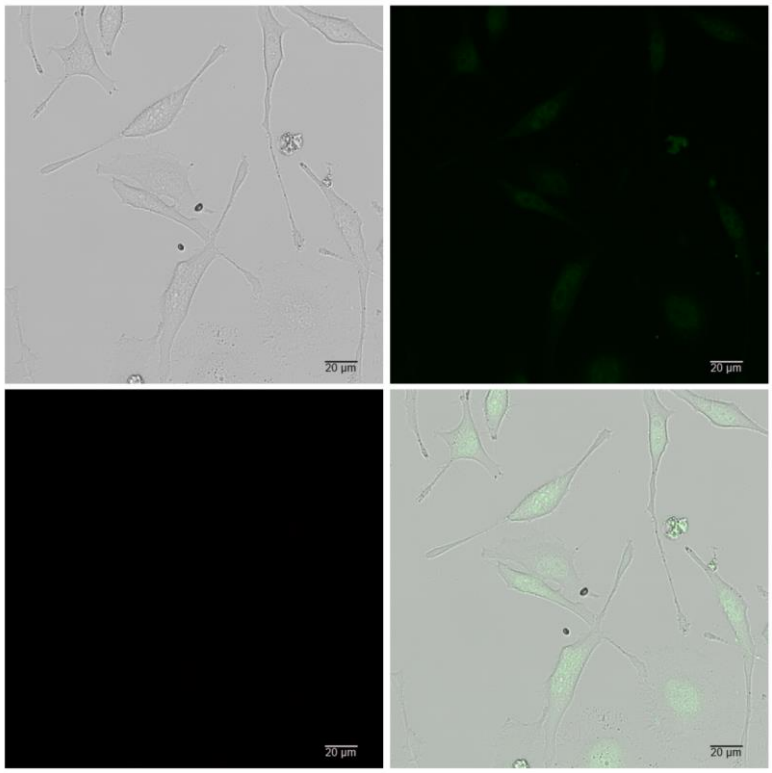

Figure S9: Live-cell CLSM images (20x) of HeLa cells co-incubated with 40.5 µM construct GFP11 **24** and 40.5 µM L17E **8**. Brightfield (top left), GFP-channel (top right), TAMRA-channel (bottom left), overlay (bottom right).

PBS control:

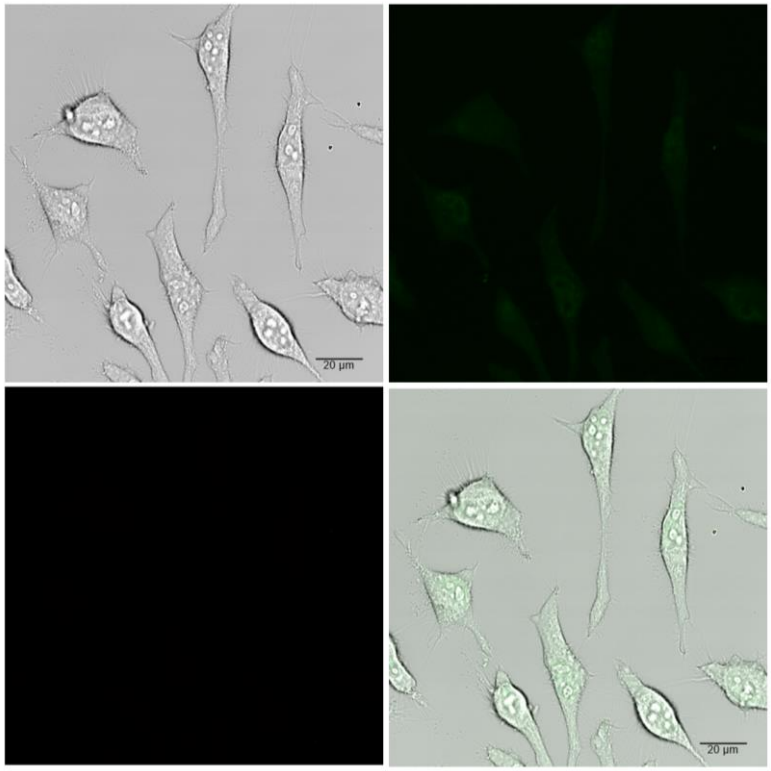

Figure S10: Live-cell CLSM images (20x) of HeLa cells treated with PBS as control. Brightfield (top left), GFP-channel (top right), TAMRA-channel (bottom left), overlay (bottom right).

1.2.2 Cell viability assay of construct **22**

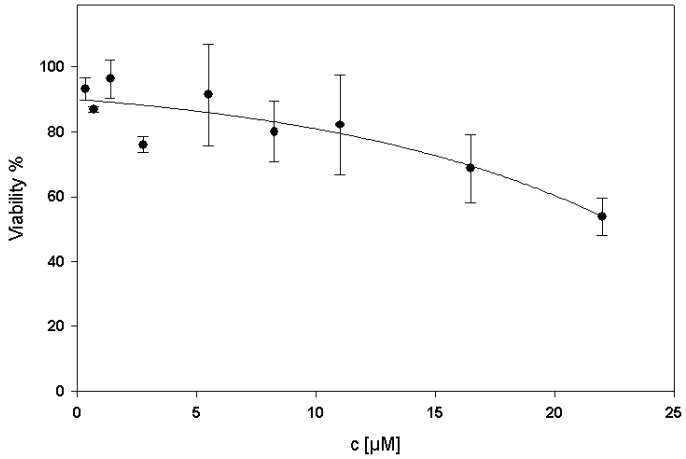

Figure S11: Cell-viability assay of construct **22** in HeLa cells. Cells were incubated for 1h with a serial dilution of **22** in serum free medium, followed by further incubation for 24 h in medium only.

1.2.3 FACS analysis

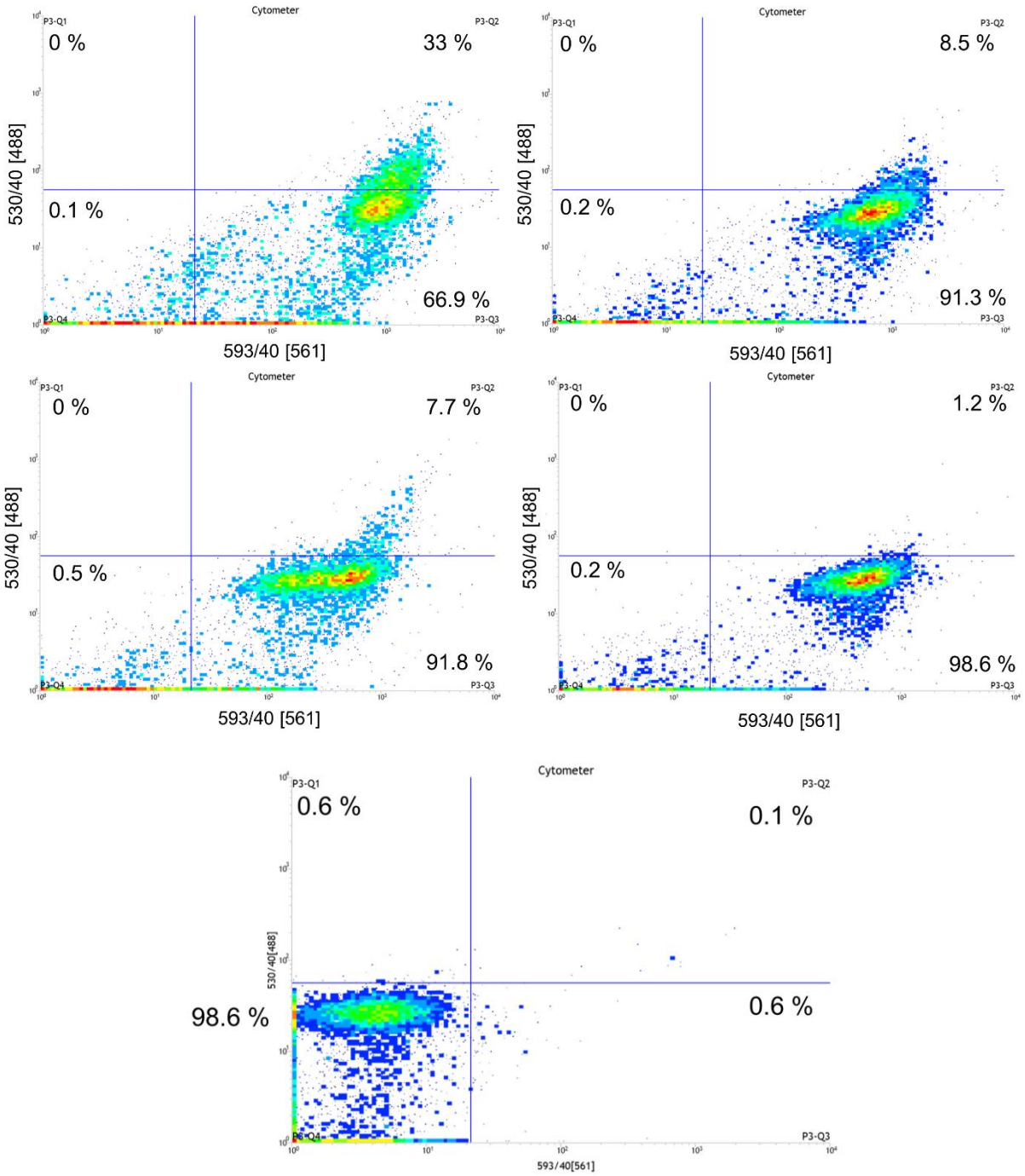

Figure S12: FACS analysis of construct **22** with TAMRA-fluorescence channel on the x-axis and GFP-fluorescence channel on the y-axis. 10 µM (top left), 7.5 µM (top right), 5 µM (middle left), 2.5 µM (middle right) and PBS control (bottom).

1.3 L17E-PNA(10.5)-dextran **29** uptake in HeLa-eGFP654 cells

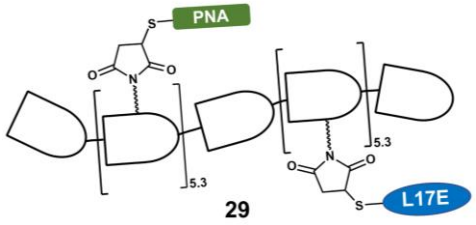

29

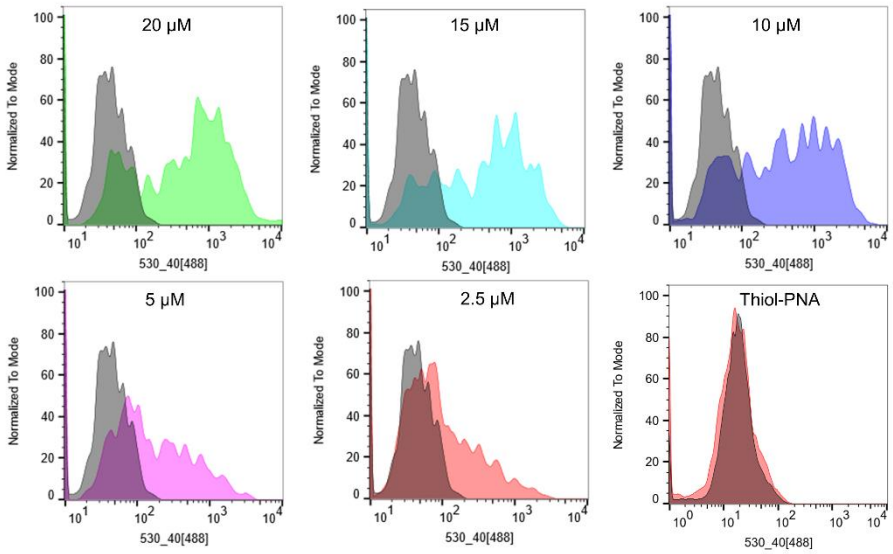

Figure S13: FACS analysis with GFP-fluorescence channel on the x-axis, grey histograms represent cells treated only with PBS. L17E-PNA(10.5)-dextran **29** (top left to bottom middle), thiol-PNA **28** (20 µM, bottom right). Please note that the experiment with thiol-PNA was performed independently from the experiment with construct **29**.

1.4 Uncaging studies of DEACM protected L17E-3PG **34** and L17E-5PG **35**

Uncaging studies were performed by irradiation of peptide solutions (10 µM in PBS-buffer at pH = 7.0 with 10% DMSO) at 405 nm and room temperature. Aliquots were analyzed by analytical RP-HPLC at 380 nm as a function of time. After 120 s over 95% of the starting material had been consumed (Figure 2) and the fully deprotected product could be identified *via* mass spectrometry (Figure S15 and Figure S17).

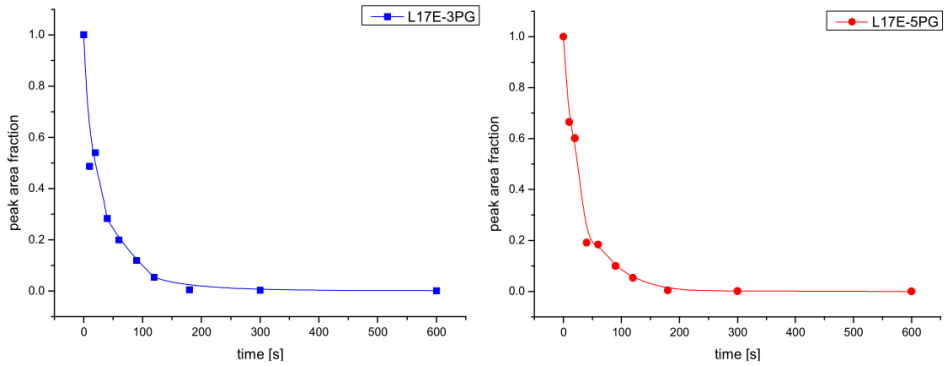

Figure S14: Time course of photolysis of photocaged peptides L17E-3PG (left) and L17E-5PG (right) as peak area fractions of the starting materials.

1.4.1 Uncaging of L17E-3PG **34**

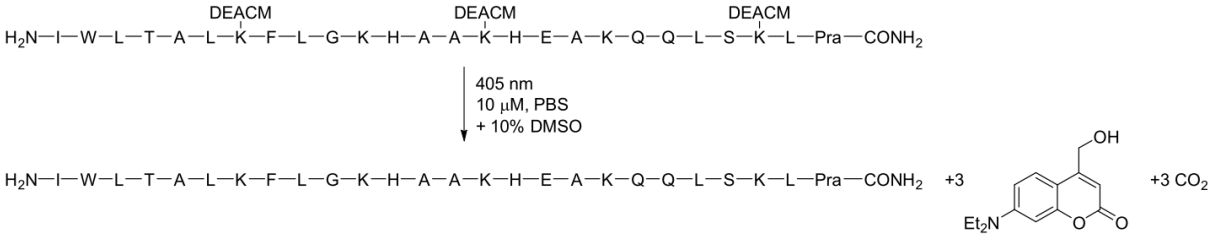

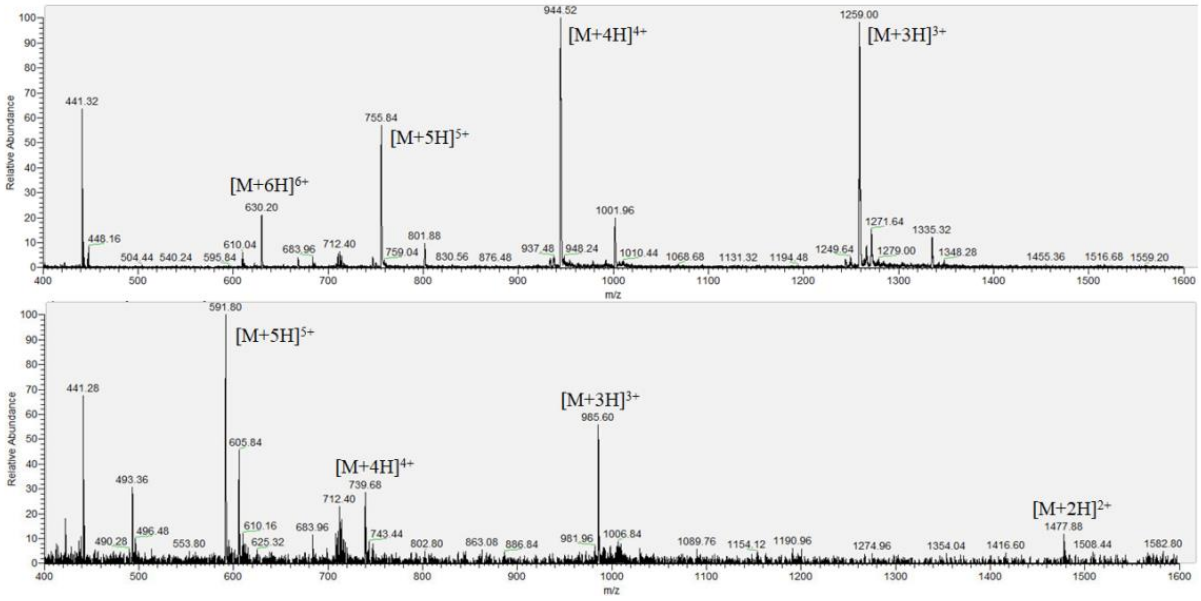

Figure S15: LC-MS mass spectrum of the uncaging of L17E-3PG after 0 s (top) and 600 s (bottom). Masses correspond to the fully caged and uncaged peptide, respectively.

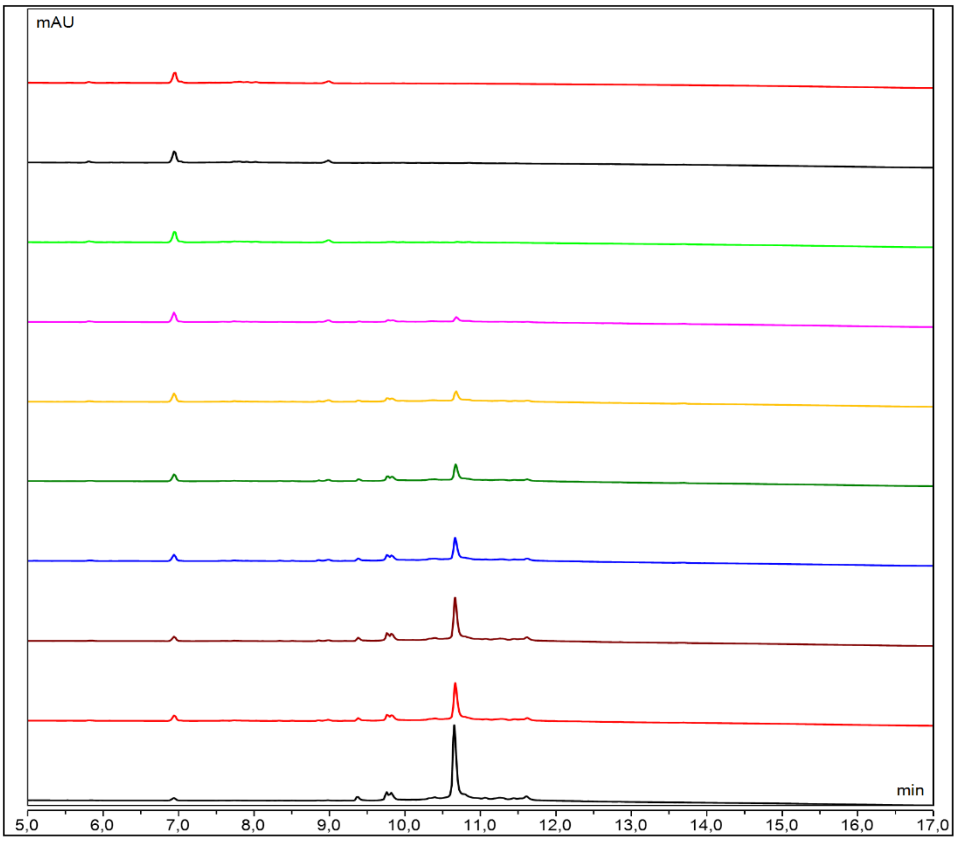

Figure S16: Excerpt of the analytical RP-HPLC chromatogram of the uncaging of L17E-3PG. Gradient: 5-95% B in 15 min, detection at 380 nm. Analysis of aliquots (from bottom to top) after 0, 10, 20, 40, 60, 90, 120, 180, 300 and 600 s. The peak at 10.65 min corresponds to the starting material, while the peak at 6.95 min corresponds to DEACM-OH.

1.4.2 Uncaging of L17E-5PG **35**

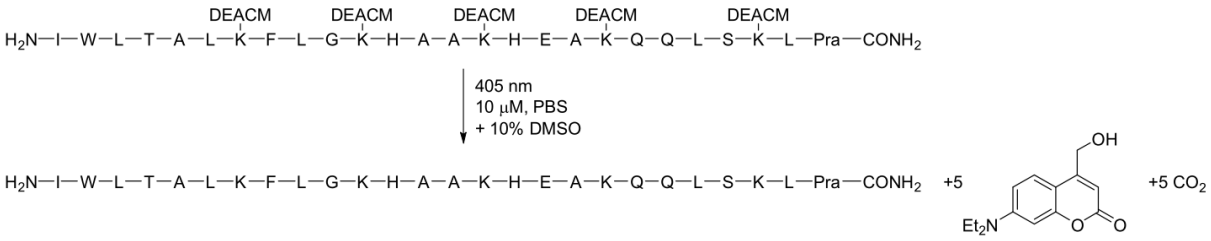

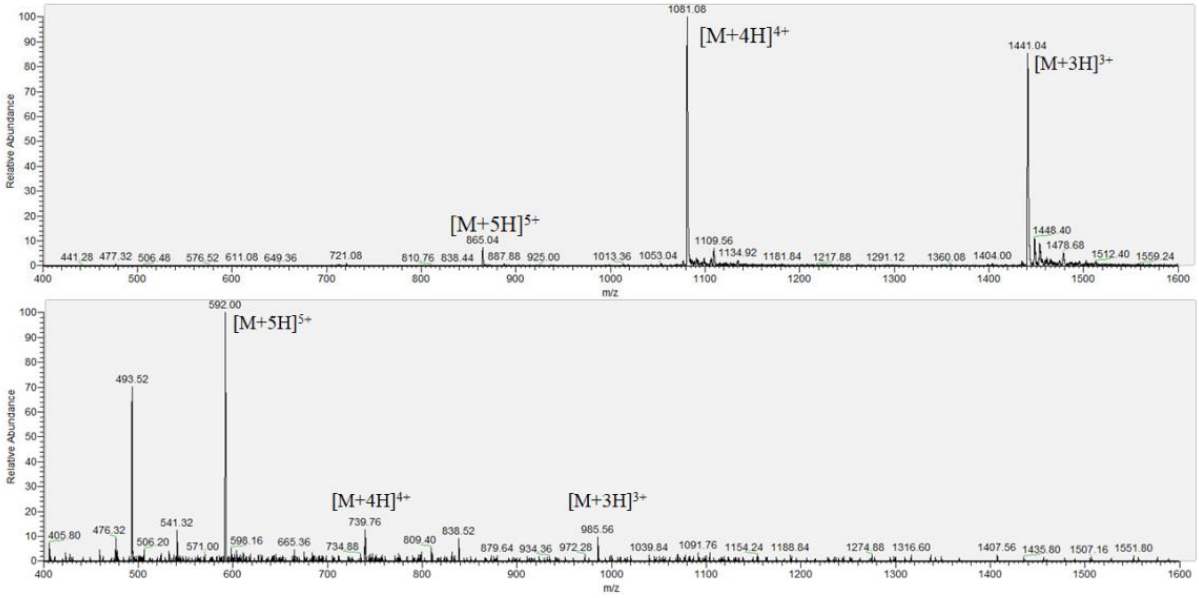

Figure S17: LC-MS mass spectrum of the uncaging of L17E-5PG after 0 s (top) and 600 s (bottom). Masses correspond to the fully caged and uncaged peptide, respectively.

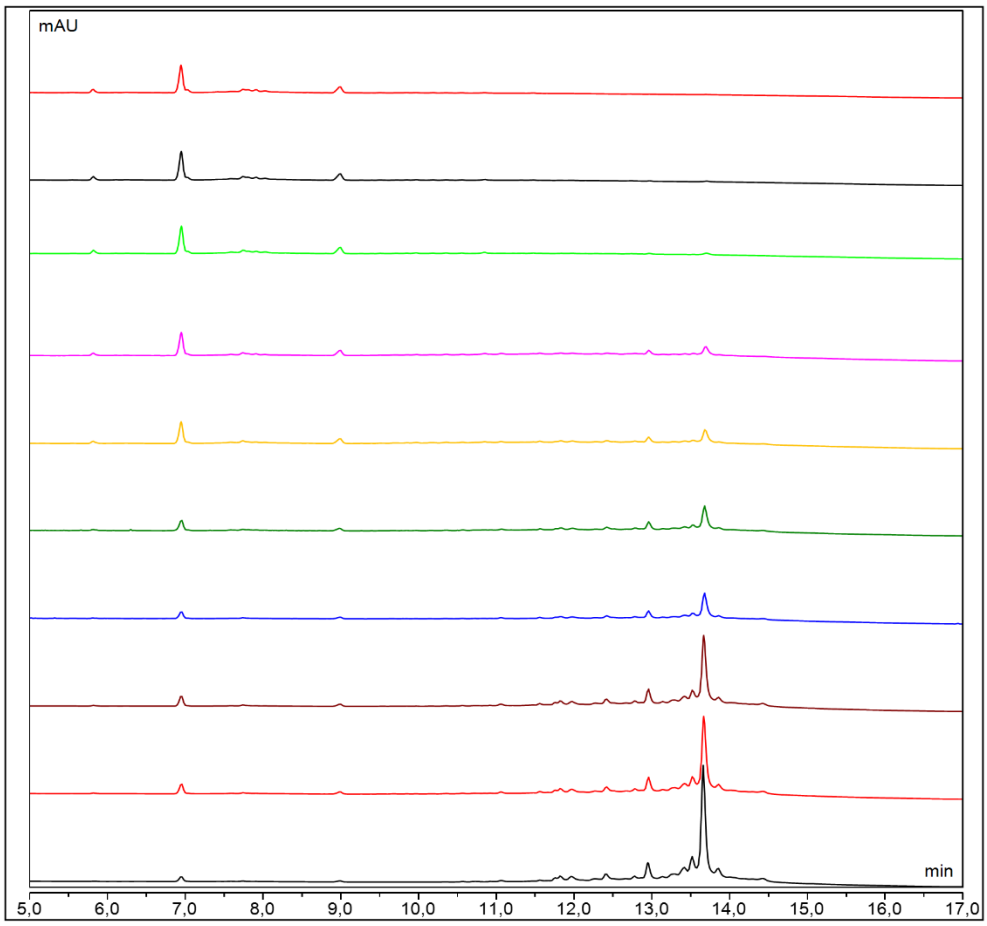

Figure S18: Excerpt of the analytical RP-HPLC chromatogram of the uncaging of L17E-5PG. Gradient: 5-95% B in 15 min, detection at 380 nm. Analysis of aliquots (from bottom to top) after 0, 10, 20, 40, 60, 90, 120, 180, 300 and 600 s. The peak at 13.66 min corresponds to the starting material, while the peak at 6.95 min corresponds to DEACM-OH.

2 Experimental Part – Synthetical Details and Analytical Data

2.1 Synthesis of L17E **8**

Sequence: IWLTALKFLGKHAAKHEAKQQLSKL-NH_2

Chemical Formula: $C_{134}H_{220}N_{38}O_{31}$

M_W: 2859.47 g/mol

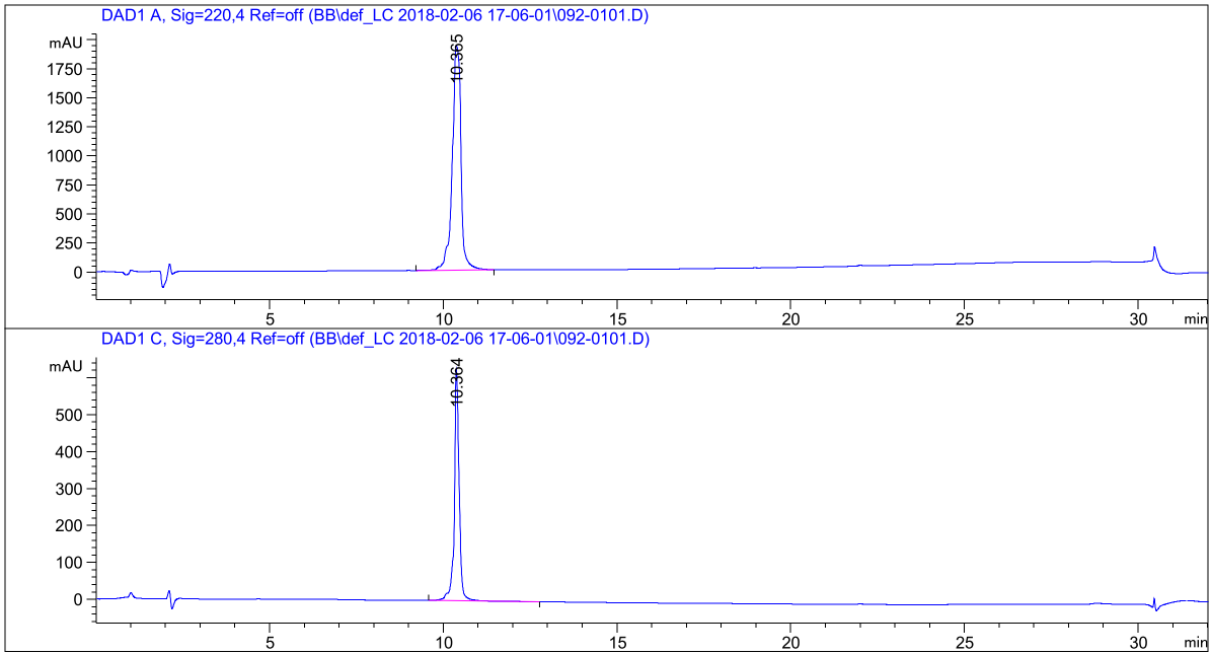

Figure S19: Analytical RP-HPLC chromatogram of purified L17E peptide, 20 to 100% B (gradient 20 min), 220, 280 nm, RT = 10.365 min.

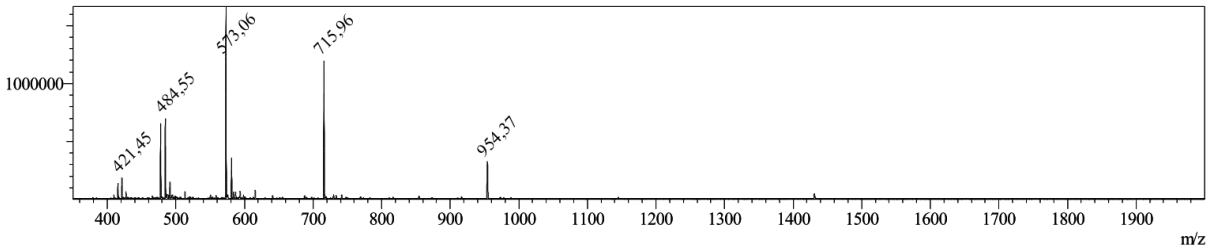

Figure S20: MS (ESI) calculated: $[M+H]^+$ = 2859.47; $[M+3H]^{3+}$ = 954.16; $[M+4H]^{4+}$ = 715.87; $[M+5H]^{5+}$ = 572.89; observed: $[M+3H]^{3+}$ = 954.37; $[M+4H]^{4+}$ = 715.96; $[M+5H]^{5+}$ = 573.06.

2.2 Synthesis of GFP11 **24**

Sequence: RDHMVLHEYVNAAGIT-NH_2

Chemical Formula: $C_{79}H_{125}N_{25}O_{23}S$

M_W: 1825.06 g/mol

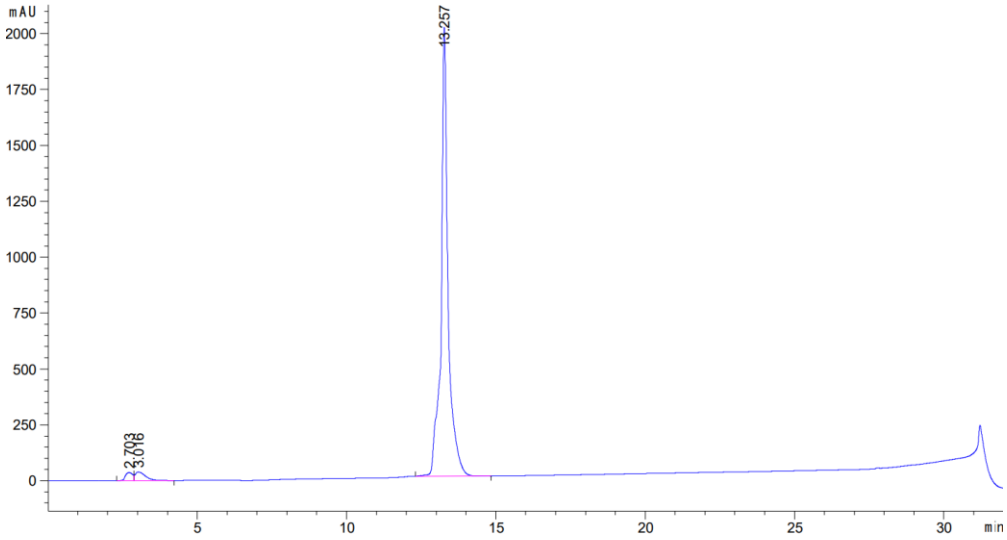

Figure S21: Analytical RP-HPLC chromatogram of purified GFP11 peptide, 10 to 60% B (gradient 20 min), 220 nm, RT = 13.257 min.

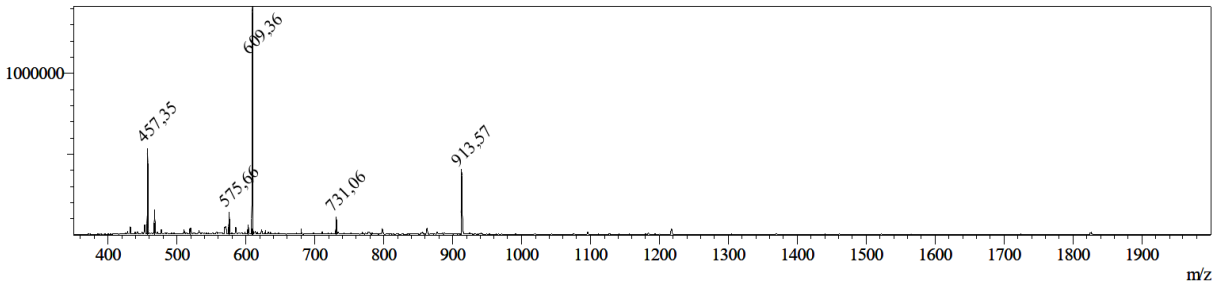

Figure S22: MS (ESI) calculated: $[M+2H]^{2+}$ = 913.53, $[M+3H]^{3+}$ = 609.35, $[M+4H]^{4+}$ = 457.27; observed: $[M+2H]^{2+}$ = 913.57; $[M+3H]^{3+}$ = 609.36; $[M+4H]^{4+}$ = 457.35.

2.3 Synthesis of L17E-Cys **14**

Sequence: IWLTALKFLGKHAAKHEAKQQLSKLC-NH_2

Chemical Formula: $C_{137}H_{225}N_{39}O_{32}S$

M_W: 2962.61 g/mol

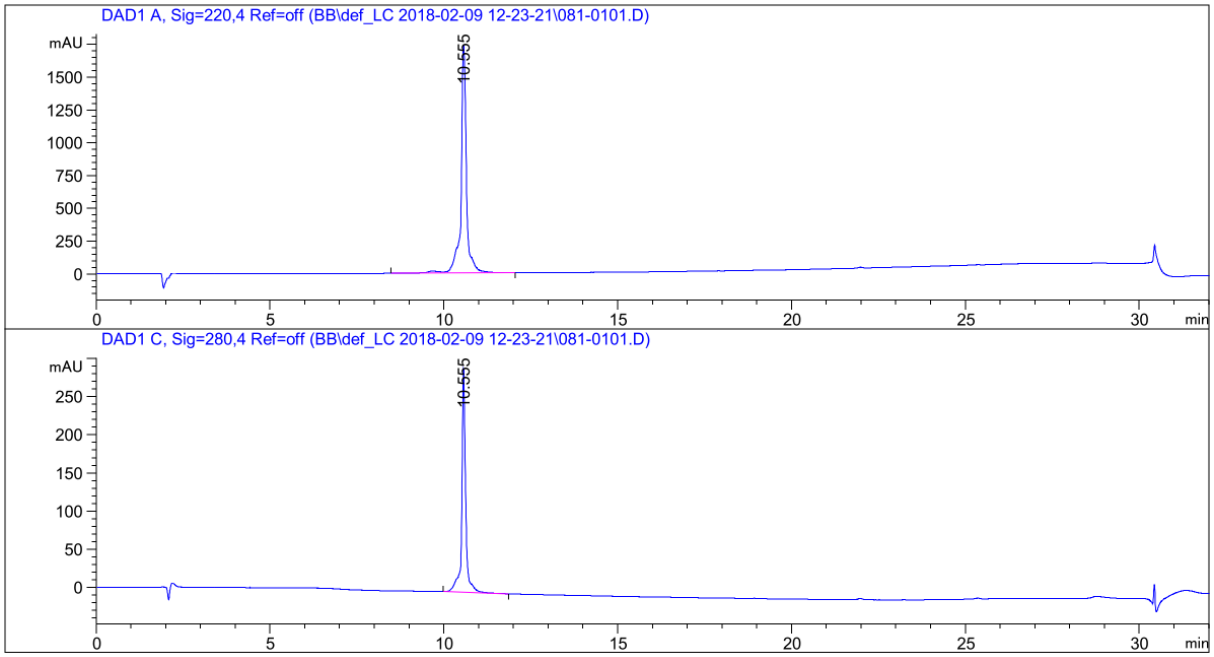

Figure S23: Analytical RP-HPLC chromatogram of purified L17E-Cys peptide, 20 to 100% B (gradient 20 min), 220, 280 nm, RT = 10.555 min.

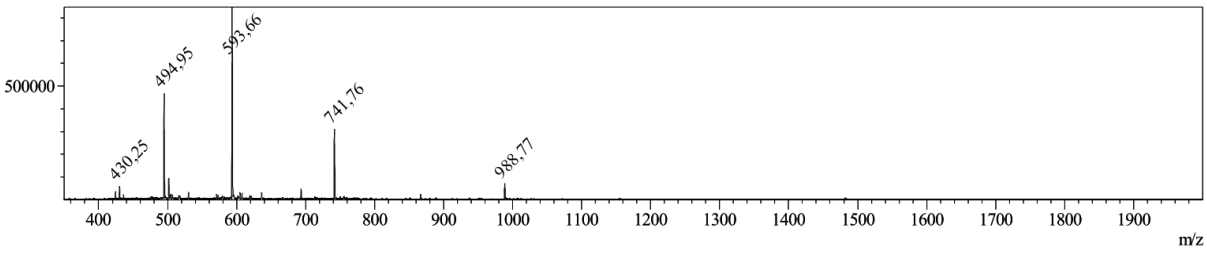

Figure S24: MS (ESI) calculated: $[M+H]^+$ = 2962.61; $[M+3H]^{3+}$ = 988.53; $[M+4H]^{4+}$ = 741.65; $[M+5H]^{5+}$ = 593.52; $[M+6H]^{6+}$ = 494.76; observed: $[M+3H]^{3+}$ = 988.77; $[M+4H]^{4+}$ = 741.76; $[M+5H]^{5+}$ = 593.66; $[M+6H]^{6+}$ = 494.95.

2.4 Synthesis of L17E-Pra **1**

Sequence: IWLTALKFLGKHAAKHEAKQQLSKL-Pra-NH_2

Chemical Formula: $C_{139}H_{225}N_{39}O_{32}$

Molecular Weight: 2954.57 g/mol

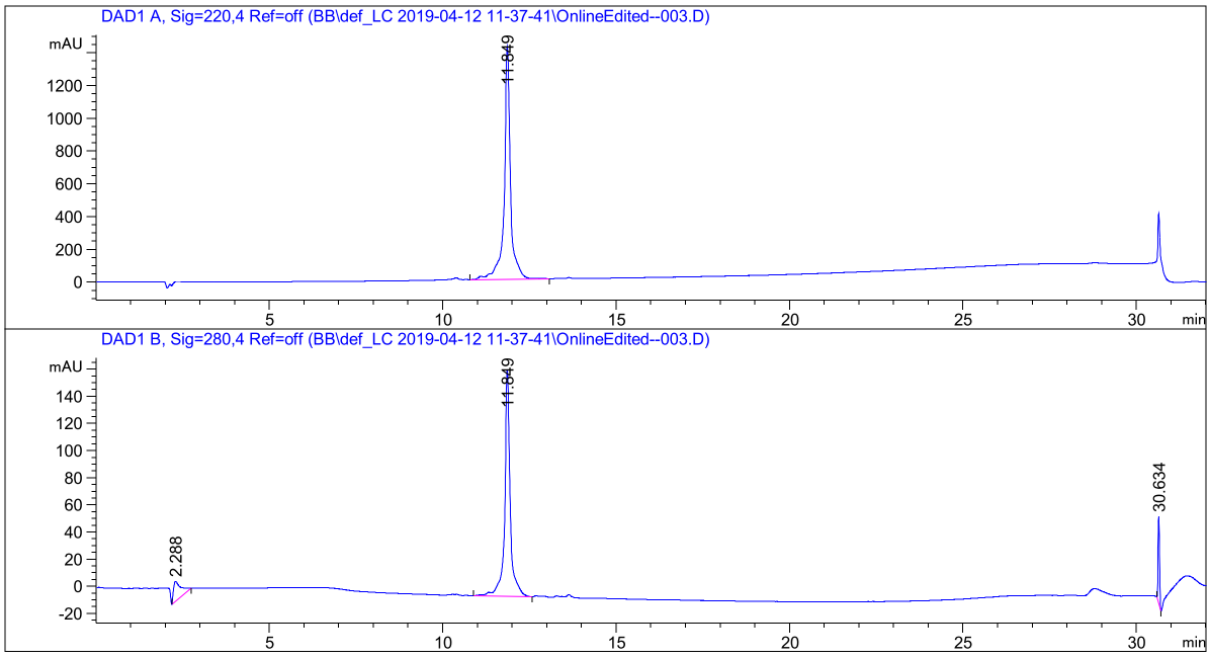

Figure S25: Analytical RP-HPLC chromatogram of purified L17E-Pra peptide, 20 to 100% B (gradient 20 min), 220, 280 nm, RT = 11.849 min.

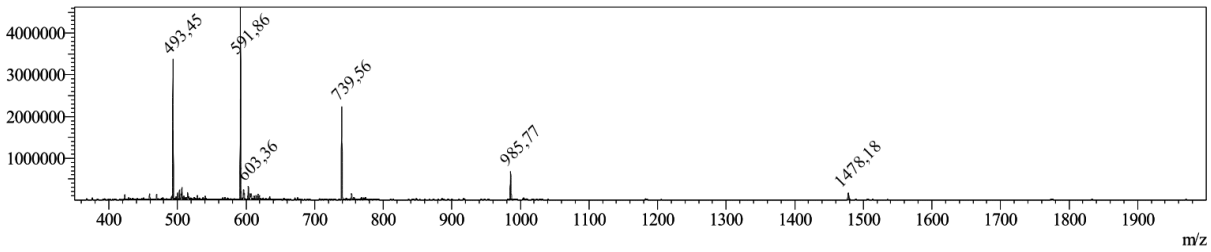

Figure S26: MS (ESI) calculated: $[M+H]^{+}$ = 2955.57; $[M+2H]^{2+}$ = 1478.29; $[M+3H]^{3+}$ = 985.86; $[M+4H]^{4+}$ = 739.64; $[M+5H]^{5+}$ = 591.91; $[M+6H]^{6+}$ = 493.43; observed: $[M+2H]^{2+}$ = 1478.18; $[M+3H]^{3+}$ = 985.77; $[M+4H]^{4+}$ = 739.56; $[M+5H]^{5+}$ = 591.86; $[M+6H]^{6+}$ = 493.45.

2.5 Synthesis of alkyne-GFP 11 **21**

Chemical Formula: $C_{94}H_{145}N_{29}O_{30}S$

M_w = 2193.40 g/mol

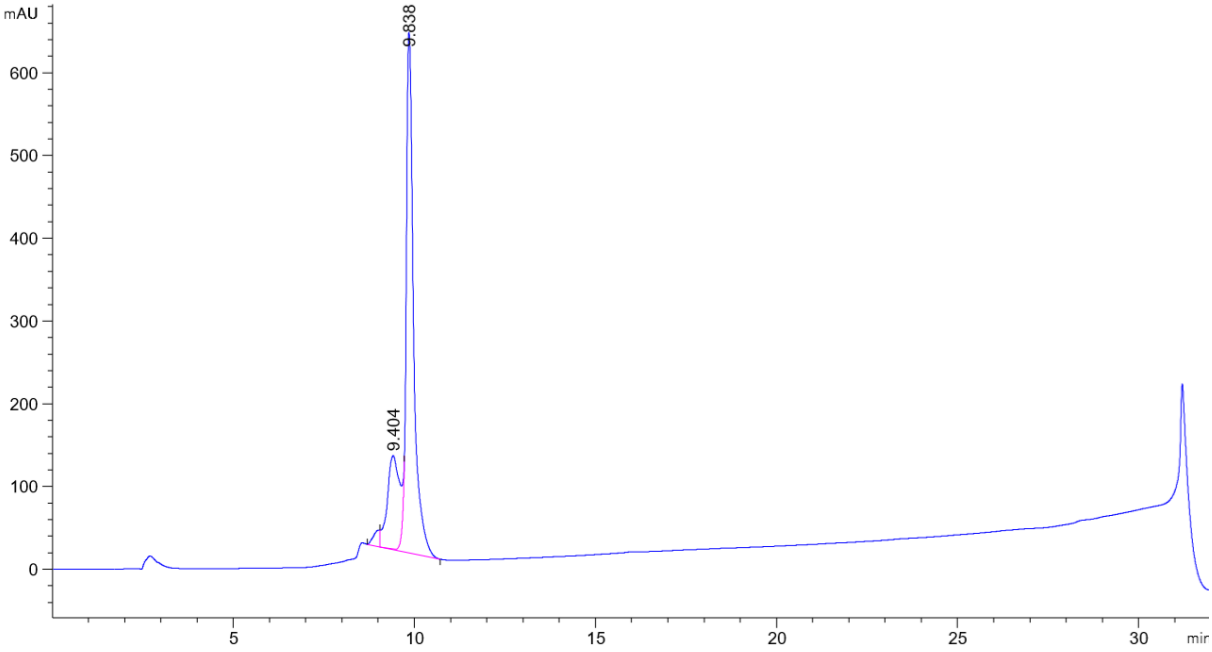

Figure S27: Chromatographic trace of purified alkyne-GFP11 peptide, 20 to 80% B (gradient 20 min), λ = 220 nm, RT = 9.838 min.

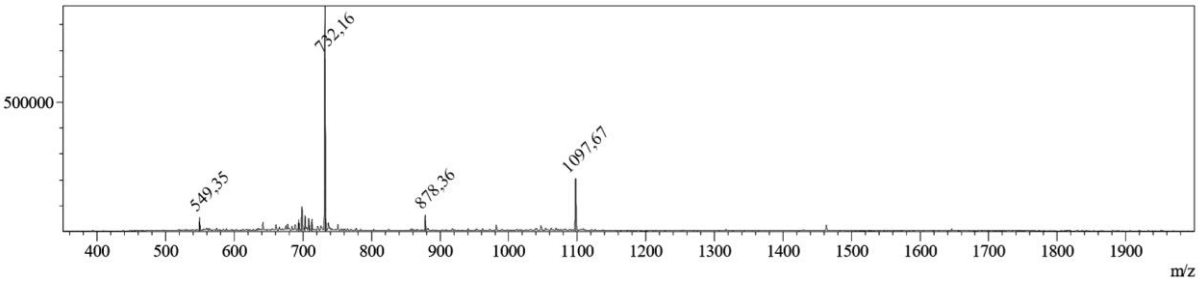

Figure S28: MS (ESI) calculated: $[M+2H]^{2+}$ = 1097.70, $[M+3H]^{3+}$ = 732.13, $[M+4H]^{4+}$ = 549.35; observed: $[M+2H]^{2+}$ = 1097.67; $[M+3H]^{3+}$ = 732.16; $[M+4H]^{4+}$ = 549.35.

2.6 Synthesis of thiol-PNA **28**

2.6.1 Synthesis of S-Trityl-3-mercaptopropionic acid **25**

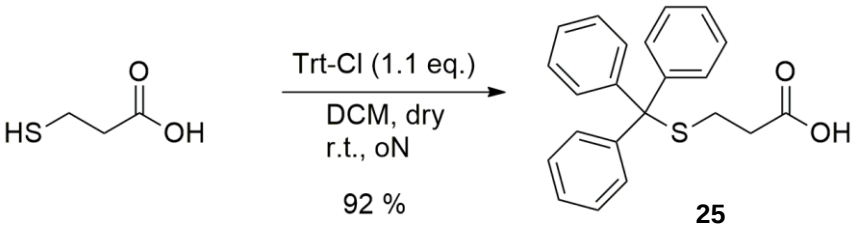

Figure S29: Synthesis of S-Trityl-3-mercaptopropionic acid.

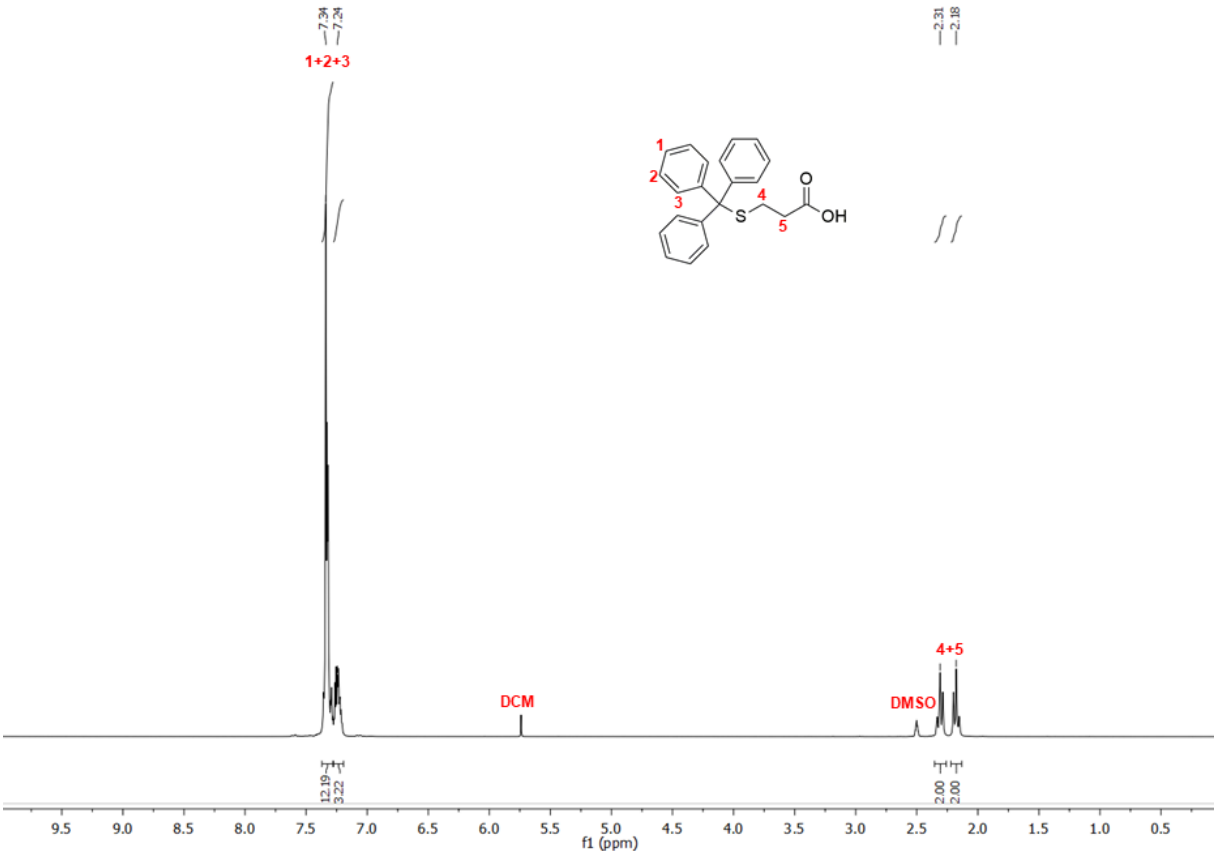

Figure S30: ^{1}H-NMR of S-Trityl-3-mercaptopropionic acid.

^{1}H NMR (300 MHz, DMSO-d$_6$) δ = 7.38 – 7.28 (m, 12H), 7.28 – 7.19 (m, 3H), 2.36 – 2.26 (m, 2H), 2.24 – 2.13 (m, 2H).

2.6.2 Synthesis of thiol-PNA **28**

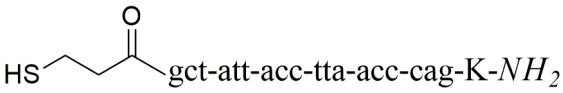

Chemical Formula: $C_{201}H_{258}N_{102}O_{56}S$

M_w = 5030.91 g/mol

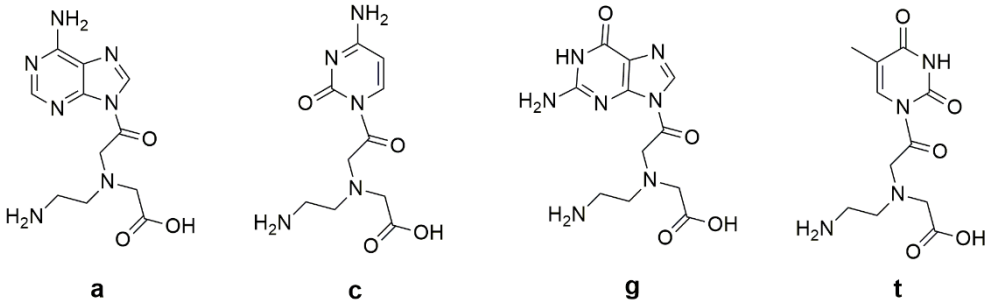

Figure S31: Structure of the four PNA monomers present in thiol-PNA **28**.

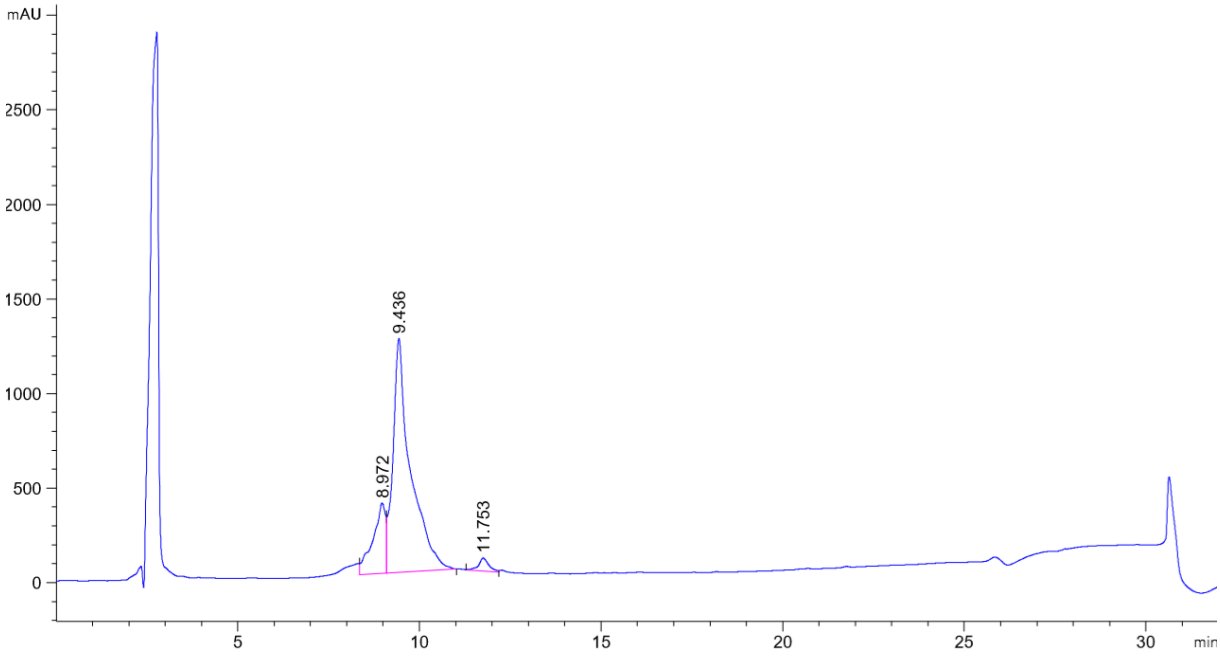

Figure S32: Chromatographic trace of thiol-PNA, 10 to 60 % B (gradient = 20 min), λ = 220 nm, RT = 9.436 min.

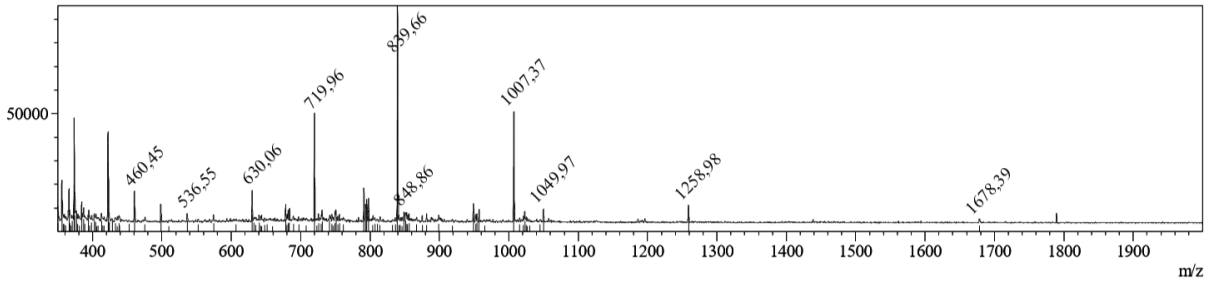

Figure S33: MS (ESI) calculated: $[M+4H]^{4+}$ = 1258.73, $[M+5H]^{5+}$ = 1007.18, $[M+6H]^{6+}$ = 839.49; $[M+7H]^{7+}$ = 719.70, $[M+8H]^{8+}$ = 629.86, observed: $[M+4H]^{4+}$ = 1258.98, $[M+5H]^{5+}$ = 1007.37, $[M+6H]^{6+}$ = 839.66; $[M+7H]^{7+}$ = 719.96, $[M+8H]^{8+}$ = 630.06

2.7 Synthesis of L17E(4.8)-dextran-cadaverine **7**

2.7.1 Synthesis of *N*-(5-aminopentyl)-2-azidoacetamide **4**

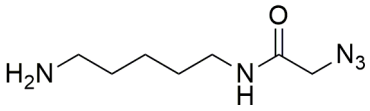

4

m = 0,390g (65 %). MS (ESI) calcd. for $C_7H_{15}N_5O$ $[M+H]^+$ = 186.23, observed: 186.52

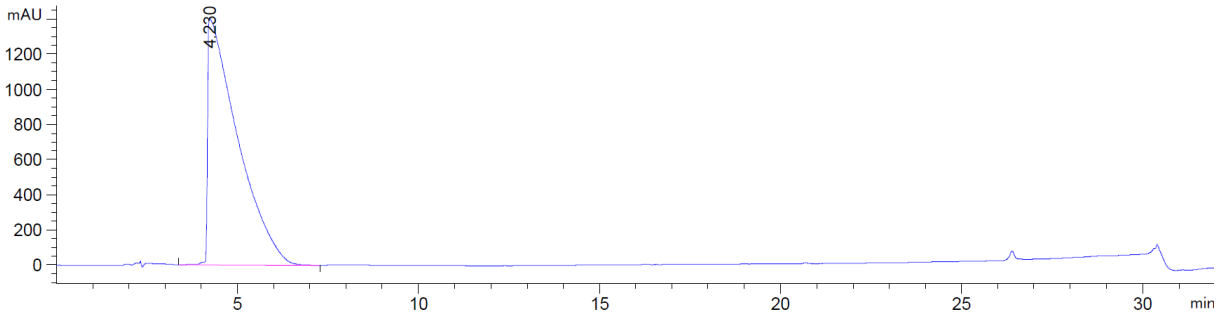

Figure S34: Analytical RP-HPLC chromatogram of purified azide linker **4**, 0 to 80% B (gradient 20 min), 220 nm, RT = 4.230 min.

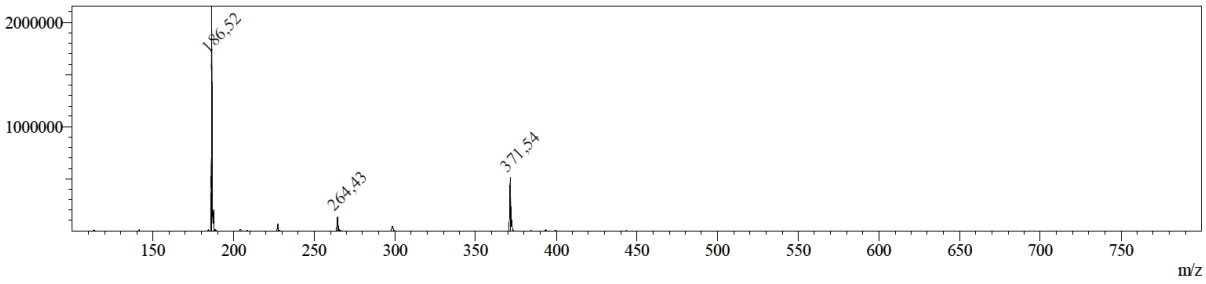

Figure S35: MS (ESI) calculated: $[M+H]^+$ = 186.23, observed: $[M+H]^+$ = 186.52.

2.7.2 Synthesis of N_3(4.8)-dextran-cadaverine **6**

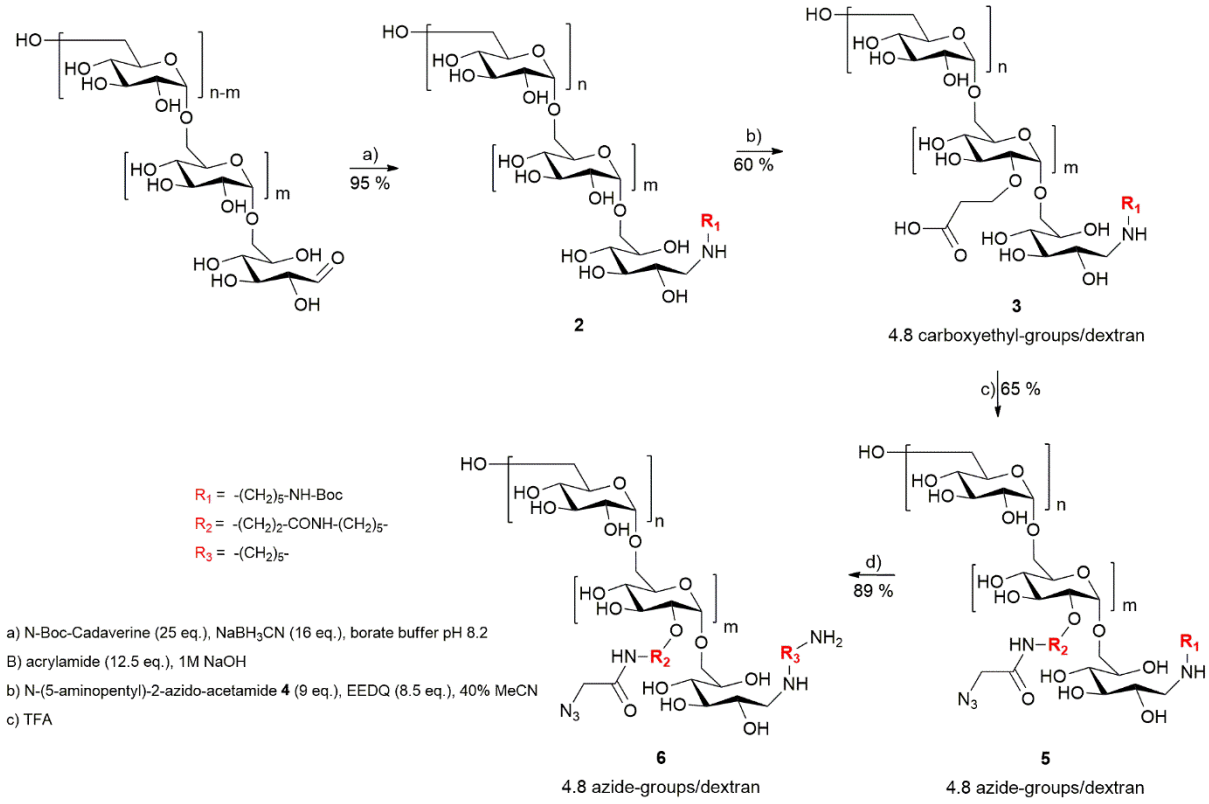

Figure S36: Dextran modification: Carboxyethylation followed by EEDQ activated conjugation of azide linker and subsequent removal of the Boc protection.

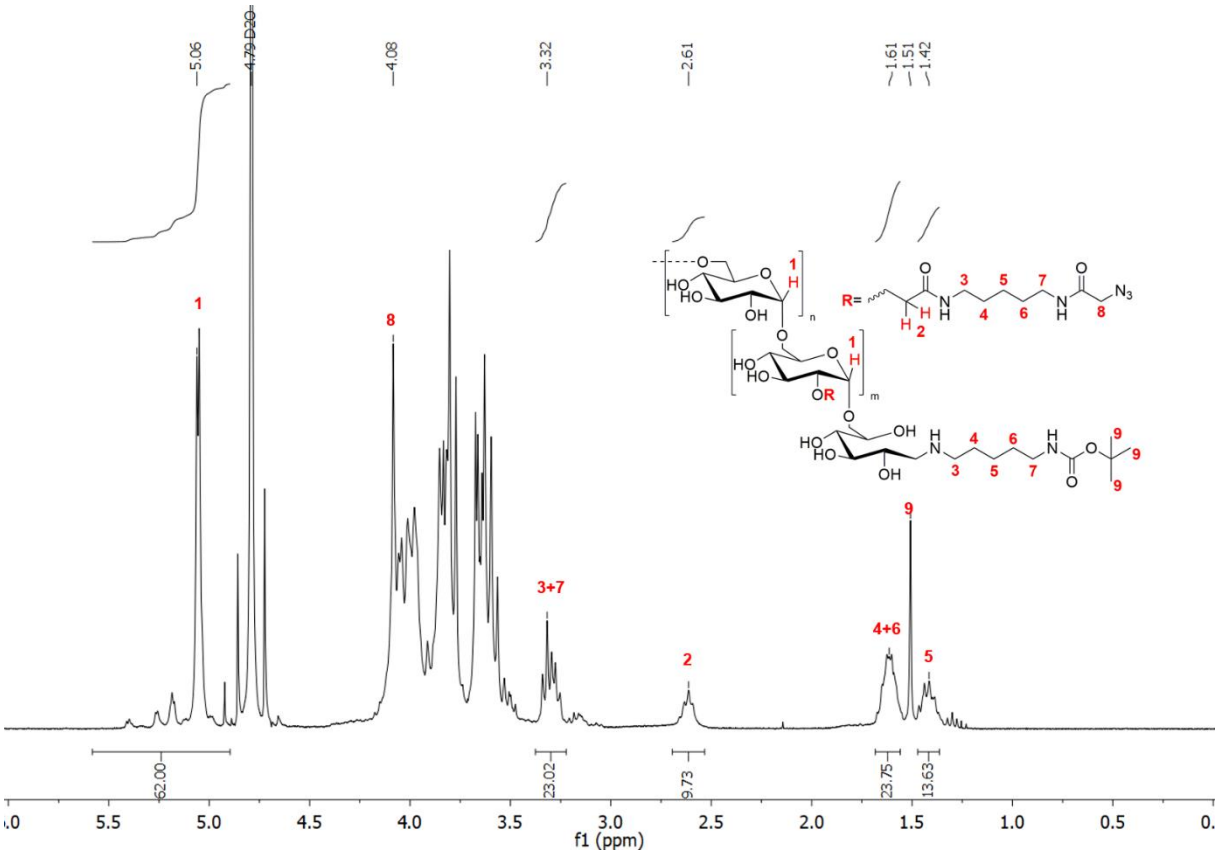

Figure S37: ^{1}H NMR spectrum of N_3(4.8)-dextran-*N*-Boc-cadaverine **5** showing tagged signals used for quantification of carboxyl groups and azide-linker.

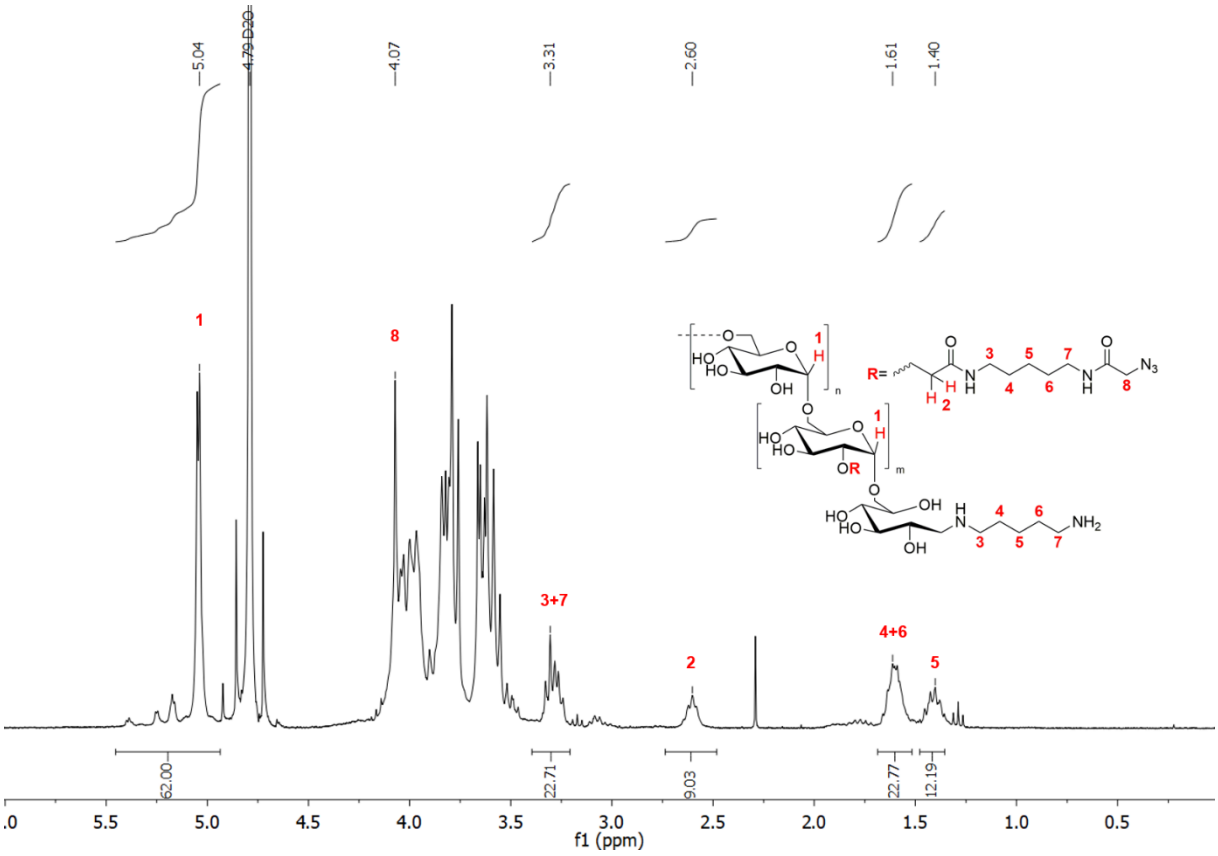

Figure S38: ^{1}H NMR spectrum of N_3(4.8)-dextran-cadaverine **6** showing tagged signals used for quantification of carboxyl groups and azide-linker.

According to the literature,[1] quantification of the azide moieties per dextran was performed *via* ^{1}H NMR spectroscopy using the integrated signals stated in Figure S37 and Figure S38, leading to 4.76 azide moieties per dextran.

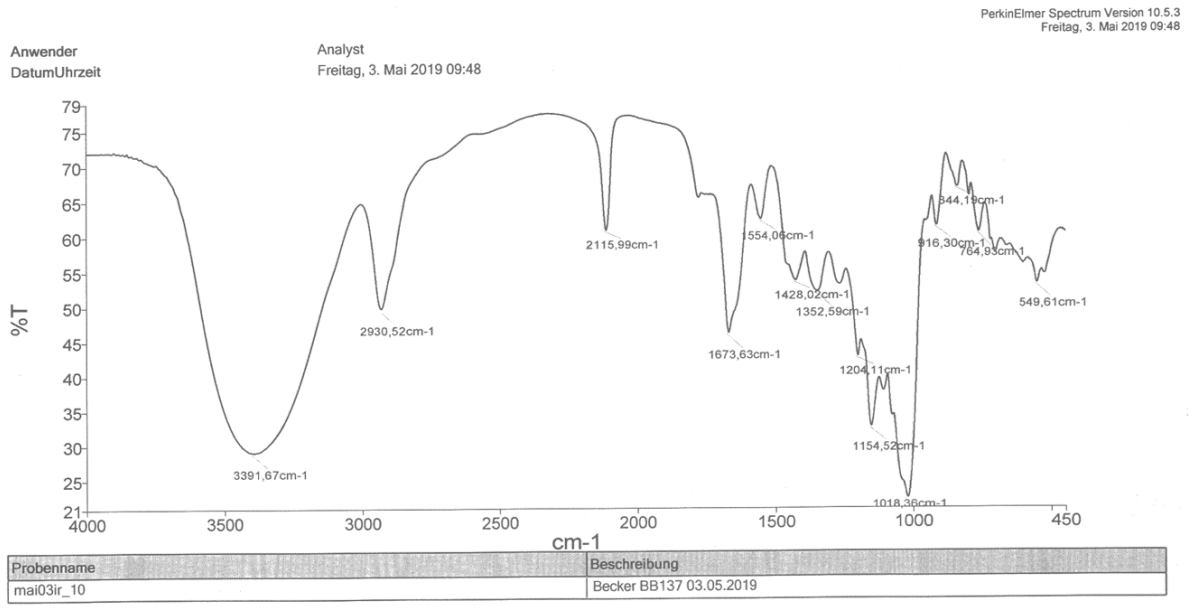

Figure S39: IR spectrum of azide modified dextran-cadaverine **6** showing the corresponding azide band at a wavenumber of 2116 cm^{-1}.

2.7.3 CuAAC of N_3(4.8)-dextran-cadaverine **7** with L17E-Pra **1**

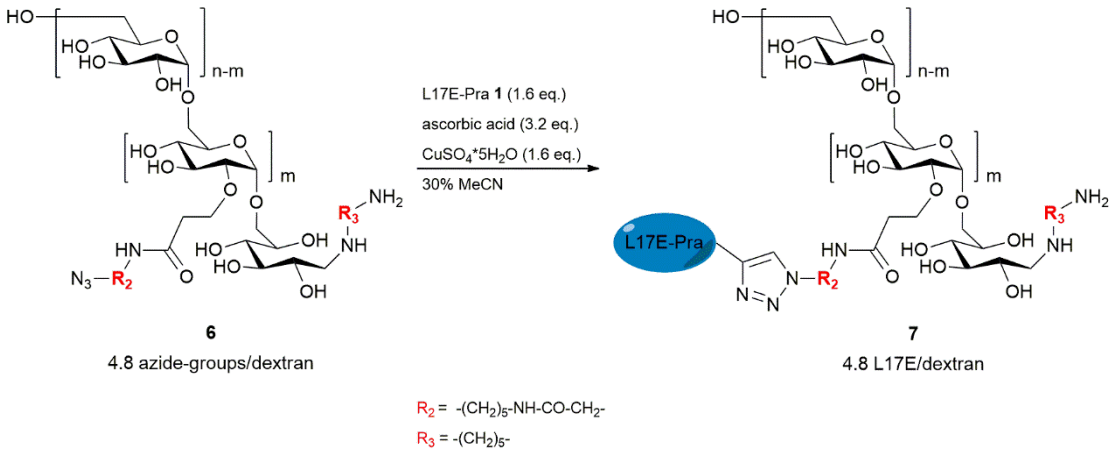

Figure S40: Copper catalyzed azide-alkyne cycloaddition of N3(4.8)-dextran-cadaverine with L17E-Pra. Stated equivalents relating to azide groups per dextran.

The quantitative turnover of the azide-alkyne cycloaddition was controlled *via* IR spectroscopy and UV-Vis photometry. The N_3-dextran-cadaverine starting material showed a characteristic azide-band at a wavenumber of around 2116 cm^{-1} (Figure S39) which disappeared in the product after CuAAC (Figure S41).

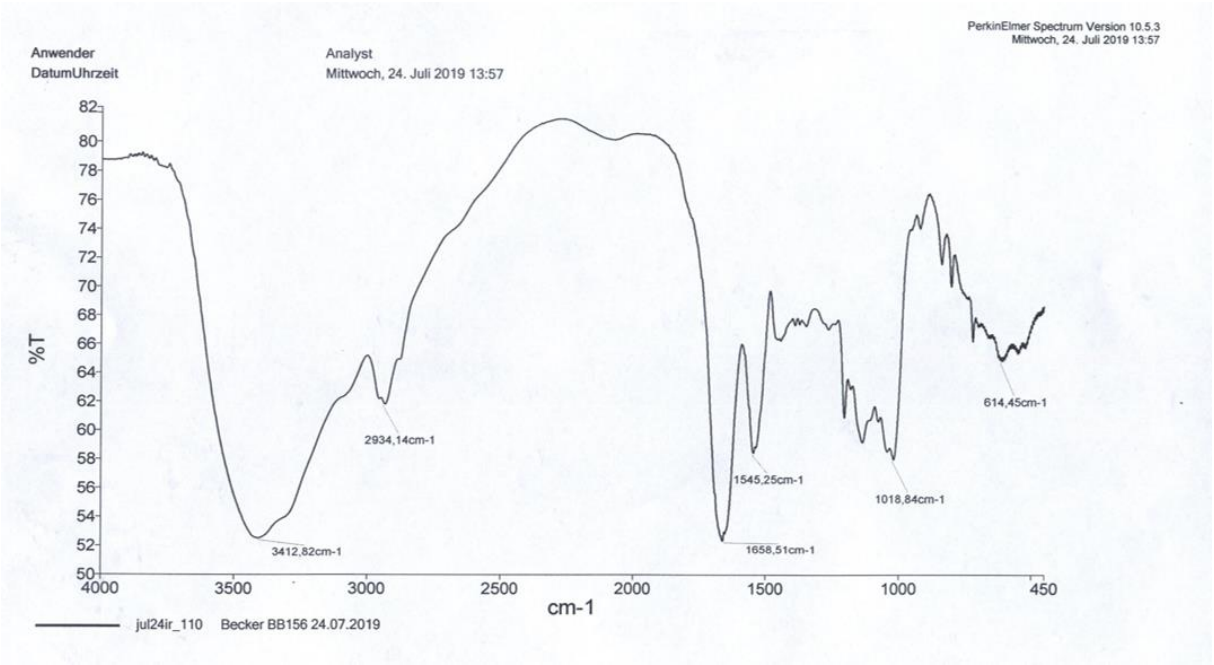

Figure S41: IR spectrum of L17E-dextran-cadaverine **7**. The azide band at a wavenumber of 2116 cm^{-1} disappeared after CuAAC.

2.7.4 UV-Vis photometrical verification of quantitative L17E conjugation *via* CuAAC

In addition to IR spectroscopy, the complete conjugation of L17E-Pra was controlled by UV-Vis photometry. Therefore, a calibration curve of L17E-Pra at a wavelength of 280 nm was generated and the molar extinction coefficient was determined (Figure S42). The absorption at 280 nm of a product sample with known concentration (weighted sample, with assumed molecular weight of quantitative reaction product) was measured and the resultant L17E concentration was calculated according to *Lambert-Beer* law. The ratio of measured L17E concentration to sample concentration gave information about the amount of L17E per dextran. The calculated ratio of 4.86 coincided with the number of addressable azide groups per dextran, determined *via* ^{1}H NMR spectroscopy, and together with the IR spectroscopy indicated the quantitative turnover of CuAAC. Hence, it can be assumed that CuAAC conjugations in subsequent experiments were quantitative as well.

Table S2: Serial dilution of three different samples of L17E-Pra with measured absorbance at 280 nm for determination of the molar extinction coefficient *via* generation of a calibration curve.

c [mmol/L]	A sample 1	A sample 2	A sample 3	**A mean**	standard deviation
0.176	0.612	0.602	0.651	**0.622**	0.021
0.117	0.408	0.402	0.438	**0.416**	0.016
0.078	0.270	0.269	0.291	**0.277**	0.010
0.052	0.181	0.179	0.195	**0.185**	0.007
0.035	0.121	0.120	0.131	**0.124**	0.005
0.023	0.078	0.081	0.087	**0.082**	0.004
0.015	0.051	0.054	0.059	**0.055**	0.003
0.010	0.032	0.035	0.040	**0.036**	0.003
0.007	0.020	0.023	0.028	**0.024**	0.003
0.005	0.021	0.016	0.019	**0.019**	0.002
0.003	0.006	0.010	0.014	**0.010**	0.003

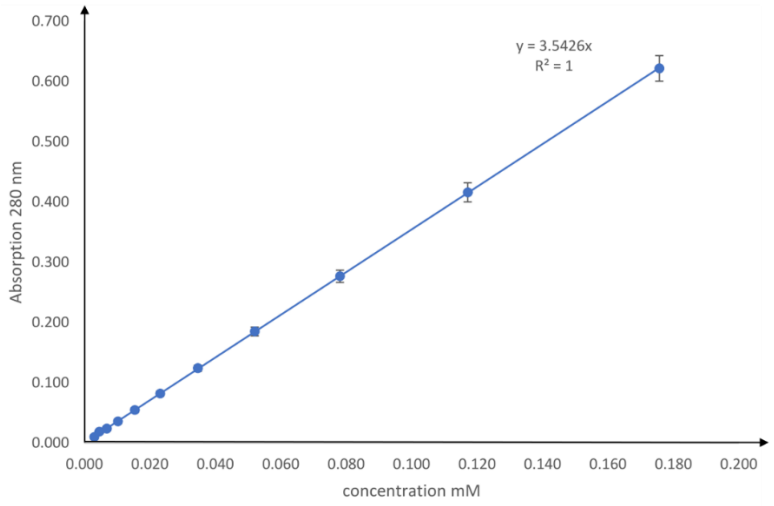

Figure S42: Calibration curve for determination of the molar extinction coefficient (280 nm) of L17E-Pra **1** based on data shown in Table S2. The extinction coefficient of L17E-Pra at 280 nm was determined as 3542.6 L/(mol*cm).

Measurement of absorbance at 280 nm of sample with known concentration and calculation of loading X, L17E per dextran, using Lambert-Beer law:

$$A = \varepsilon * c * d$$

A_{280}(sample) = 0.302

d = 1 cm

ε_{280}(L17E-Pra) = 3542.6 L/(mol*cm)

c(sample) = 1.75 * 10^{-5} mol/L

$$c(L17E) = \frac{A280(sample)}{\varepsilon 280(L17E\text{—}Pra) * d} = \frac{0.302}{3542.6\ \frac{L}{mol * cm} * 1\ cm}$$

$$c(L17E) = 8.5 * 10^{-5}\ \frac{mol}{L}$$

$$X = \frac{L17E}{dextran} = \frac{c(L17E)}{c(sample)} = \frac{8.5 * 10^{-5}\ \frac{mol}{L}}{1.75 * 10^{-5}\ \frac{mol}{L}} = 4.86$$

The photometric determination of a loading of 4.86 L17E per dextran matched the quantification of azide groups per dextran *via* ^{1}H NMR spectroscopy.

2.8 Synthesis of TAMRA-L17E(3.8)-dextran-*N*-Boc-cadaverine **16**

2.8.1 Synthesis of *N*-(2-aminoethyl)maleimide **12**

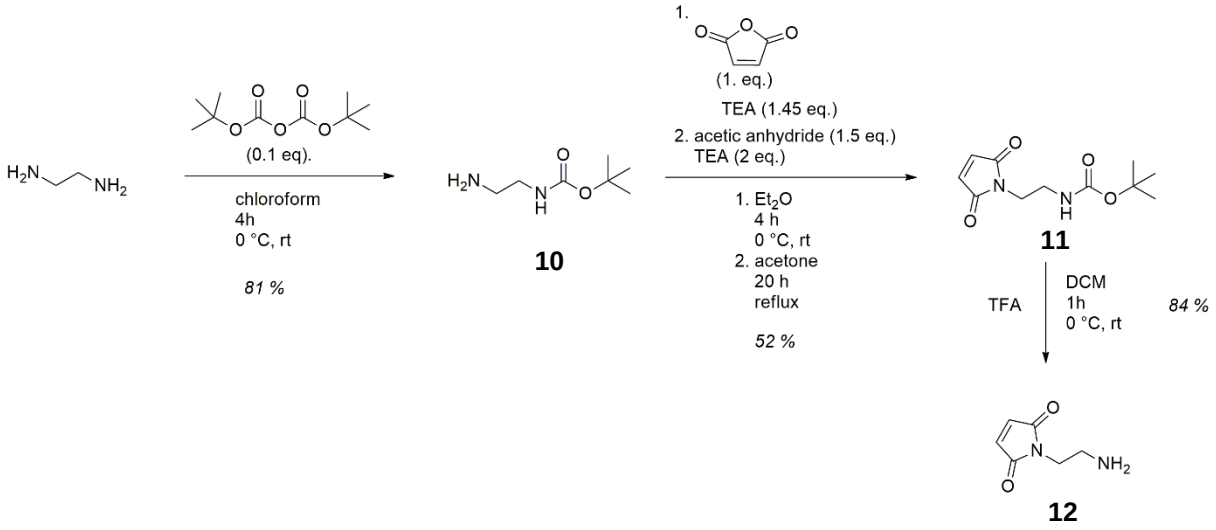

Figure 43: Synthetic approach to maleimide-linker **12.**

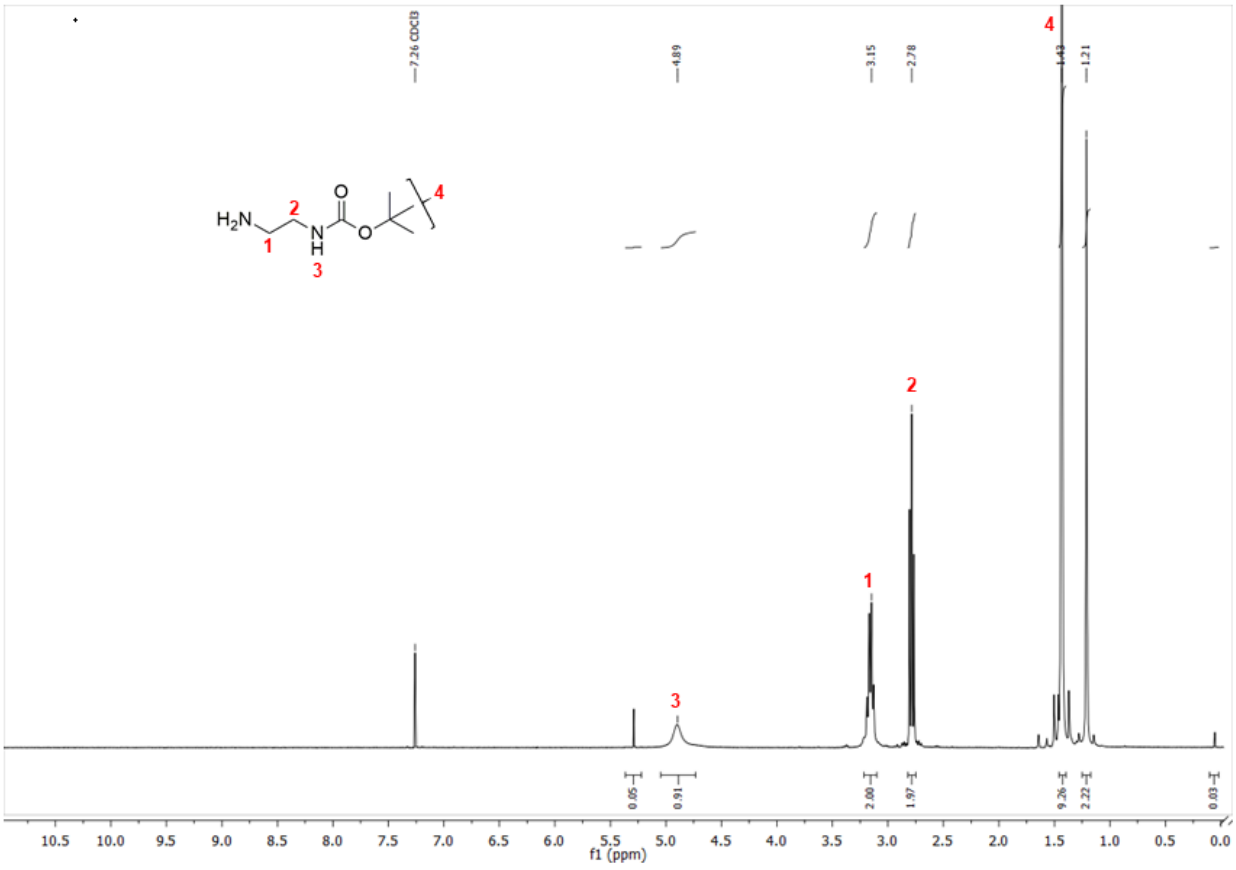

Figure 44: ^{1}H NMR spectrum of *N*-Boc-ethylendiamine **10.**

^{1}H NMR (300 MHz, Chloroform-d) δ =4.89 (s, 1H), 3.26 – 3.06 (m, 2H), 2.88 – 2.70 (m, 2H), 1.43 (s, 9H).

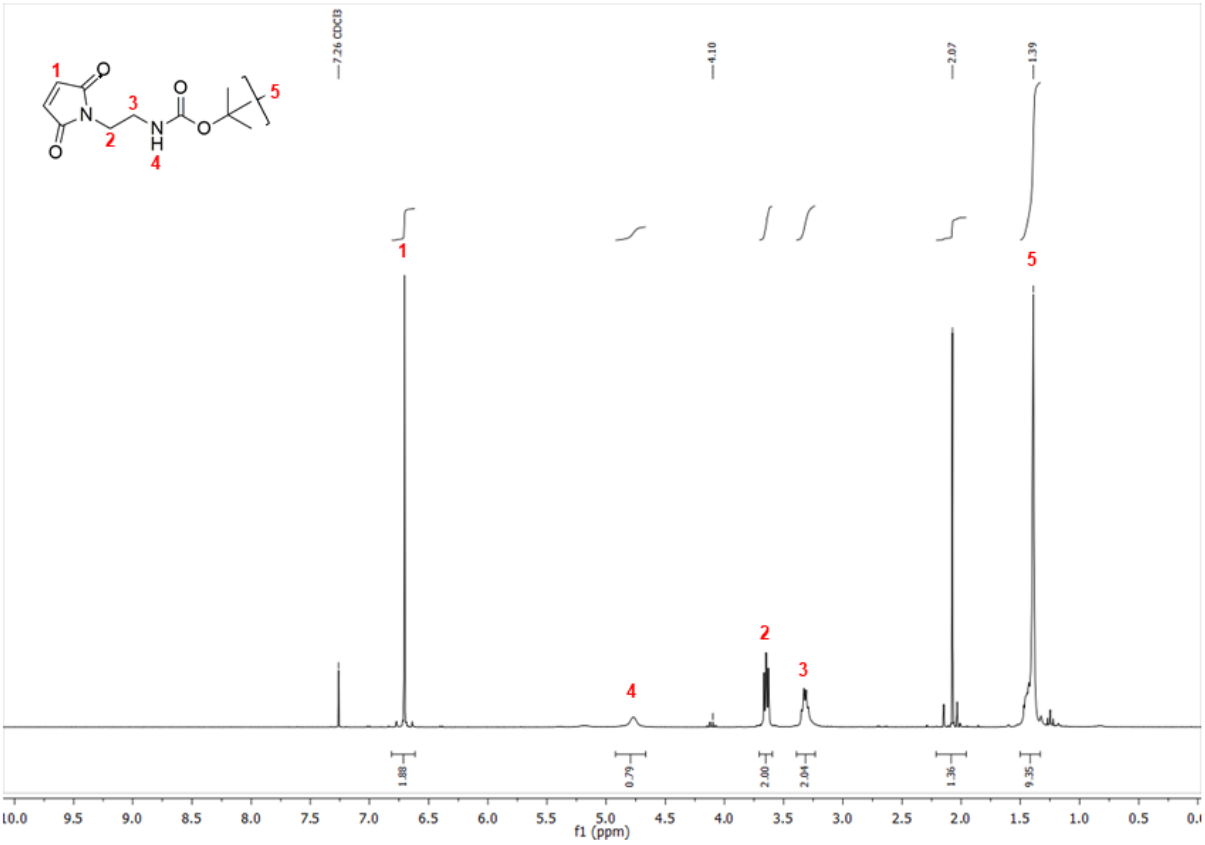

Figure 45: ^{1}H NMR spectrum of 1-((*N*-Boc)-2-aminoethyl)maleimide **11**. Please note that the integral of the maleimide protons is lower than expected.

^{1}H NMR (300 MHz, Chloroform-d) δ = 6.70 (s, 2H), 4.77 (s, 1H), 3.76 – 3.53 (m, 2H), 3.43 – 3.20 (m, 2H), 1.39 (s, 9H).

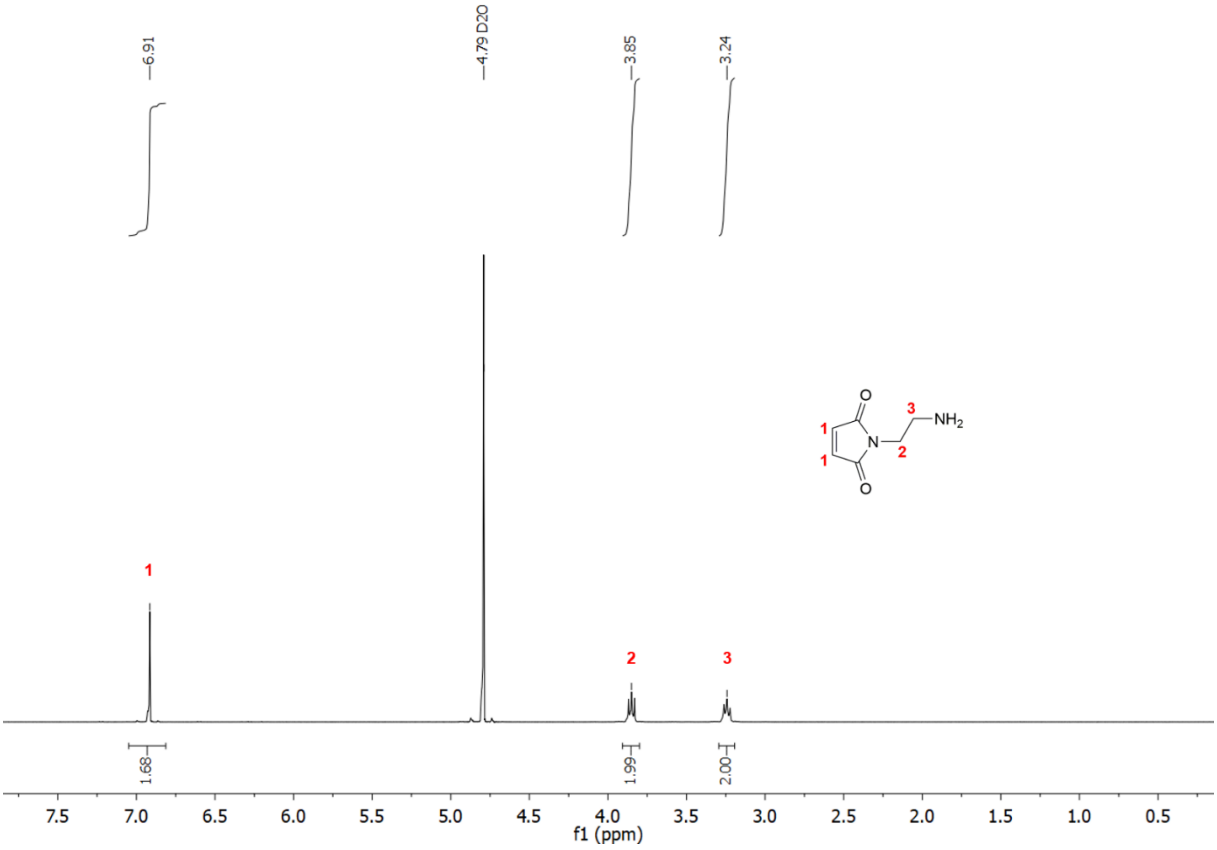

Figure S46: ^{1}H NMR spectrum of *N*-(2-aminoethyl)maleimide **12**. The signal of the maleimide is lower than expected, like in the starting compound.

^{1}H NMR (300 MHz, Deuterium Oxide) δ = 6.92 (s, 2H), 3.93 – 3.78 (m, 2H), 3.24 (t, J = 5.8 Hz, 2H).

2.8.2 Synthesis of TAMRA-thiol **15**

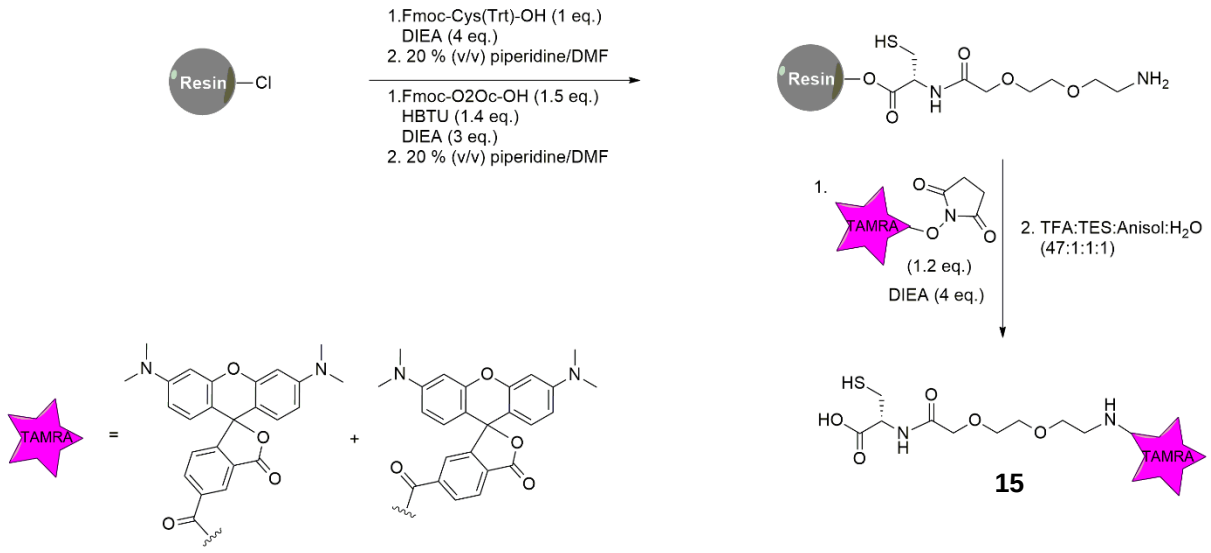

Figure S47: Solid phase synthesis approach to TAMRA-thiol **9** and structure of 5(6)-TAMRA, bottom left.

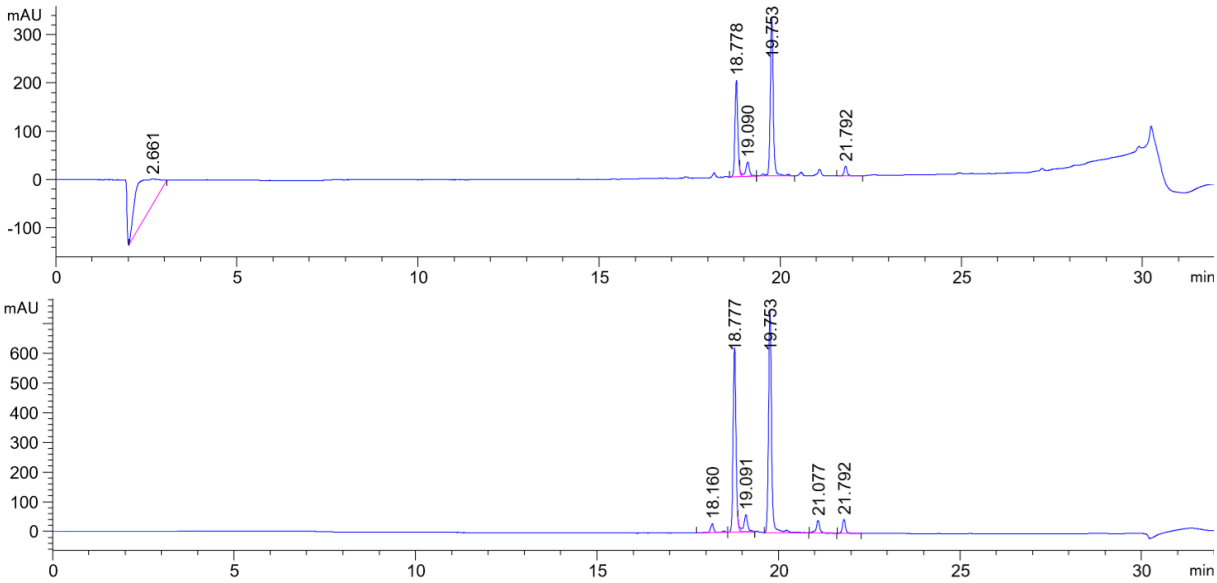

Figure S48: Chromatographic trace of TAMRA-thiol **15**, 0 to 60% B (gradient 20 min), λ = 220 nm (top), λ = 550 nm (bottom), RT = 18.778 min, 19.753 min (corresponding to TAMRA-isomers).

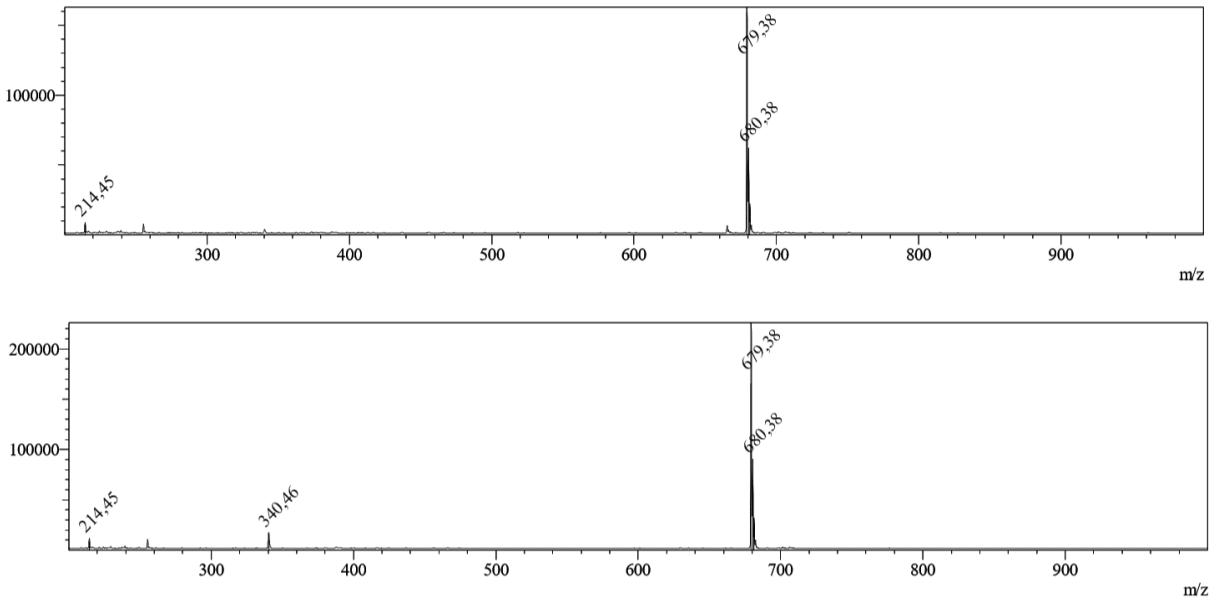

Figure S49: MS (ESI) calculated: $[M+H]^+$ = 679.24, $[M+2H]^{2+}$ = 340.12, observed: $[M+H]^+$ = 679.38, $[M+2H]^{2+}$ = 340.46 (bottom spectrum).

2.8.3 Synthesis of maleimide(6.5)-dextran-*N*-Boc-cadaverine **13**

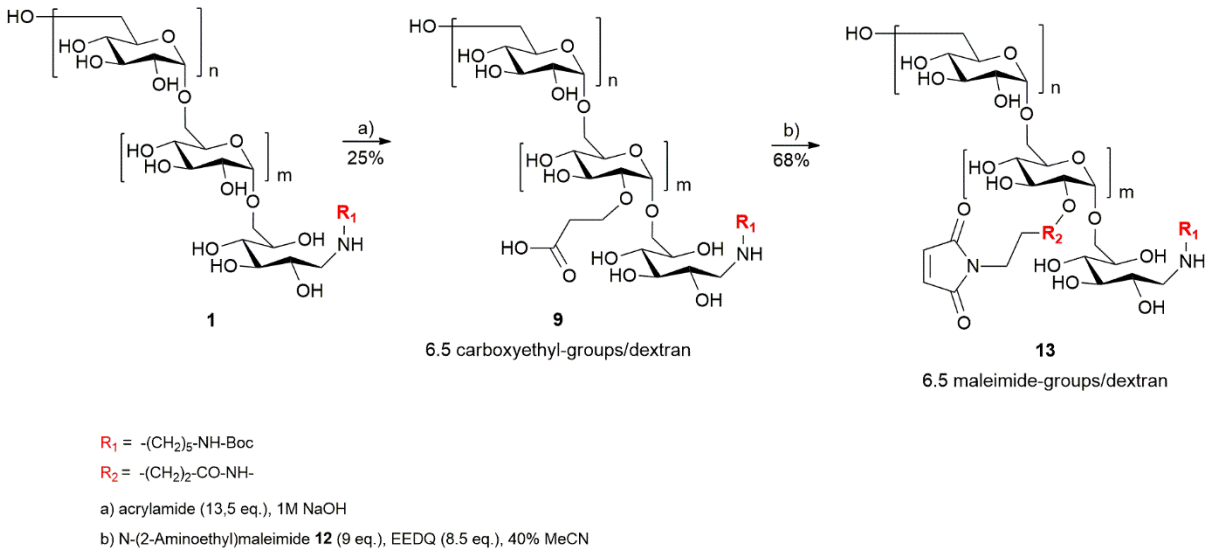

Figure S50: Dextran modification: Reductive amination followed by carboxyethylation and subsequent EEDQ activated conjugation of maleimide linker.

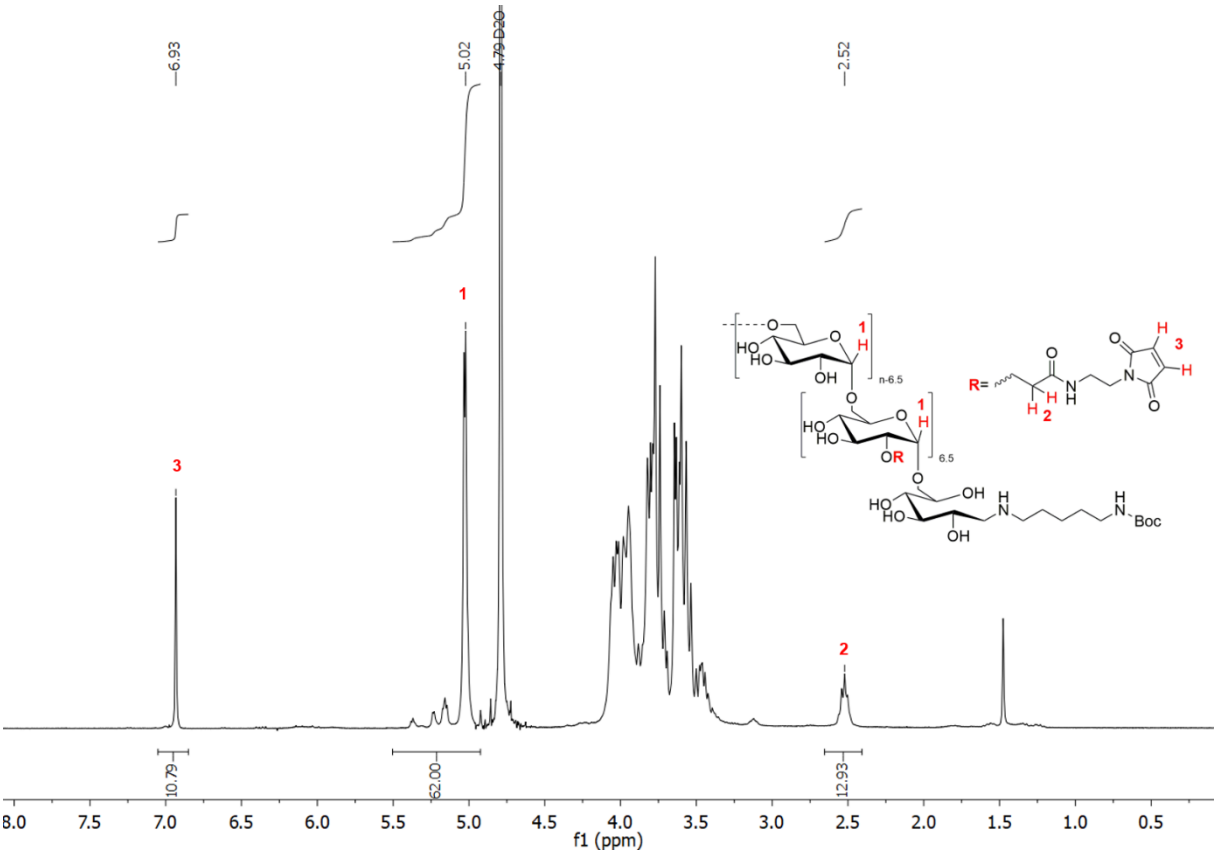

Figure S51: ^{1}H NMR spectrum of maleimide(6.5)-dextran-N-Boc-cadaverine **13** showing tagged signals used for quantification of carboxyl and maleimide groups.

According to the literature,[1] quantification of the carboxyethyl groups and functional maleimide moieties was performed *via* ^{1}H NMR spectroscopy, leading to 6.5 carboxyethyl groups and maleimide moieties per dextran on average. The integrated proton signal of the maleimide double bond was generally observed slightly less than expected. However, the corresponding signal was decreased in the maleimide starting material (**11** and **12**), too.

2.8.4 Maleimide-thiol conjugation of L17E-Cys **14** and TAMRA-thiol **15**

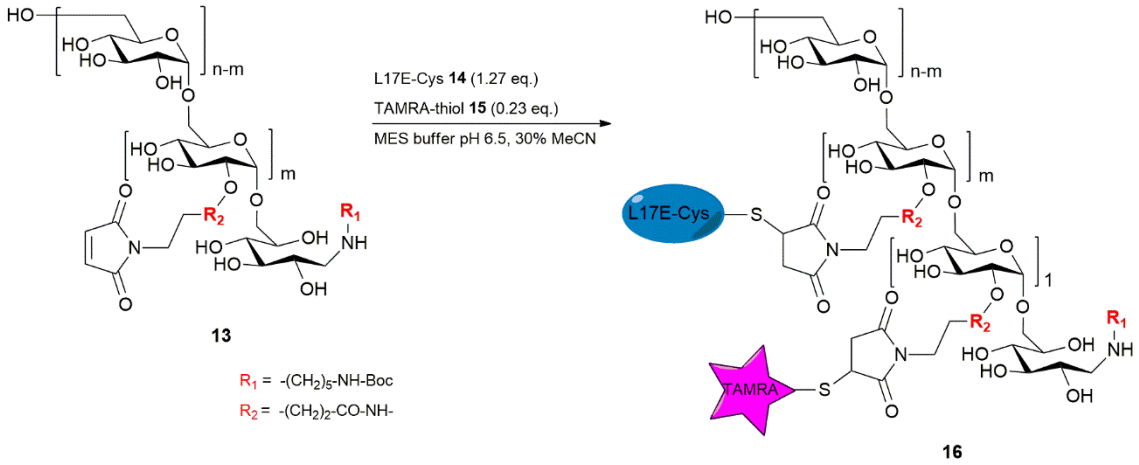

Figure S52: Synthesis of TAMRA-L17E-dextran-*N*-Boc-cadaverine **16** *via* maleimide-thiol Michael addition. A stoichiometric mixture containing 5.5 parts L17E-Cys and 1 part TAMRA-thiol was added to the maleimide modified dextran.

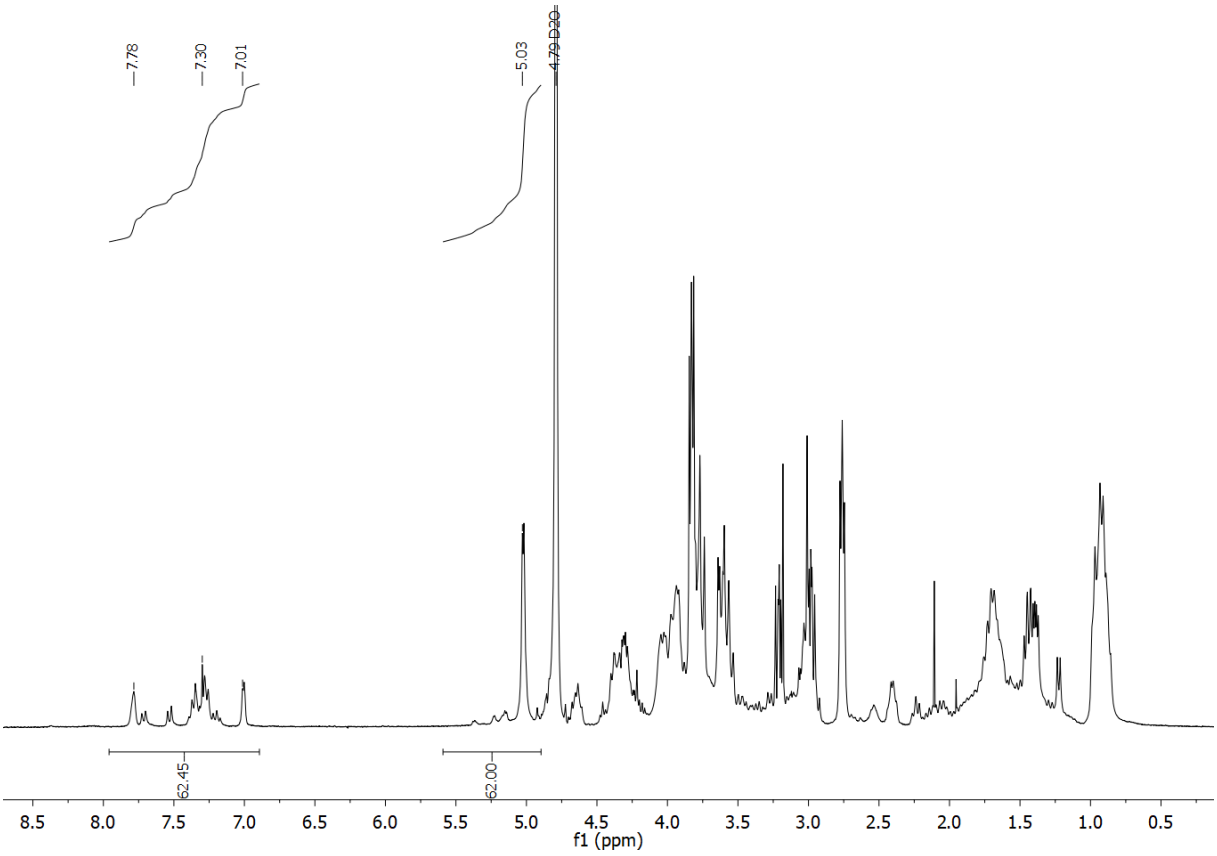

Figure S53: ^{1}H NMR analysis of **16**: Aromatic signals and signals of the anomeric protons of the glucose repeating units at a chemical shift of 5.0-5.5 ppm were of interest for quantification.

According to the literature,[1] quantification of the maleimide-thiol addition product was performed *via* ^{1}H NMR spectroscopy. Only signals of the anomeric proton of the dextran glucose repeating units and aromatic signals were relevant. The product exhibited 62.45 aromatic protons per dextran. Knowing that L17E peptide comprised 14 aromatic protons and assuming that 1 TAMRA fluorophore, corresponding to 9 aromatic protons, is conjugated per dextran, the product contains 3.8 conjugated L17E per dextran on average.

2.9 Synthesis of GFP11/L17E-dextran-TAMRA **22**

2.9.1 Synthesis of N_3(5.4)-dextran-cadaverine **19**

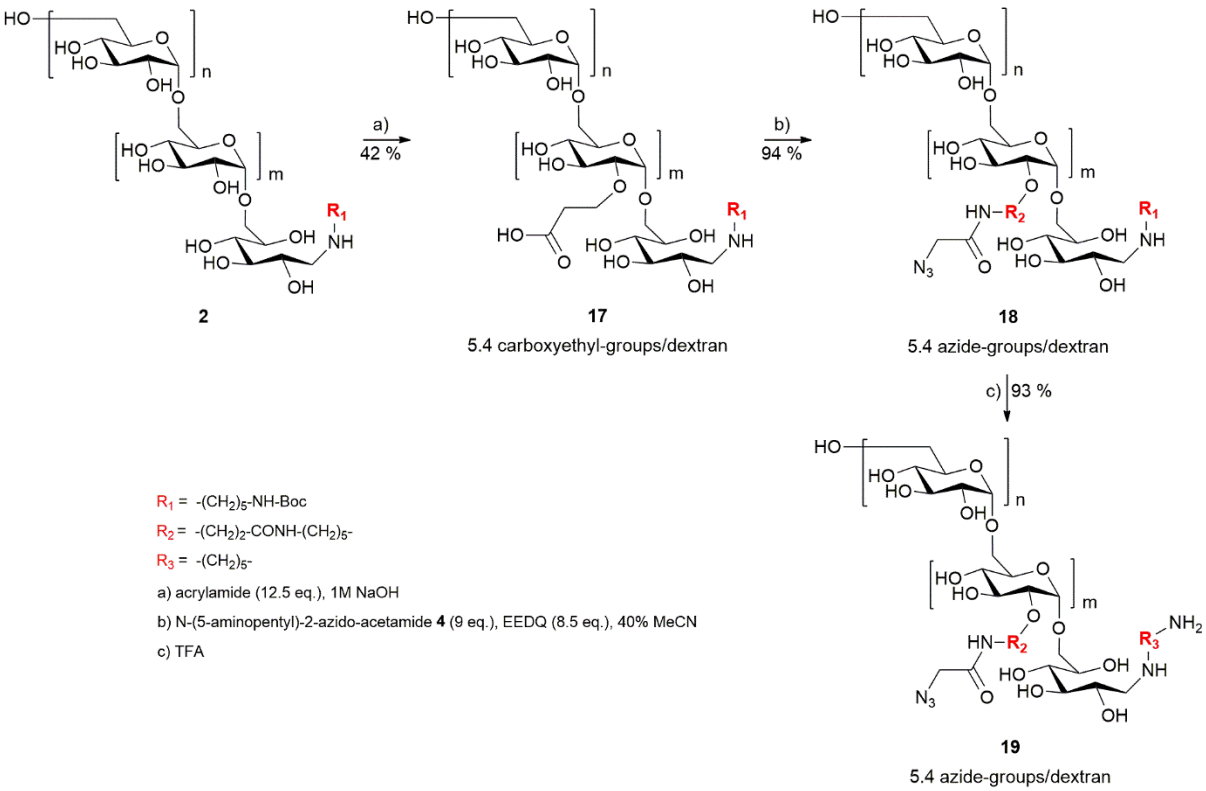

Figure S54: Dextran modification: Carboxyethylation followed by EEDQ activated conjugation of azide linker and subsequent removal of the Boc protection.

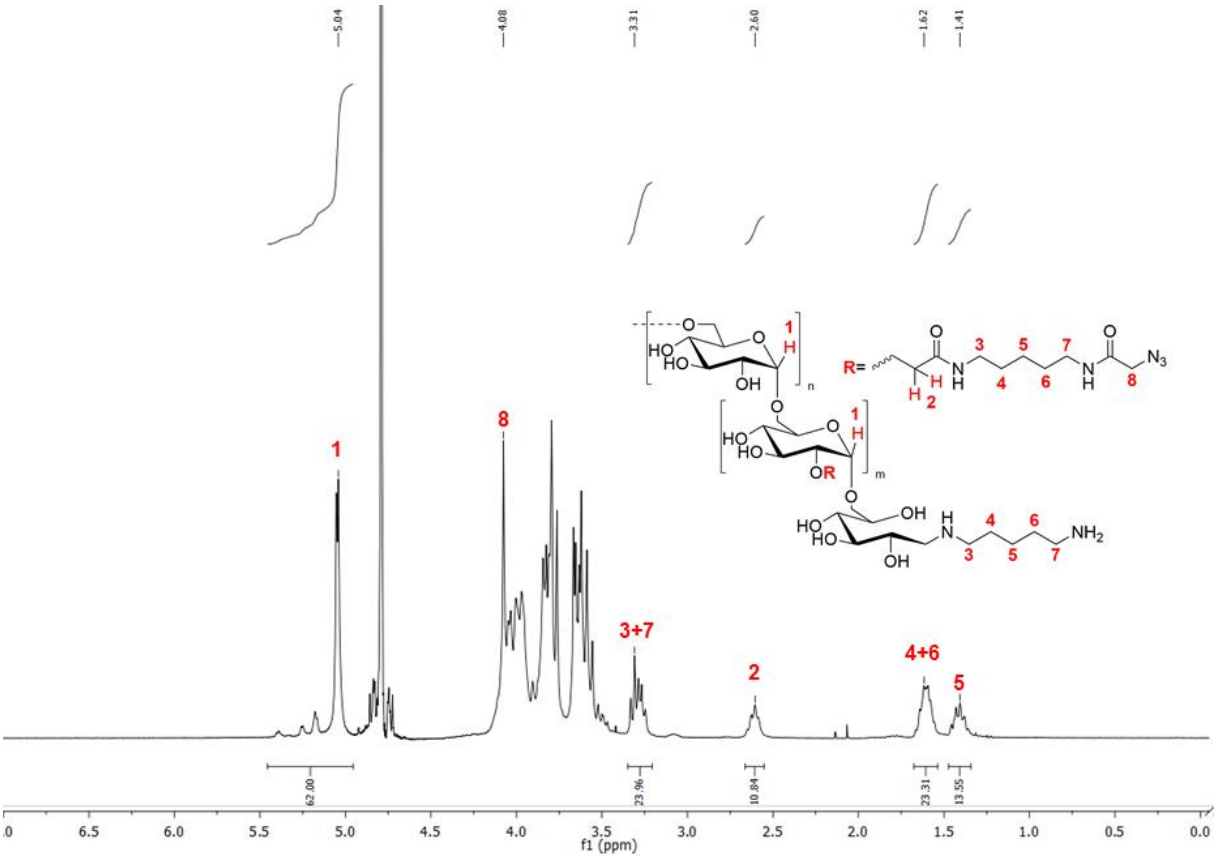

Figure S55: ^{1}H-NMR of N_3-(5.4)-dextran-cadaverine **19**.

2.9.2 Synthesis of N_3(5.4)-dextran-TAMRA **20**

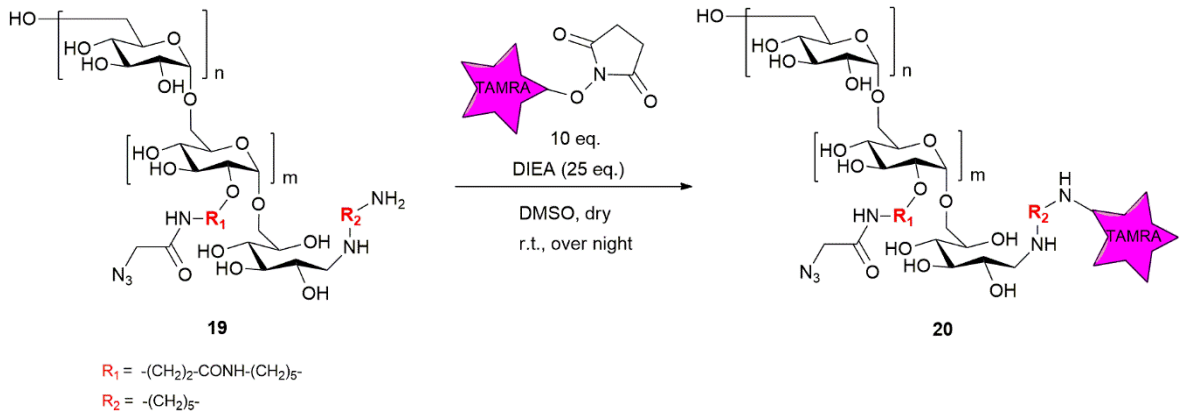

Figure S56: Conjugation of TAMRA to the reducing end of N_3(5.4)-dextran-cadaverine.

Purity of the product was determined by SEC-HPLC:

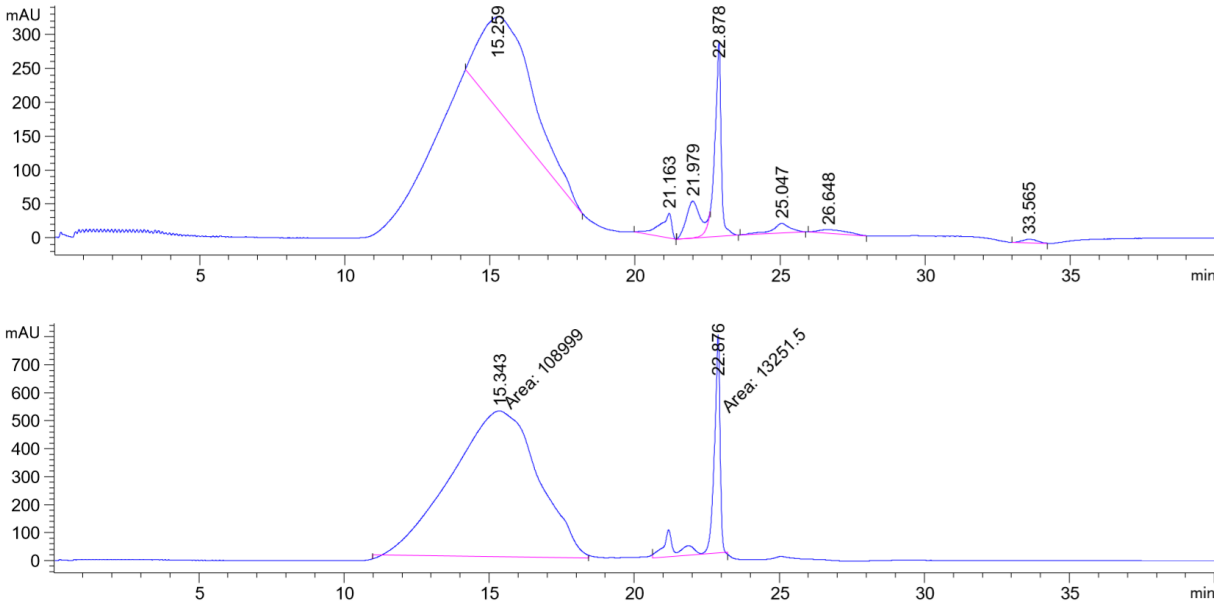

Figure S57: SEC-chromatogram of N_3(5.4)-dextran-TAMRA **20**, 30 % B isocratic flow over 40 min, λ = 220 nm (top), λ = 550 nm (bottom).

The ratio of N_3(5.4)-dextran-TAMRA (RT ~ 11 – 18 min) to impurities (RT ~ 21 -23 min) was estimated upon peak surface area calculated by the software and was 89 %.

For quantification of turnover, the concentration of TAMRA in the product was determined by UV/Vis-spectroscopy as described in section S2.7.4. Therefore, a calibration curve of TAMRA was prepared.

Table S3: Serial dilution of three different samples TAMRA-NHS in water; absorbance was measured at λ = 557 nm.

c [µmol/L]	A (sample 1)	A (sample 2)	A (sample 3)	A (mean)	Stand. Dev.
0.78	0.044	0.047	0.047	**0.046**	0.00173205
1.56	0.098	0.096	0.098	**0.097**	0.0011547
3.13	0.195	0.194	0.199	**0.196**	0.00264575
6.25	0.398	0.387	0.397	**0.394**	0.00608276
12.5	0.756	0.75	0.756	**0.754**	0.0034641

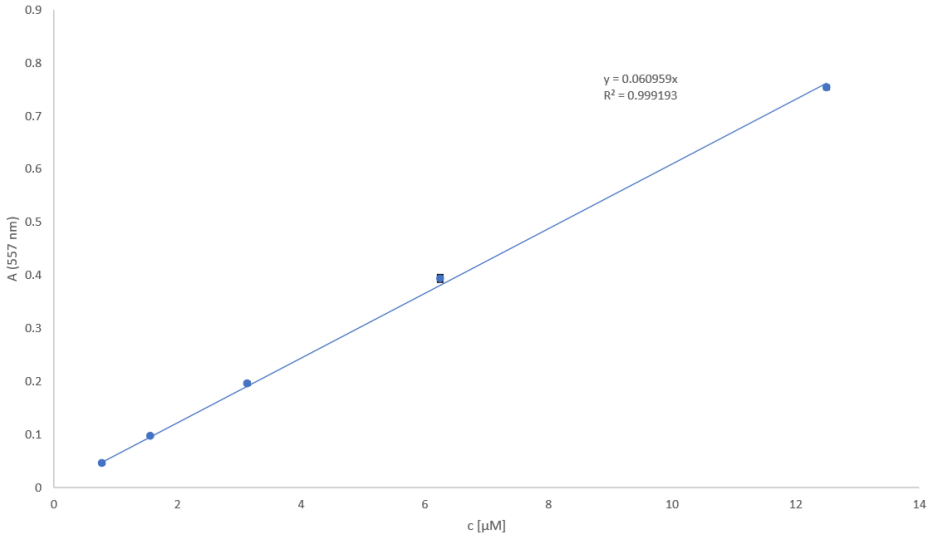

Figure S58: Calibration curve of TAMRA-NHS in water at λ = 557 nm for determination of the molecular extinction coefficient.

All product was dissolved in water and diluted 1:500, followed by measurement of the absorption at λ = 557 nm.

$$A = \varepsilon * c * d$$

A_{557}(sample) = 0.072 (1:500 dilution)

d = 1 cm

ε_{557}(TAMRA-NHS) = 60959 L/(mol*cm)

c (sample, according to weight) = 672 µM

$$c = \frac{0.072}{60959 \frac{L}{mol * cm} * 1\ cm} = 1.18\ \mu M; \quad c\ (undiluted) = 590\ \mu M$$

According to the SEC-chromatogram, 89 % of TAMRA in the product was coupled to dextran, hence the concentration of N_3(5.4)-dextran-TAMRA **20** is c = 525 µM.

$$TAMRA\ per\ dextran: \frac{c_{photometric}}{c_{weight}} = \frac{525\ \mu M}{672\ \mu M} = 0.78$$

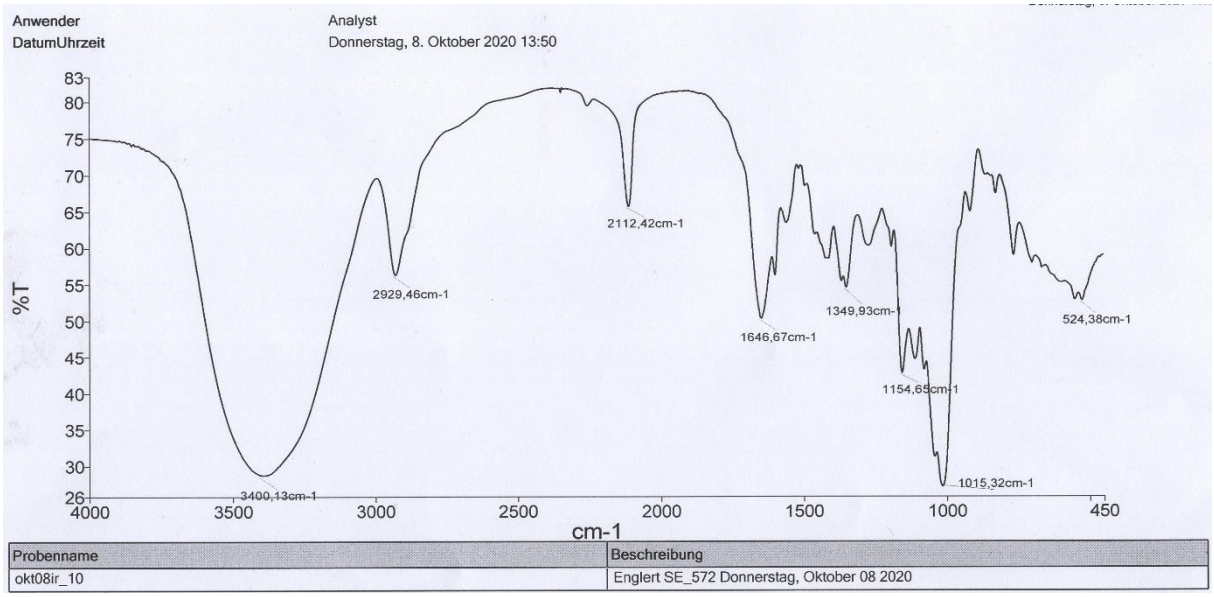

Figure S59: IR-spectrum of N_3(5.4)-dextran-TAMRA **20**. The azide band is at a wavenumber of 2112 cm^{-1}.

2.9.3 CuAAC of N_3(5.4)-dextran-TAMRA **20** with alkyne-GFP11 **21** and L17E-Pra **15**

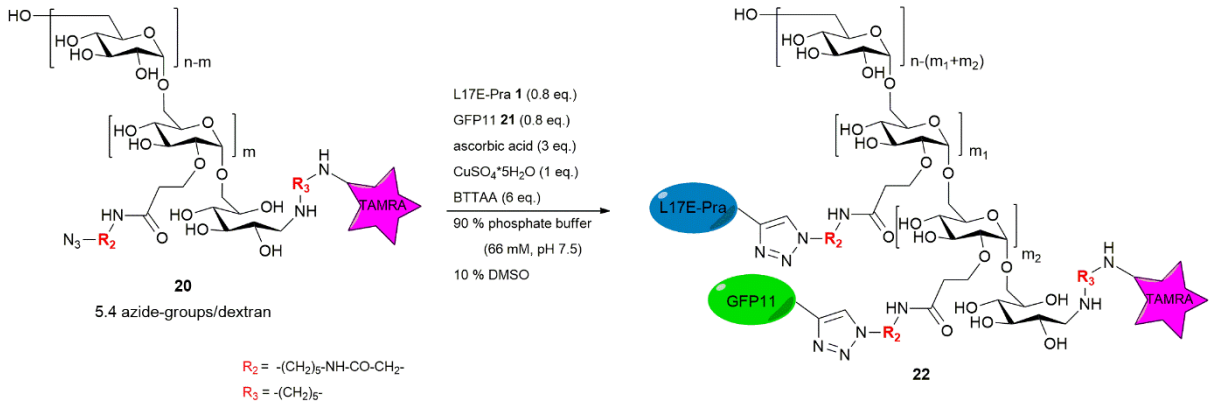

Figure S60: Decoration of N_3(5.4)-dextran-TAMRA with L17E-Pra and alkyne-GFP11 peptide by CuAAC.

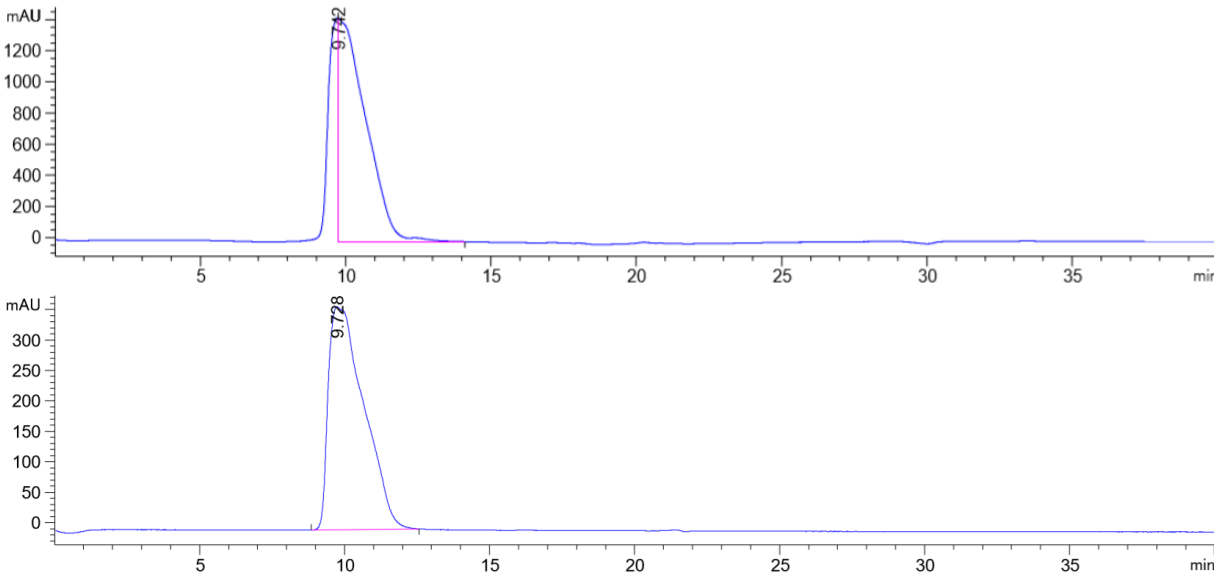

Figure S61: SEC-chromatogram of L17E-GFP11-(5.4)-dextran-TAMRA **22**, 30 % B isocratic flow over 40 min, λ = 220 nm (top), λ = 550 nm (bottom).

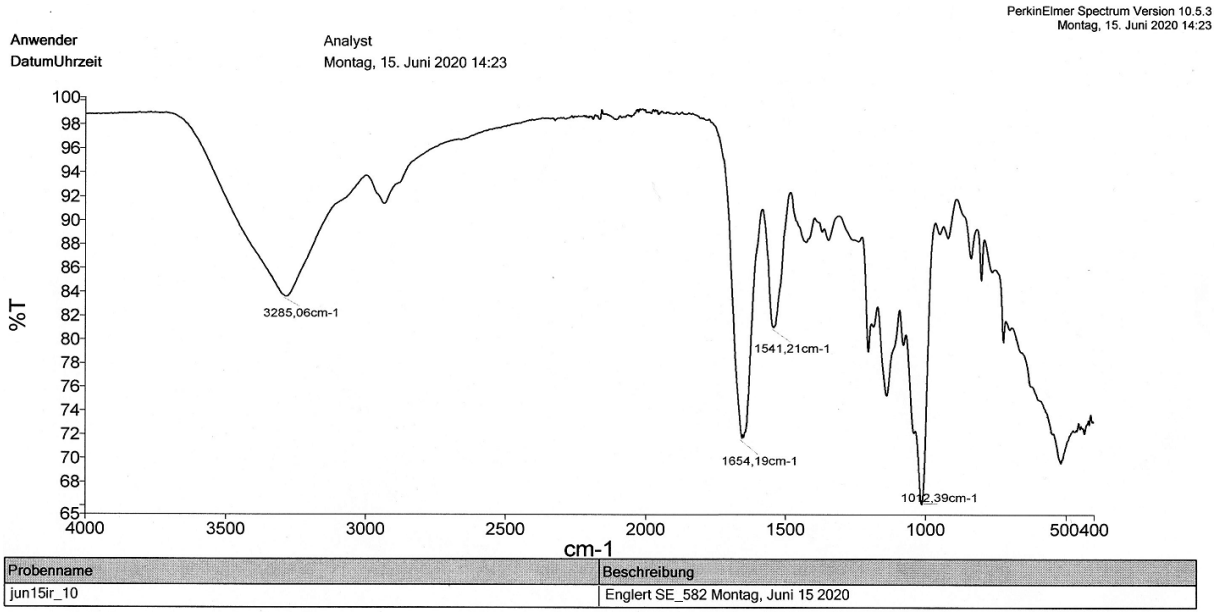

Figure S62: IR-spectrum of **22**. Please note that contrary to previous IR spectra, ATR-IR instead of KBr pellet-based IR was performed. The azide band at wavenumber 2109 cm^{-1} from the parent dextran completely disappeared.

2.9.4 CuAAC of N_3(5.4)-dextran-TAMRA **20** with alkyne-GFP11 **21**

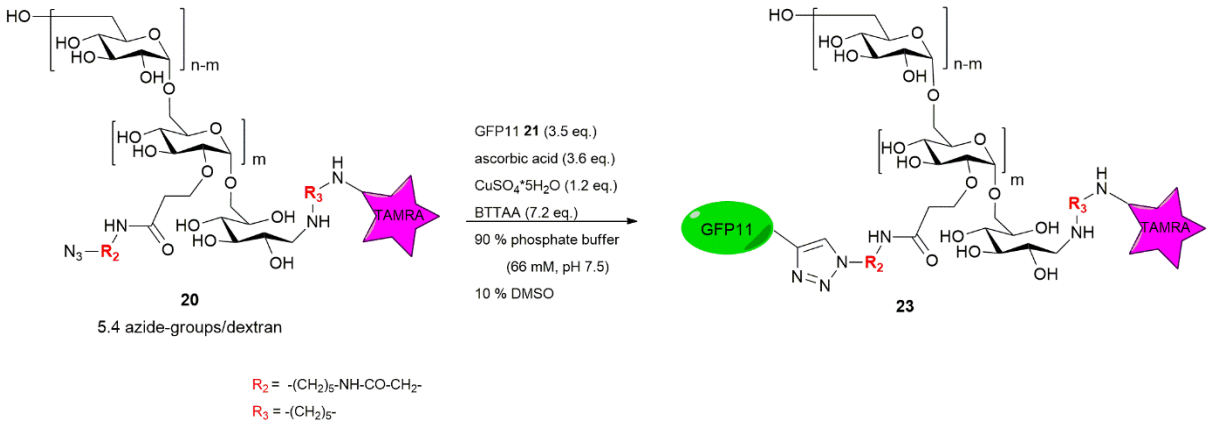

Figure S63: Decoration of N_3(5.4)-dextran-TAMRA with alkyne-GFP11 peptide by CuAAC. Please note that contrary to previous CuAAC, the equivalents correspond to the amount of dextran and not it´s azide functionalities.

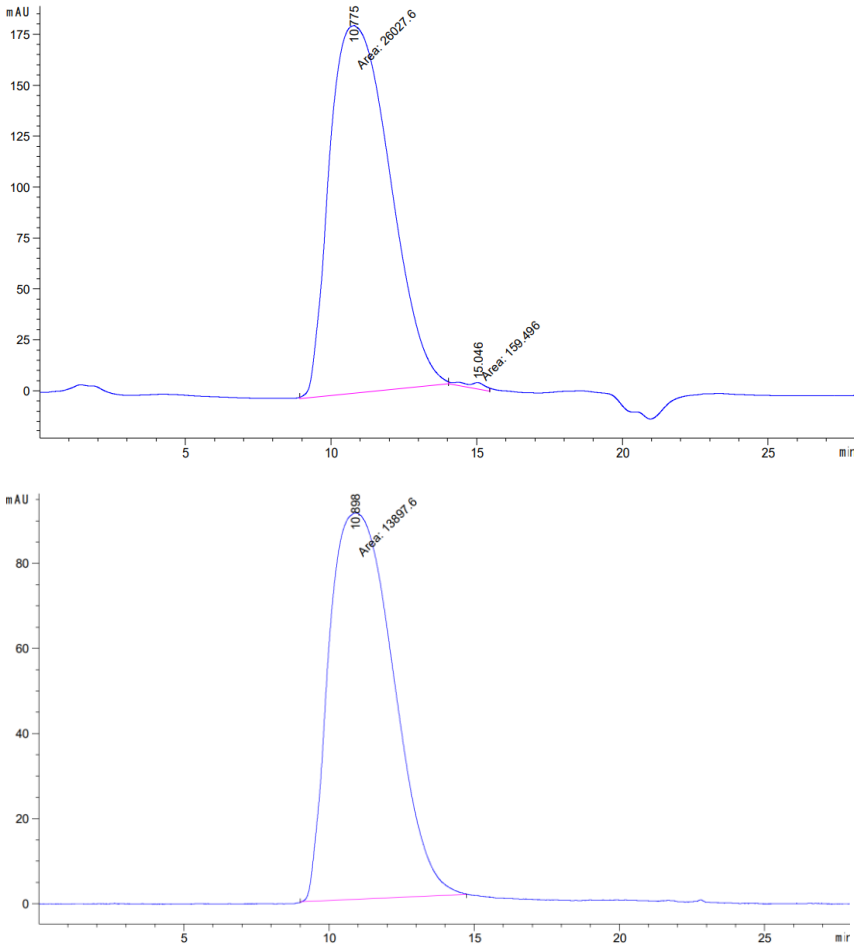

Figure S64: SEC-chromatograms of GFP11-dextran-TAMRA **23**, 30 % B isocratic flow over 28 min, λ = 220 nm (top), λ = 550 nm (bottom).

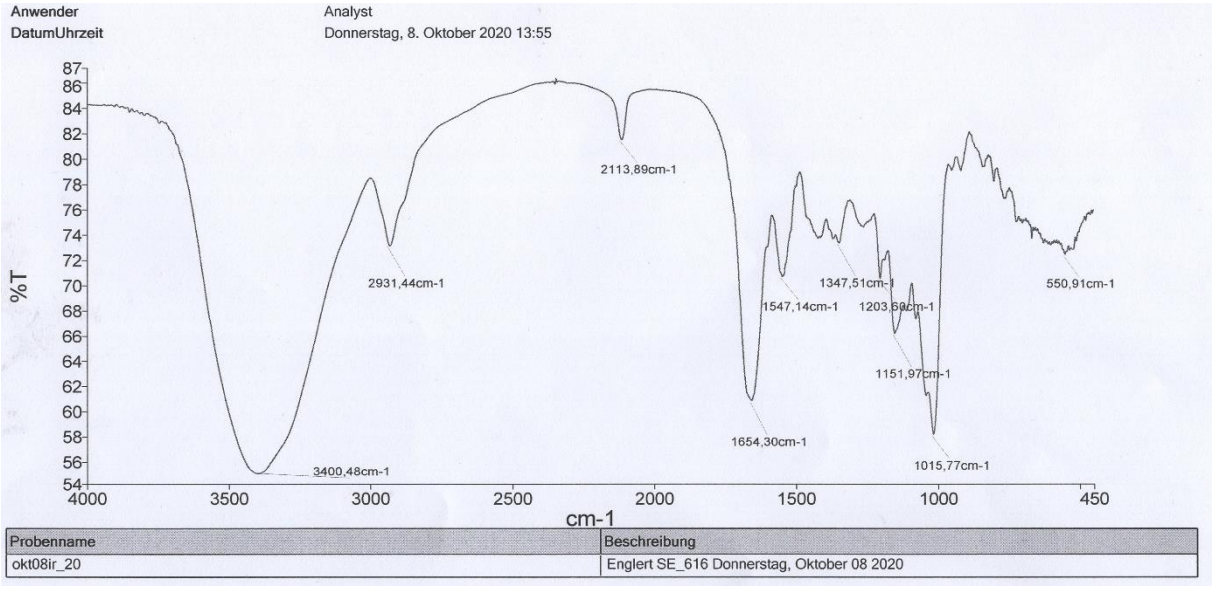

Figure S65: IR-spectrum of **23**. Compared to the parent dextran **20**, the azide band at wavenumber 2114 cm^{-1} is distinctly reduced in intensity.

2.10 Synthesis of PNA/L17E-dextran-*N*-Boc-cadaverine **29**

2.10.1 Synthesis of maleimide(10.5)-dextran-*N*-Boc-cadaverine **27**

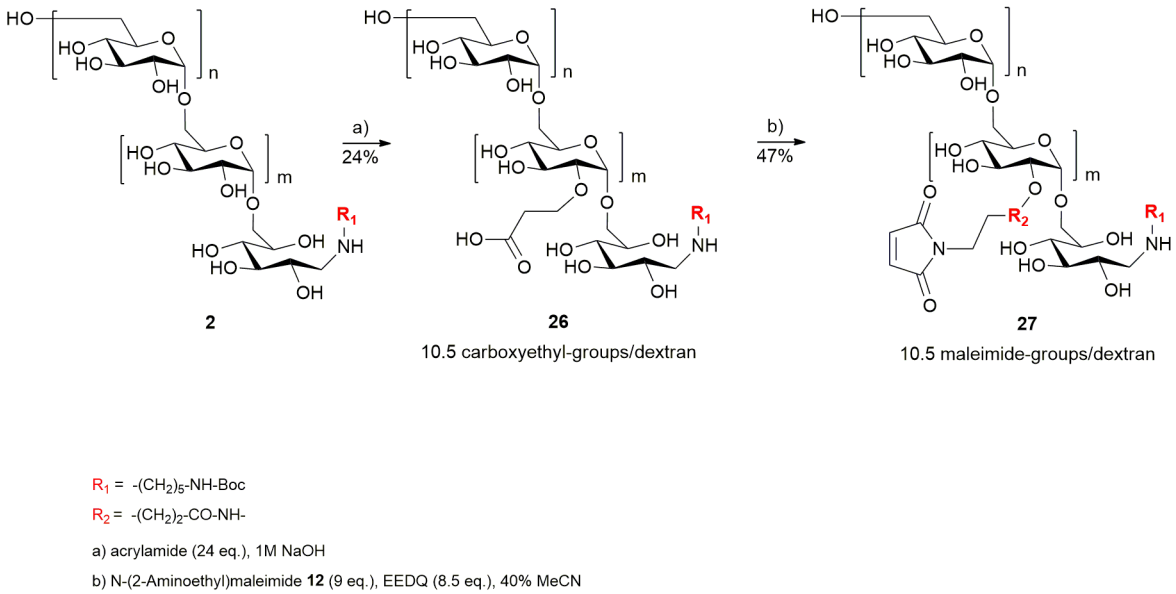

Figure S66: Reaction scheme of dextran modification, starting with dextran-*N*-Boc-cadaverine, followed by carboxyethylation and EEDQ-activated conjugation of maleimide functionalities.

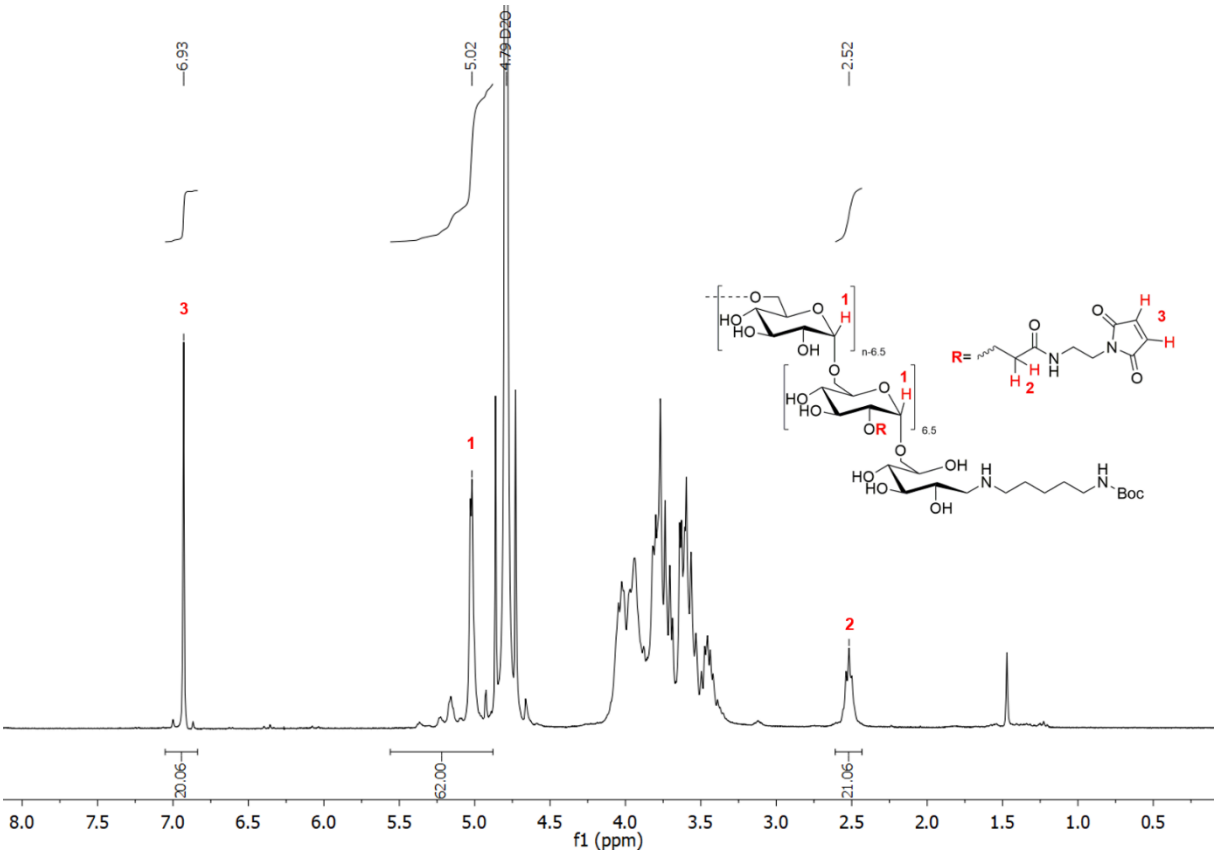

Figure S67: ^{1}H NMR spectrum showing tagged signals used for quantification of carboxyl and maleimide groups.

According to the literature,[1] quantification of the carboxyethyl groups and functional maleimide moieties was performed *via* ^{1}H NMR spectroscopy, leading to 10.5 carboxyethyl groups and maleimide moieties per dextran on average. The integrated proton signal of the maleimide double bond was generally observed slightly less than expected. However, the corresponding signal was decreased in the maleimide starting material, too.

2.10.2 Maleimide-thiol conjugation of L17E-Cys **14** and thiol-PNA **28**

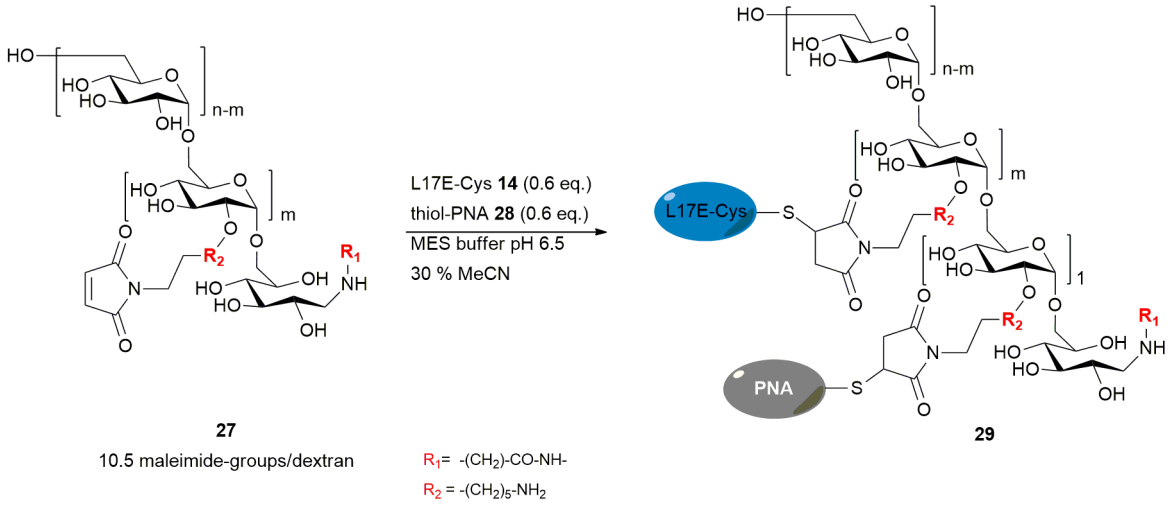

Figure S68: Synthesis of PNA/L17E-dextran-*N*-Boc-cadaverine *via* maleimide-thiol Michael addition. An equimolar mixture containing of L17E-Cys and thiol-PNA was added to the maleimide modified dextran.

2.11 Synthesis of Fmoc-L-Lys(DEACM)-OH **33** building block

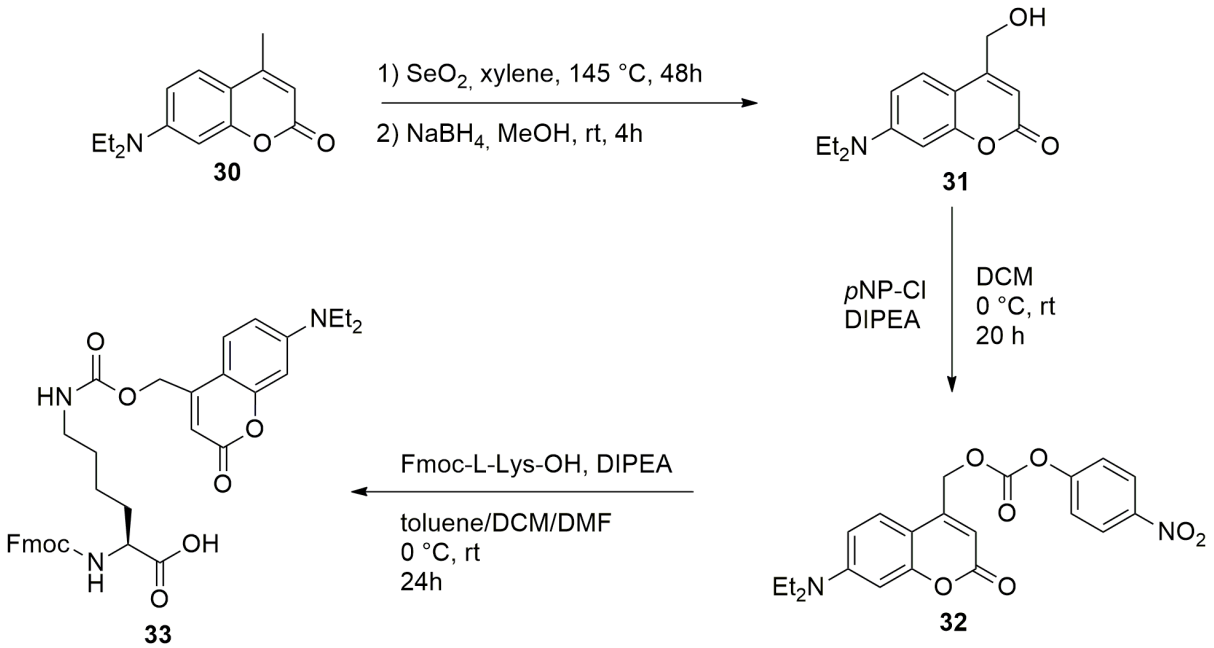

Figure S69: Synthetic scheme for the photocaged amino acid Fmoc-L-Lys(DEACM)-OH.

2.11.1 Synthesis of DEACM-OH **31**

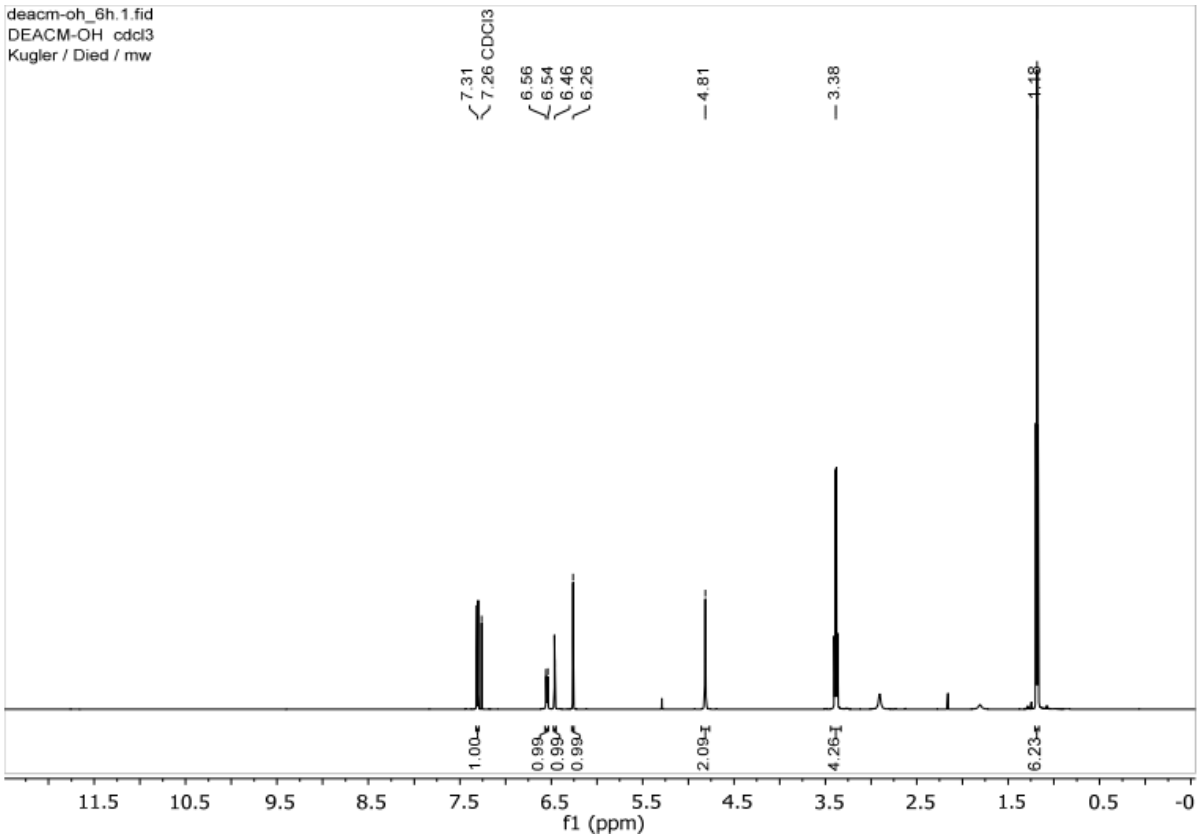

^{1}H-NMR (600 MHz, $CDCl_3$): δ = 7.31 (d, $^{3}J_{HH}$ = 9.0 Hz, 1 H, *H*5), 6.56-6.54 (dd, $^{3}J_{HH}$ = 9.0 Hz, $^{4}J_{HH}$ = 2.6 Hz, 1 H, *H*6), 6.46 (d, $^{4}J_{HH}$ = 2.6 Hz, 1 H, *H*8), 6.26 (t, $^{4}J_{HH}$ = 1.3 Hz, 1 H, *H*3), 4.81 (s, 2 H, C*H*$_2$OH), 3.88 (q, $^{3}J_{HH}$ = 7.2 Hz, 4 H, C*H*$_2$CH$_3$), 1.18 (t, $^{3}J_{HH}$ = 7.2 Hz, 6 H, CH$_2$C*H*$_3$) ppm.

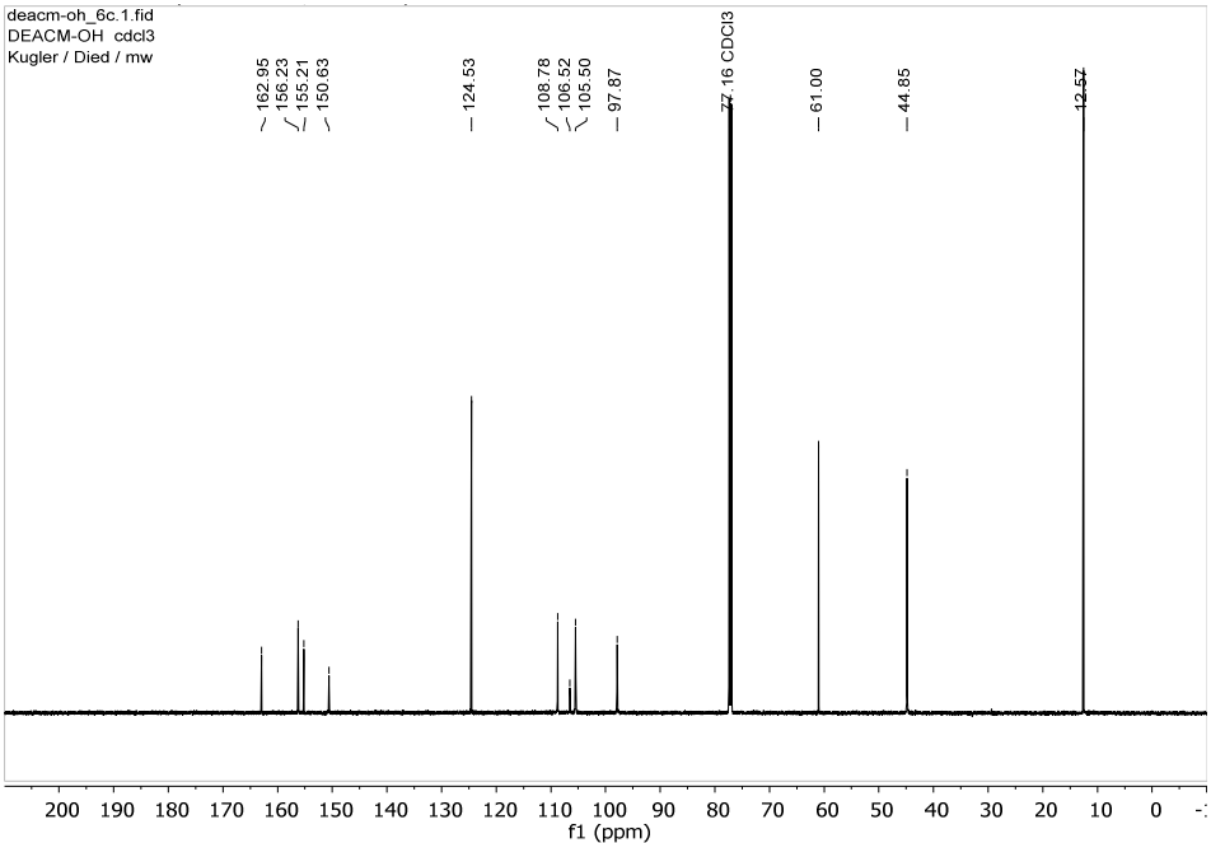

^{13}C-NMR (150 MHz, $CDCl_3$): δ = 163.0 (*C*2), 156.2 (*C*8'), 155.2 (*C*4), 150.6 (*C*7), 124.5 (*C*5), 108.8 (*C*6), 106.5 (*C*4'), 105.5 (*C*3), 97.9 (*C*8), 61.0 (CH_2OH), 44.9 (CH_2CH_3), 12.6 (CH_2CH_3) ppm.

HR-MS (ESI+): calcd. for $C_{14}H_{17}NO_3$: 248.1281; found: 248.1283.

2.11.2 Synthesis of DEACM-*p*NP **32**

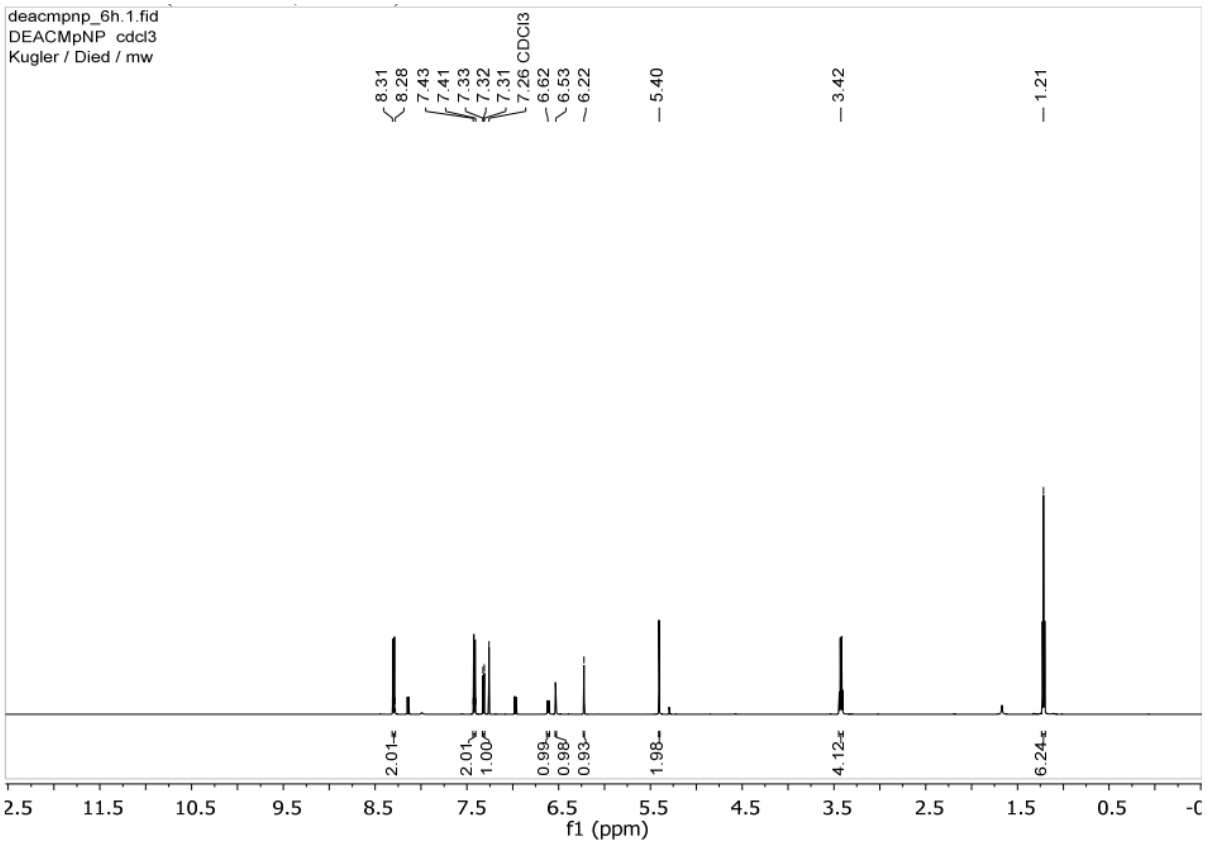

^{1}H-NMR (600 MHz, $CDCl_3$): δ = 8.31-8.28 (dt, $^3J_{HH}$ = 9.3 Hz, $^4J_{HH}$ = 5.4 Hz, $^5J_{HH}$ = 3.1 Hz, 2H, *H*3$_{pNP}$), 7.43-7.41 (dt, $^3J_{HH}$ = 9.3 Hz, $^4J_{HH}$ = 5.4 Hz, $^5J_{HH}$ = 3.1 Hz, 2H, *H*2$_{pNP}$), 7.32 (d, $^3J_{HH}$ = 9.0 Hz, 1 H, *H*5), 6.62 (dd, $^3J_{HH}$ = 9.0 Hz, $^4J_{HH}$ = 2.6 Hz, 1 H, *H*6), 6.53 (d, $^4J_{HH}$ = 2.6 Hz, 1 H, *H*8), 6.22 (t, $^4J_{HH}$ = 1.2 Hz, 1 H, *H*3), 5.40 (d, 2 H, $^4J_{HH}$ = 1.2 Hz, C*H*$_2$OR), 3.42 (q, $^3J_{HH}$ = 7.1 Hz, 4 H, C*H*$_2$CH$_3$), 1.18 (t, $^3J_{HH}$ = 7.1 Hz, 6 H, CH$_2$C*H*$_3$) ppm.

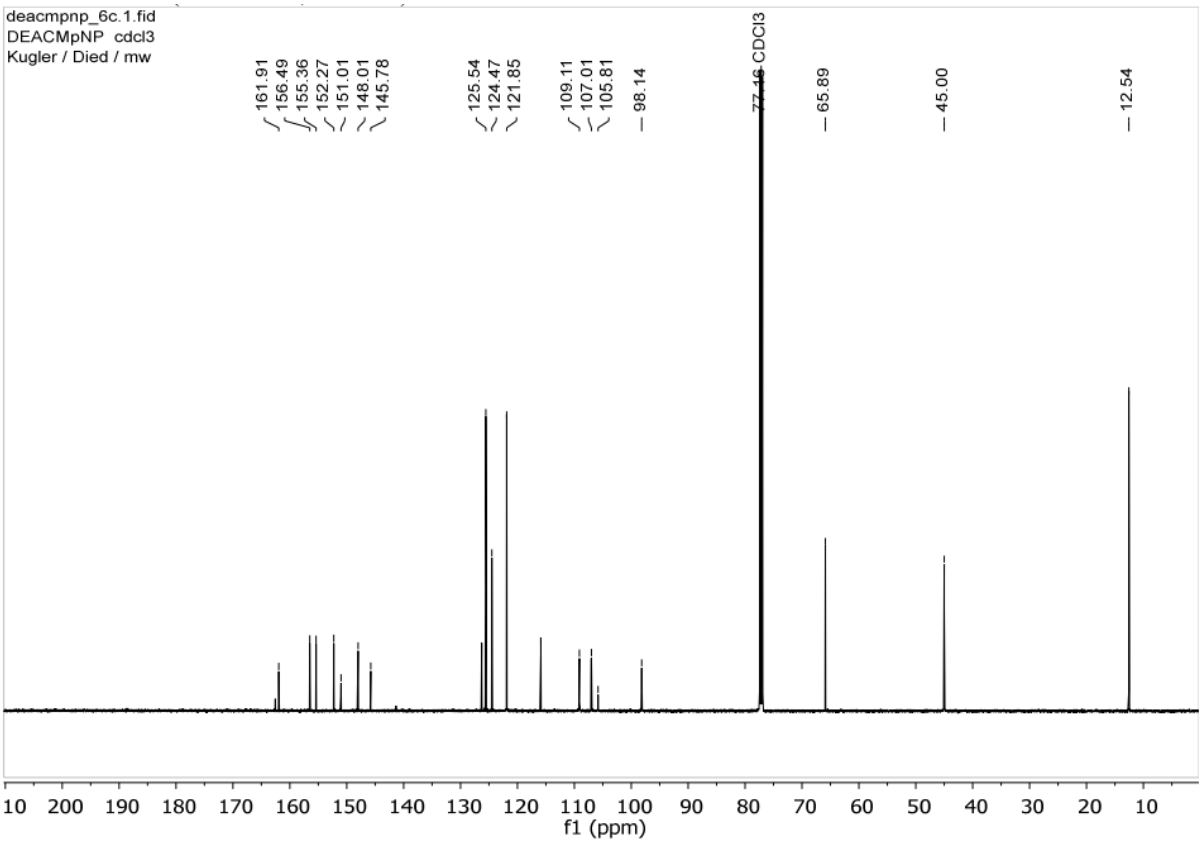

^{13}C-NMR (150 MHz, $CDCl_3$): δ = 161.9 (*C*2), 156.5 (*C*8'), 155.4 (*C*1$_{p\text{NP}}$), 152.3 (C=O), 151.0 (*C*7), 148.0 (*C*4), 145.8 (*C*4$_{p\text{NP}}$), 125.5 (*C*3$_{p\text{NP}}$), 124.4 (*C*5), 121.9 (*C*2$_{p\text{NP}}$), 109.1 (*C*6), 107.0 (*C*3), 105.8 (*C*4'), 98.1 (*C*8), 65.9 (CH_2OR), 45.0 (CH_2CH_3), 12.5 (CH_2CH_3) ppm.

HR-MS (ESI+) calcd. for $C_{21}H_{20}N_2O_7$: 413.1343; found: 413.1344.

2.11.3 Synthesis of Fmoc-L-Lys(DEACM)-OH **33**

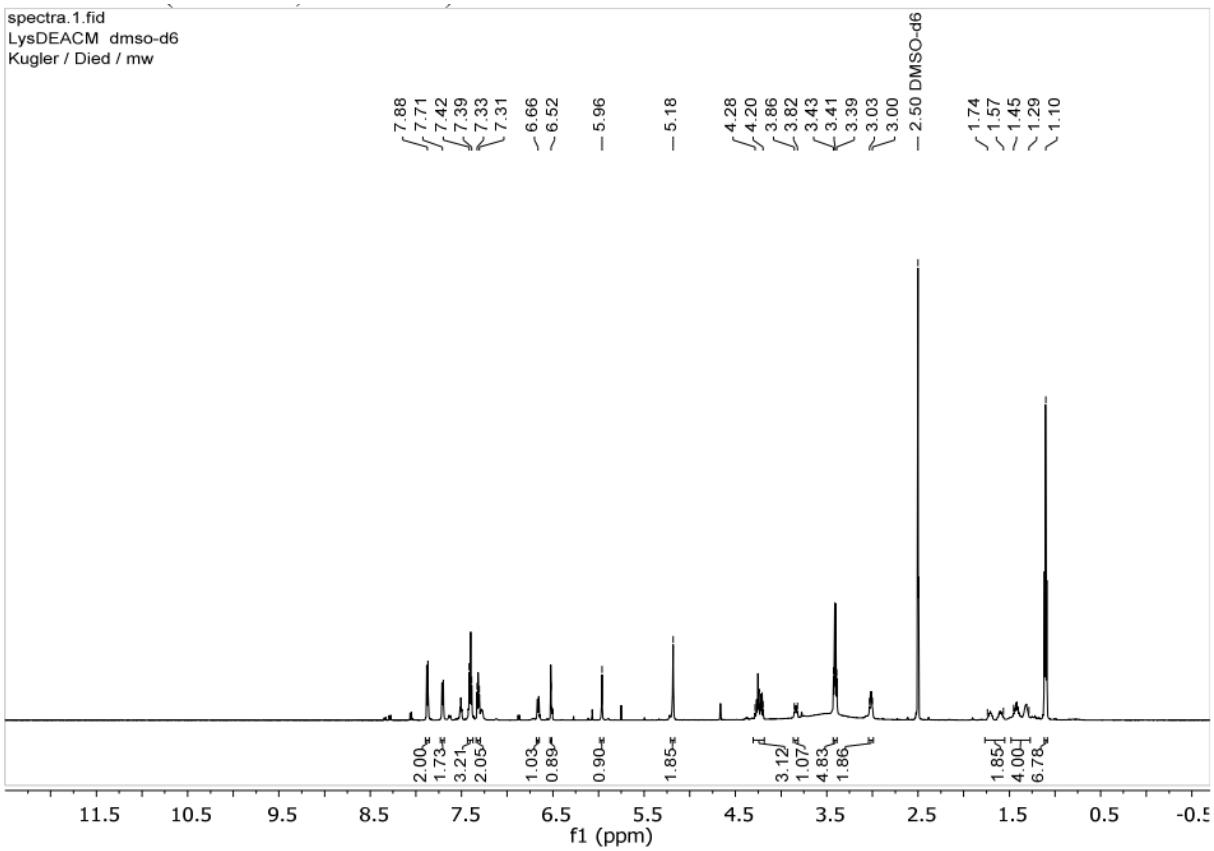

^{1}H-NMR (600 MHz, DMSO-d_6): δ = 7.88 (d, $^3J_{HH}$ = 7.4 Hz, 2 H, *H*4$_{Fmoc}$), 7.71 (d, $^3J_{HH}$ = 7.4 Hz, 2 H, *H*1$_{Fmoc}$), 7.42-7.39 (m, 3 H, *H*5, *H*3$_{Fmoc}$), 7.33-7.31 (m, 2 H, *H*2$_{Fmoc}$), 6.66 (dd, $^3J_{HH}$ = 8.9 Hz, $^4J_{HH}$ = 2.6 Hz, 2 H, *H*6), 6.52 (d, $^4J_{HH}$ = 2.6 Hz, 1 H, *H*8), 5.96 (s, 1 H, *H*3), 5.18 (s, 2 H, C*H*$_2$OR), 4.28-4.20 (m, 3 H, C*H*$_{2,\ Fmoc}$, C*H*$_{Fmoc}$), 3.86-3.82 (m, 1 H, CH$^{\alpha}$), 3.41 (q, 4 H, $^3J_{HH}$ = 7.0 Hz, C*H*$_2$CH$_3$), 3.03-3.00 (m, 2 H, CH$_2^{\varepsilon}$), 1.74-1.57 (m, 2 H, CH$_2^{\beta}$), 1.45-1.29 (m, 4 H, CH$_2^{\gamma}$, CH$_2^{\delta}$), 1.10 (t, $^3J_{HH}$ = 7.0 Hz, 6 H, CH$_2$C*H*$_3$) ppm.

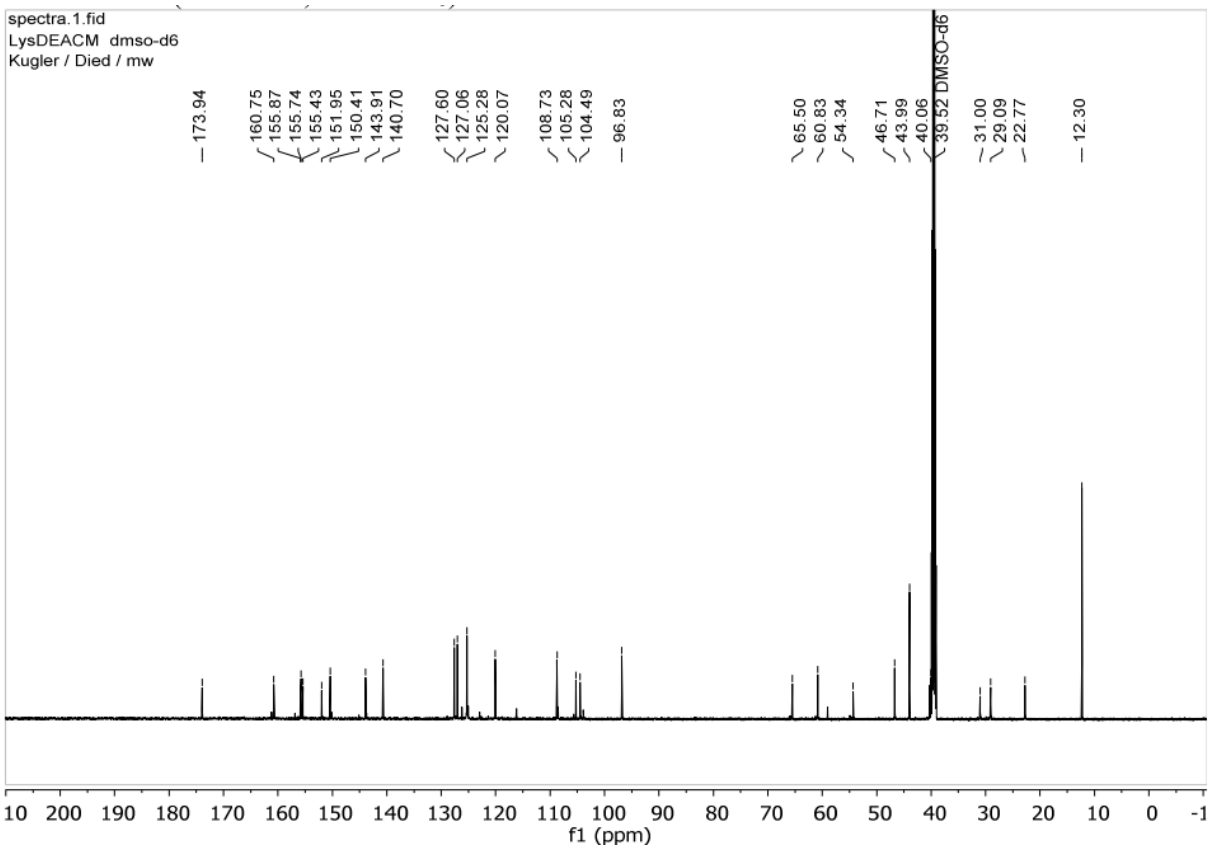

^{13}C-NMR (150 MHz, DMSO-d_6): δ = 170.9 (*C*O_2H), 160.8 (*C*2), 155.9 (*C*=O_{Fmoc}), 155.7 (*C*8'), 155.4 (C=$O_{DEACM\ carbamate}$), 152.0 (*C*4), 150.4 (C7), 143.9 (C^{q}_{Fmoc}), 140.7 (C^{q}_{Fmoc}), 127.6 ($C_{Ar,\ Fmoc}$), 127.1 ($C_{Ar,\ Fmoc}$), 125.3 (*C*5, $C_{Ar,\ Fmoc}$), 120.1 ($C_{Ar,\ Fmoc}$), 108.7 (*C*6), 105.3 (*C*4'), 104.5 (*C*3), 96.8 (*C*8), 65.5 ($CH_{2,\ Fmoc}$), 60.8 (*C*H_2OR), 54.3 (C^{α}), 46.7 (CH_{Fmoc}), 44.0 (*C*H_2CH_3) 40.1 (C^{ε}), 31.0 (C^{β}), 29.1 (C^{δ}), 22.8 (C^{γ}), 12.3 (CH_2CH_3) ppm.

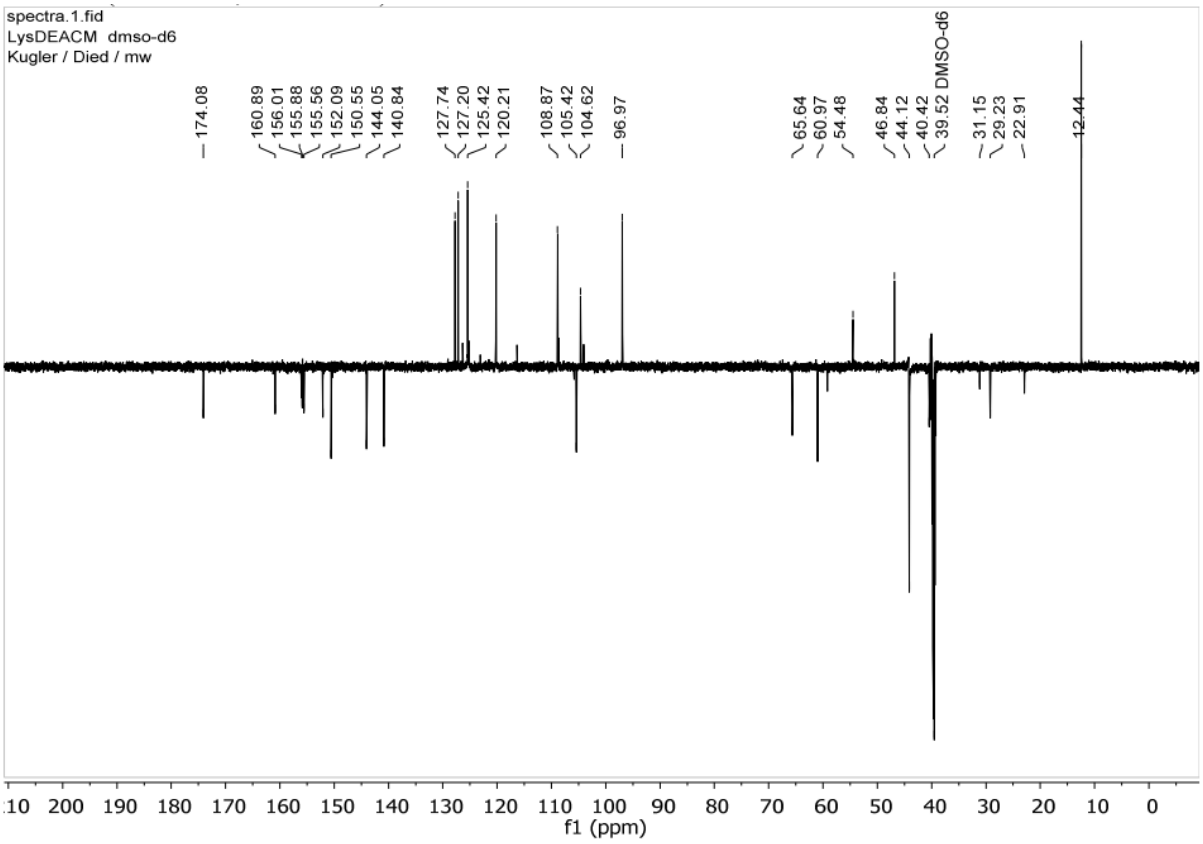

Figure S70: APT (150 MHz, DMSO-d_6).

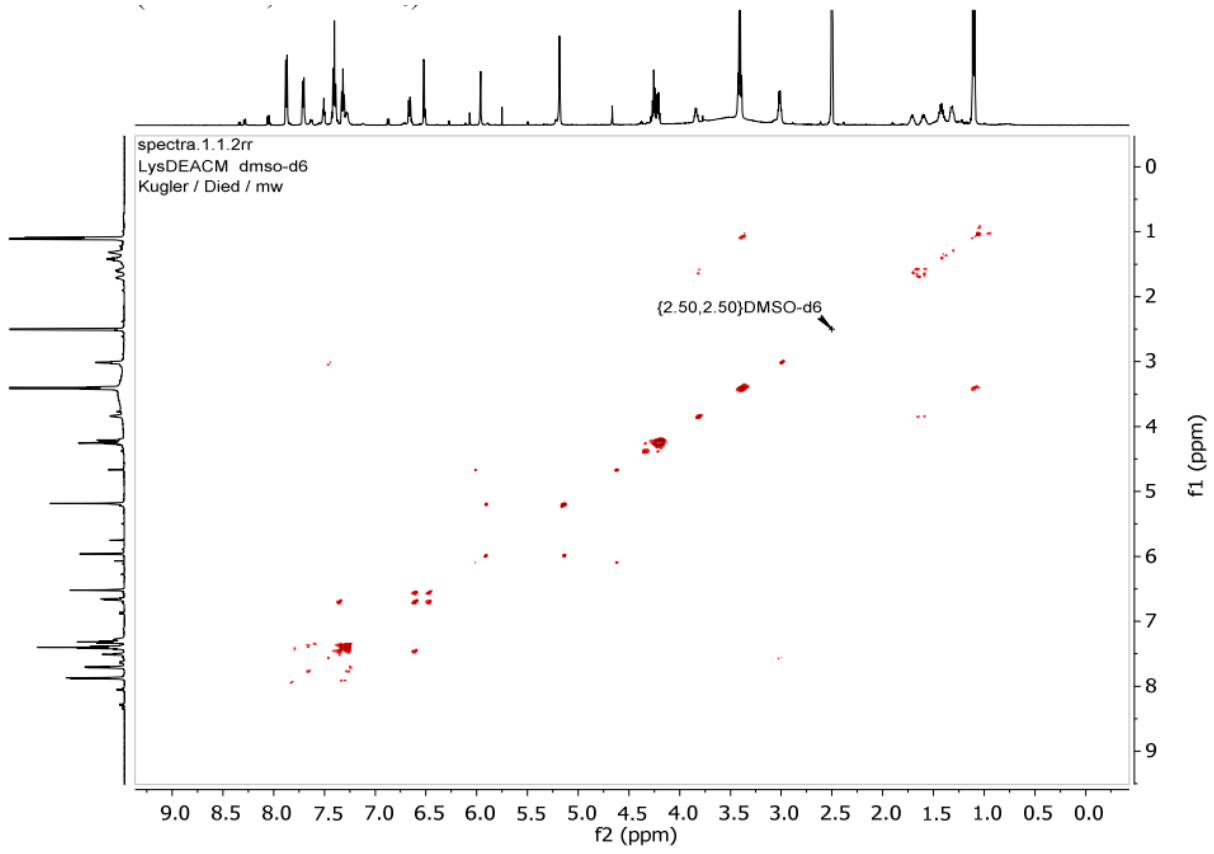

Figure S71: COSY (600 MHz, DMSO-d_6).

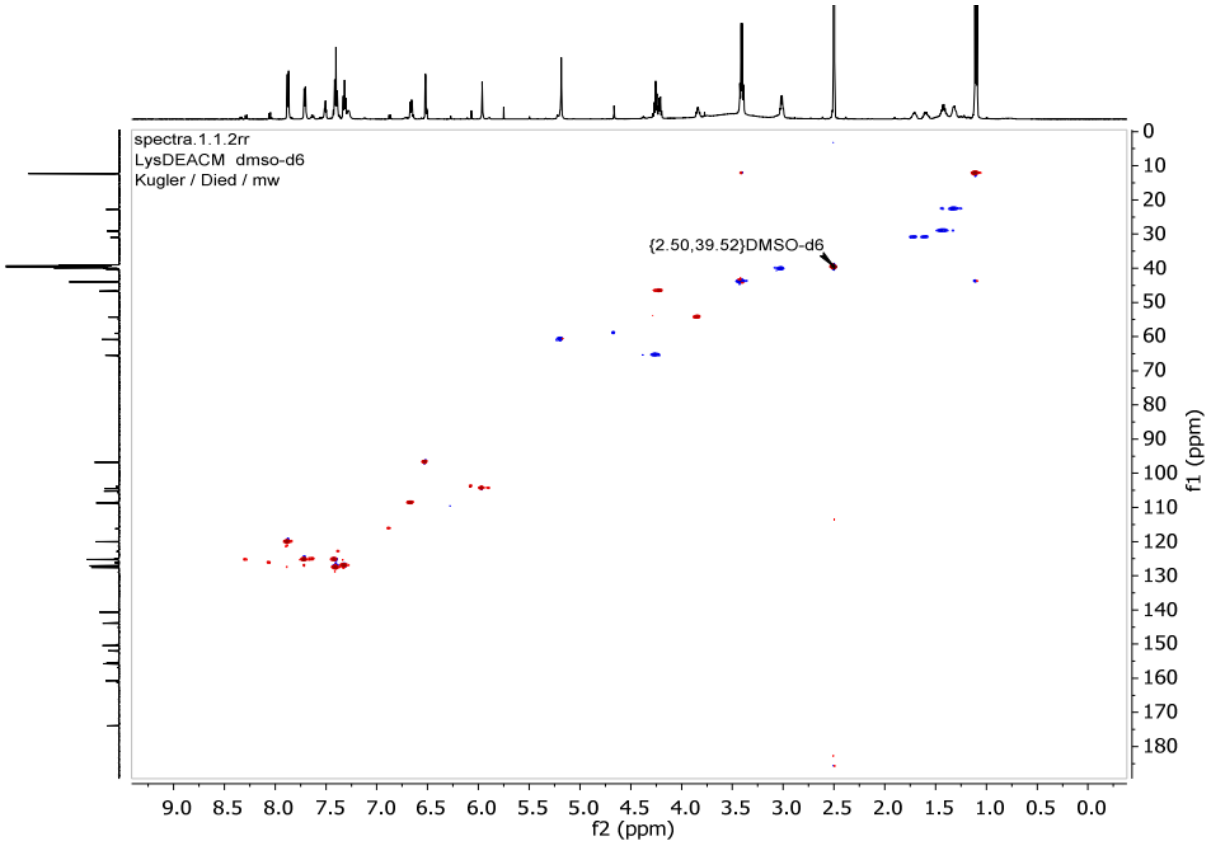

Figure S72: HSQC (600 MHz; 150 MHz, DMSO-d_6)

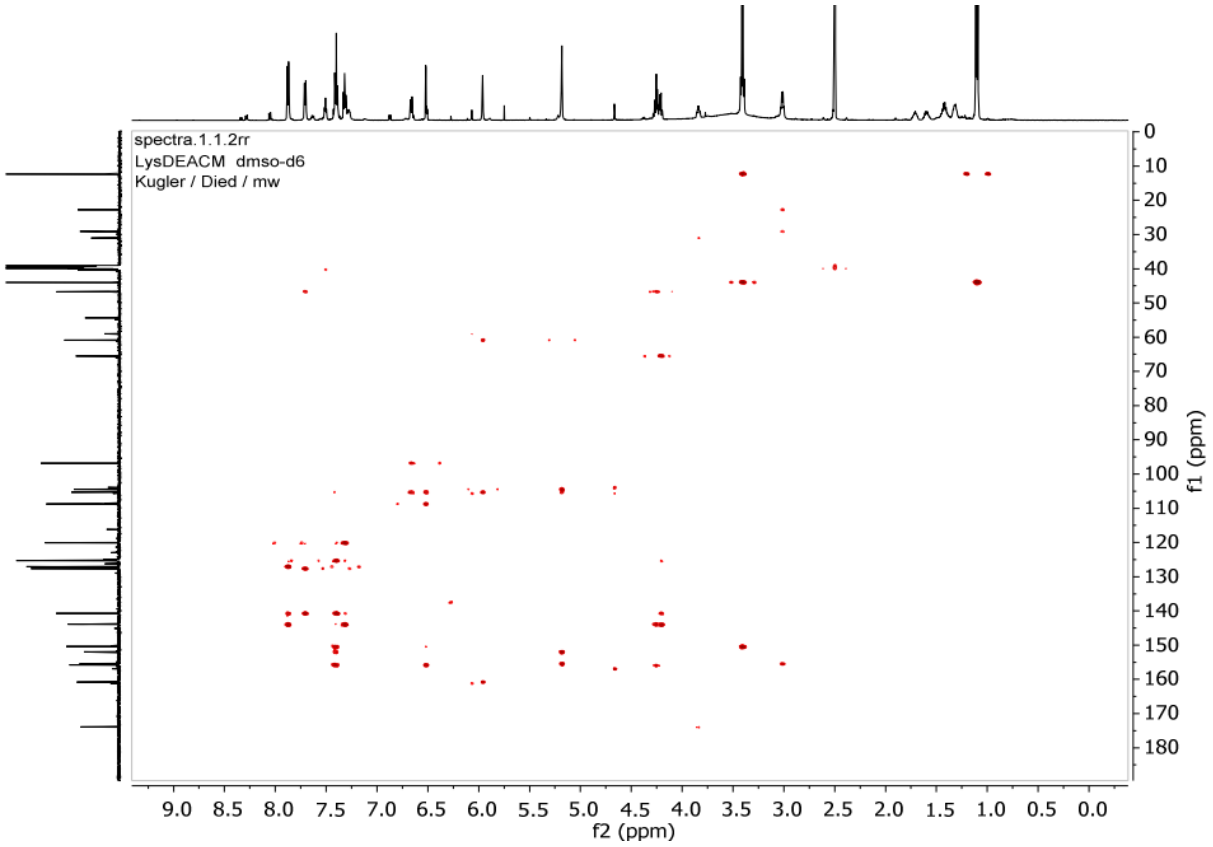

Figure S73: HMBC (600 MHz; 150 MHz, DMSO-d_6)

HR-MS (ESI+): calcd. for $C_{36}H_{39}N_3O_8$: 642.2810; found: 642.2792.

2.12 Synthesis of L17E-3PG **34**

Sequence: IWLTALK^{DEACM}FLGKHAAK^{DEACM}HEAKQQLSK^{DEACM}LPra-NH_2

Chemical Formula: $C_{184}H_{270}N_{42}O_{44}$

Molecular Weight: 3774.43 g/mol

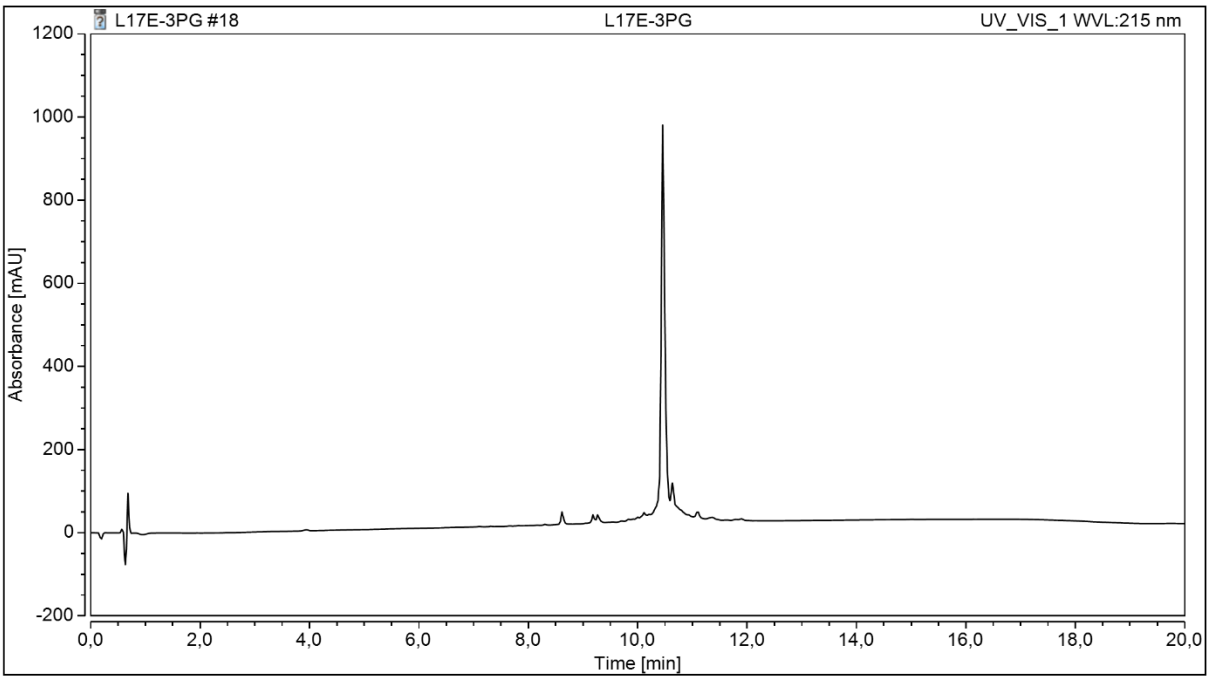

Figure S74: Analytical HPLC: ACE® Excel® 2 C18-100 column, 100x2.1 mm, 2 µM, with a 20-80% gradient of B, tR = 10.46 min, at a flow rate of 0.4 mL/min.

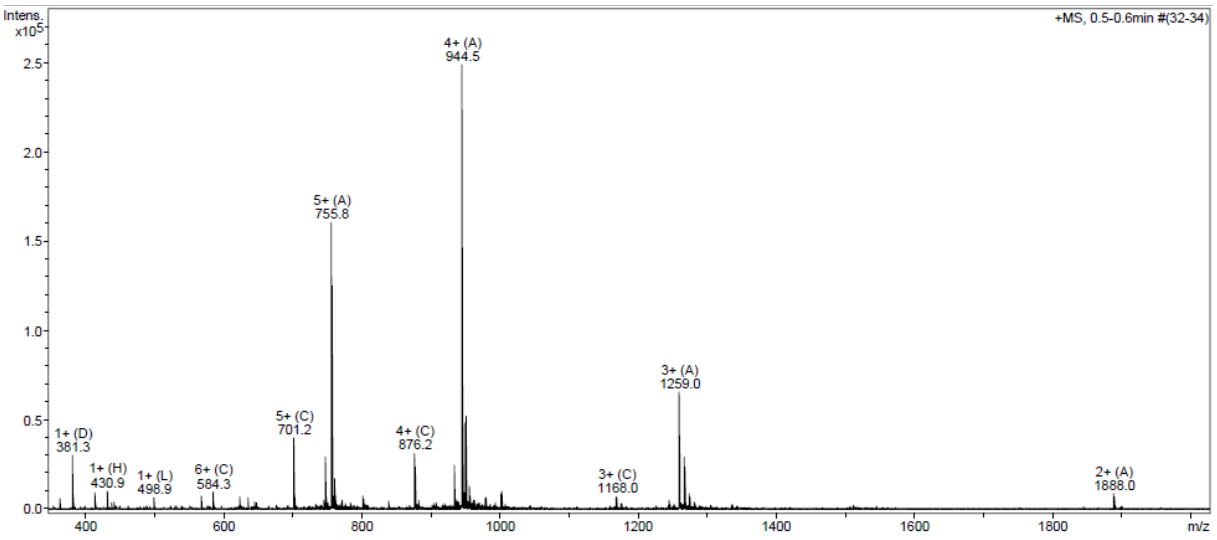

Figure S75: HR-MS (ESI+): calcd. for $[M+2H]^{2+}$: 1888.0196; found: 1888.0143, calcd. for $[M+3H]^{3+}$: 1259.0155; found: 1259.0133, calcd. for $[M+4H]^{4+}$: 944.5134; found: 944.5128, calcd. for $[M+5H]^{5+}$: 755.8122; found: 755.8114.

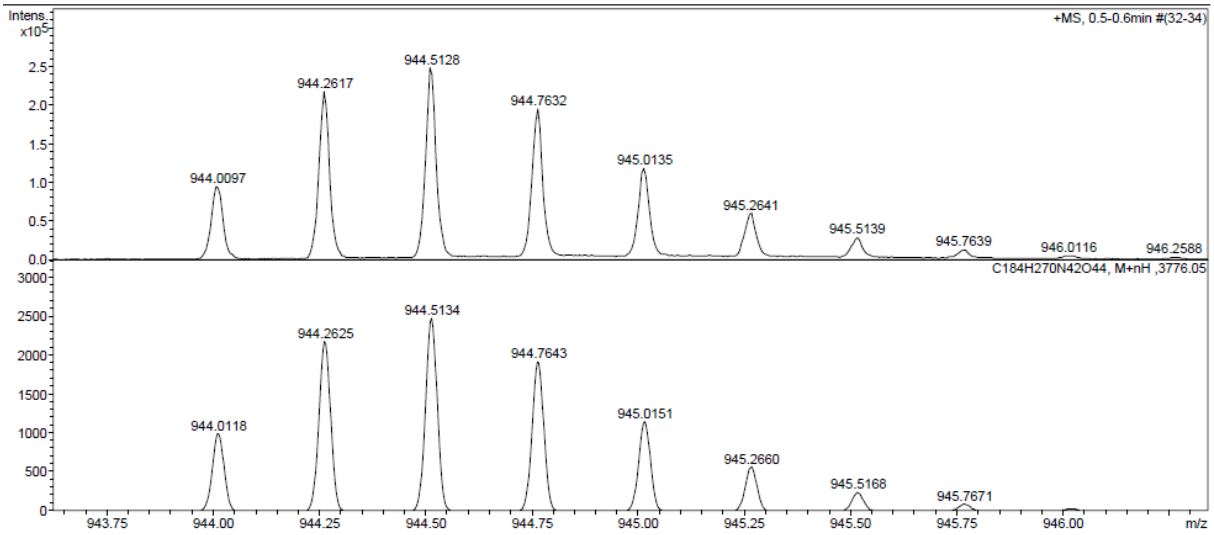

Figure S76: Measured isotopic pattern of the $[M+4H]^{4+}$ product peak (top) and its calculated isotopic pattern (bottom).

2.13 Synthesis of L17E-5PG **35**

Sequence: IWLTALK^{DEACM}FLGK^{DEACM}HAAK^{DEACM}HEAK^{DEACM}QQLSK^{DEACM}LPra-NH_2

Chemical Formula: $C_{214}H_{300}N_{44}O_{52}$

Molecular Weight: 4321,01

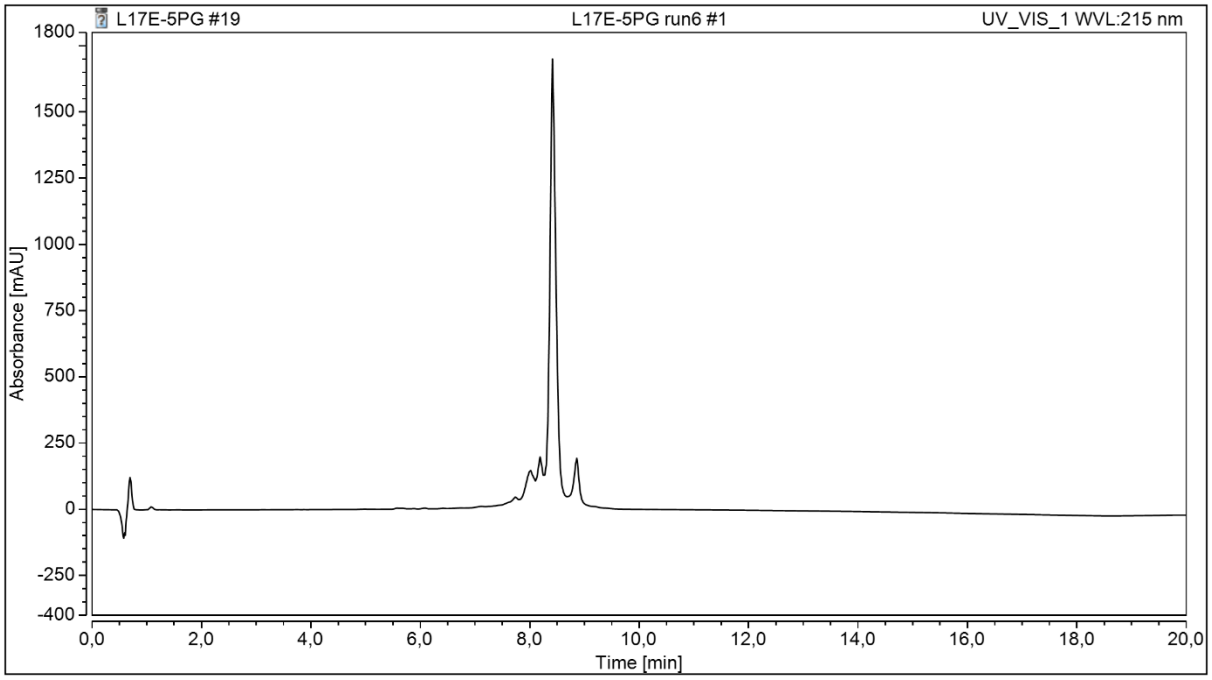

Figure S77: Analytical HPLC: ACE® Excel® 2 C18-100 column, 100x2.1 mm, 2 µM, with a 50-95% gradient of B, t_R = 8.42 min, at a flow rate of 0.4 mL/min.

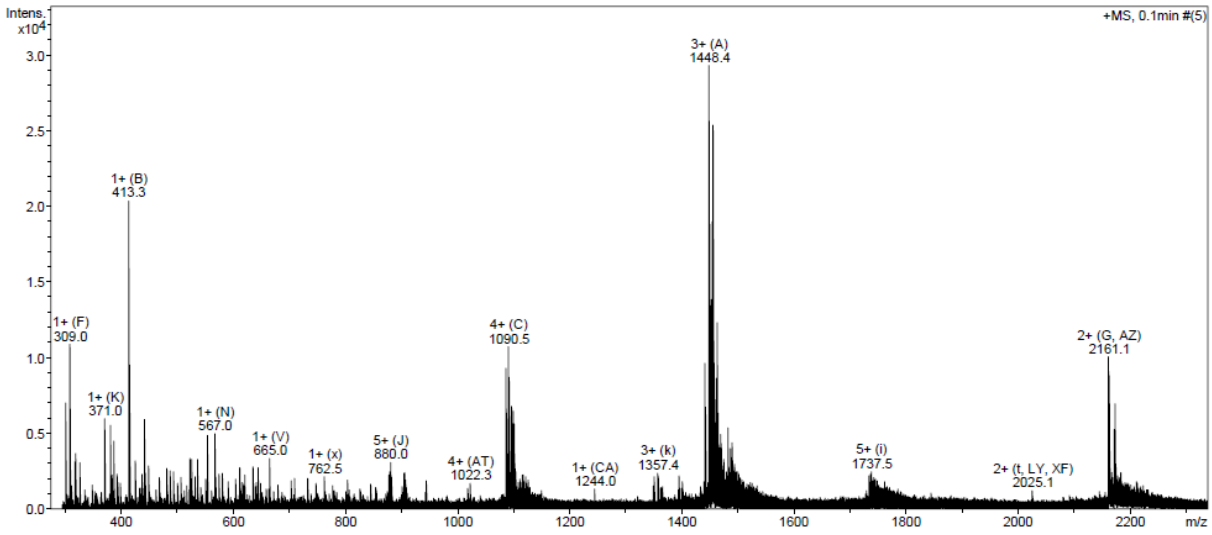

Figure S78: HR-MS (ESI+): calcd. for $[M+2H]^{2+}$: 2161.1194; found: 2161.1185, calcd. for $[M+3H]^{3+}$: 1441.0820; found: 1441.0828, calcd. for $[M+Na+H]^{2+}$: 2172.1104; found: 2172.1113, calcd. for $[M+2H+Na]^{3+}$: 1448.4093; found: 1448.4095, calcd. for $[M+3H+Na]^{4+}$: 1086.5588; found: 1086.5577.

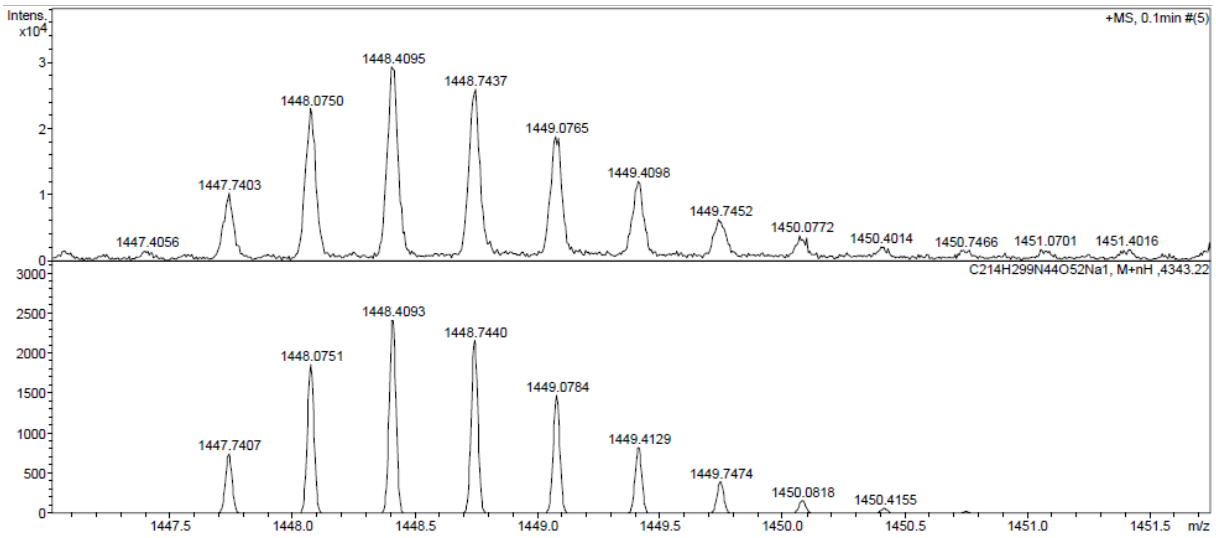

Figure S79: Measured isotopic pattern of the $[M+2H+Na]^{3+}$ product peak (top) and its calculated isotopic pattern (bottom).

3 Literature

[1] M. Richter, A. Chakrabarti, I. R. Ruttekolk, B. Wiesner, M. Beyermann, R. Brock, J. Rademann, *Chemistry* **2012**, *18*, 16708-16715.